

STUDY OF POLYMERIC NANOCOMPOSITES THROUGH ADDITIVE MANUFACTURING PROCESS

**Thesis Submitted
in Partial Fulfilment of the Requirements for the
Degree of
DOCTOR OF PHILOSOPHY**

**in
Mechanical Engineering**

**by
PHOOL SINGH**

(2K18/PhD/ME/12)

Under the Supervision of

Dr. RANGANATH M. SINGARI

Professor Mechanical Engineering
Delhi Technological University

Dr. R.S. MISHRA

Professor Mechanical Engineering
Delhi Technological University



**Department of Mechanical Engineering
DELHI TECHNOLOGICAL UNIVERSITY
(Formerly Delhi College of Engineering)**

Shahbad Daultpur, Main Bawana Road Delhi -110042, India

November, 2024

DECLARATION

I Phool Singh hereby certify that the work which is being presented in Thesis entitled **“Study of Polymeric Nanocomposites Through Additive Manufacturing Process”** in partial fulfilment of the requirement for the award of the degree of **Doctor of Philosophy** submitted in the Department of Mechanical Engineering, Delhi Technological University is an authentic record of my own work carried out during the period from 13th July 2018 to 19th April 2024 under the supervision of **Dr. Ranganath M. Singari**, and **Dr. R.S.Mishra**, Professors, Department of Mechanical Engineering, Delhi Technological University, Delhi.

The research work presented and reported in this thesis has not been submitted either in part or full to any other university or institute for the award of any other degree.

PHOOL SINGH

(2K18/PhD/ME/12)

This is to certify that the student has incorporated all the corrections suggested by the examiners in the thesis and the statement made by the candidate is correct to the best of our knowledge.

Signature of Supervisor (s)

Prof. Ranganath M. Singari,

Prof. R.S. Mishra



DELHI TECHNOLOGICAL UNIVERSITY

(Formerly Delhi College of Engineering)

Shahbad Dault Pur, Main Bawana Road, Delhi-42

CERTIFICATE

This is to certify that **Phool Singh** (2K18/PhD/ME/12) has carried out research work presented in the thesis entitled “**Study of Polymeric Nanocomposites through Additive Manufacturing Process**” for the award of **Doctor of Philosophy** in Mechanical Engineering under our supervision. The thesis embodies results of original work, and studies are carried out by the student himself and the contents of the thesis are not submitted for the award of any other degree to the candidate or to anybody else from this or any other University/Institution.

Dr. Ranganath M.Singari
Professor
Department of Mechanical
Engineering
Delhi Technological University
Delhi, India

Dr. R.S.Mishra
Professor
Department of Mechanical
Engineering
Delhi Technological University
Delhi, India

Date:

*Dedicated to my parents and
My Beloved Wife*

ACKNOWLEDGEMENT

I express my profound gratitude to **Dr. Ranganath M. Singari, Professor (supervisor) and Dr. R.S.Mishra, Professor (supervisor) Department of Mechanical Engineering, Delhi Technological University, Delhi**, for their inspiring guidance, encouragement, motivation, constructive criticism and valuable suggestions throughout the course of the investigation, which paved way for the completion of my Ph.D. work.

I would like to acknowledge my sincere thanks to **Prof. B.B. Arora, Head of Department, and DRC Prof. A.K. Aggrawal chairmen, Department of Mechanical Engg., Delhi Technological University, Delhi**, for providing all facilities during my research work. I am extremely thankful to **Dr. B.P. Singh, Sr. Principal Scientist, CSIR (National Physical Laboratory Delhi), Dr. Rajesh Kumar Chief Scientist, Head of Department force and hardness Metrology Section CSIR (National Physical Laboratory Delhi)**, for their whole hearted cooperation, allowing me to use their testing and production facility, suggestions and for doing my research works a delightful experience.

I would like to extend my sincere gratitude to **Dr. Mohan Singh Mehata and Dr. Deshraj Meena, Department of Physics, Delhi Technological University**, for their valuable help.

I also convey my sincere thanks to **Mr. Ali Nawaz** (Research Scholar DTU) for the technical support.

I also like to remember my parents and their blessings. It would be challenging for me to carry out the whole research work without the support of my entire family, especially **my wife (Mrs Poonam Kaur) and my two sons (Mr Himanshu Singh and Mr Vishal Singh)**, who have always supported me to do with my research work despite all constraints. It was only with their moral support that I was able to finish this task. I am always grateful and thankful to ALMIGHTY GOD for providing me with good health and patience in every best and worst situation during this research work. Thanking to all.

(Phool Singh)

TABLE OF CONTENTS

Title	Page No.
Declaration	i
Certificate by the supervisors	ii
Acknowledgement	iv
Table of Contents	v
List of Figure	ix
List of Table	xiii
List of Abbreviations	xiv
Preamble	xvi
Abstract	xvii
Flow Chart Diagram	xviii

CHAPTER 1: INTRODUCTION	1
1.1 Polymer	1
1.1.1 Generalities of Polymer	1
1.1.1.1 Polymerization Process	2
1.1.1.2 Polymer Structure	3
1.1.1.3 Confirmation	4
1.1.1.4 Polymer Morphology	6
1.1.1.5 Classes of Polymers	12
(i) Thermoplastic Polymers	12
(ii) Thermosetting polymers	12
(iii) Elastomers	13
1.1.2 Composites	13
(i) Metal matrix composites	13
(ii) Ceramic matrix composites	13
(iii) Polymer matrix composites	14
(iv) Polymer nanocomposites	15
1.1.3 Process for the preparation of nanocomposites	17
1.1.3.1 Solvent Blending	18
1.1.3.2 Melt Blending	18
1.1.3.3 In-situ Polymerisation	19
1.1.3.4 Solution mixing	20

1.1.3.5 Electrospinning	21
1.1.4 Factor affecting properties of polymer nanocomposites	23
1.1.4.1 Properties of the matrix	23
1.1.4.2 Particles, Flakes, Fibers, and Laminates Shape and Orientation of Dispersed Phase Inclusions	23
1.1.4.3 Interfacial Adhesion	24
1.1.5 Characterization of Polymer Nanocomposites	24
1.1.5.1 Spectroscopic test	24
1.1.5.2 Micromechanical Technique	25
1.1.5.3 Microscopic Technique	27
1.1.5.4 Thermodynamic Methods	28
1.1.6 Carbon nanotubes	30
1.1.6.1 Type of carbon nanotubes	30
(i) Single Walled carbon nanotubes	30
(ii) Multi-walled carbon nanotubes	31
1.1.6.2 Structure of carbon nanotubes	31
1.1.6.3 Properties of carbon nanotubes	34
1.1.6.4 Carbon nanotube-based Polymer nanocomposites	36
1.1.7 General Background of Functionalization of CNT	37
1.2 Additive Manufacturing Process	38
1.3 Challenges in existing polymeric nanocomposites	40
1.4 Need for new materials for additive manufacturing	41
1.5 Research Objectives	43
1) Study of material and characterization of polymeric nanocomposites	43
2) Development of new polymeric nanocomposites material.	44
3) Study of Mechanical Properties of the developed material.	44
4) Application of developed material with Additive manufacturing process.	44
1.6 Contribution to the field of material science	45
1.7 Advancements in Additive manufacturing	45
1.8 Potential applications	45
1.9 Technological advancements	46

1.10 Overview of Thesis	46
CHAPTER 2: LITERATURE REVIEW	49
2.1. Overview of polymeric nanocomposites	49
2.2. Significance in various industries.	51
a. Automotive Industry	52
b. Aerospace and Aviation	53
c. Electronics and Semiconductor Industries	53
d. Medical and Healthcare	53
e. Construction and Infrastructure	54
f. Energy Sector	54
2.3. Various types of Additive Manufacturing Processes.	54
2.3.1 Fused Deposition Modelling (FDM)	54
2.3.2 Stereolithography (SLA)	59
2.3.3 Laminated object manufacturing (LOM)	60
2.3.4 Selective laser sintering (SLS)	61
2.3.5 Direct energy deposition (DED)	62
2.4. Modeling and Simulation in Additive Manufacturing	64
2.4.1. Multi-scale multi-physics modelling of AM process	69
2.4.1.1. Micro-scale modeling for heat source model	69
2.4.1.2. Meso-scale modeling	69
2.4.2 Mechanical modeling for AM products using self-consistent clustering Analysis	70
2.5. A detailed survey of literature review	72
2.6. Summary of literature review	96
2.7. Motivation	97
2.8. Research gaps	98
CHAPTER 3: MATERIAL AND METHOD	99
3.1 Selection of base polymer and nanocomposites.	99
3.2 Fabrication of MWCNTs/ABS nanocomposites.	99
3.3 Preparation of specimens by microinjection moulding	101

3.4 Fused filament fabrication of MWCNTs/ABS composites	102
3.5 Preparation of specimens by FDM 3D printing	105
CHAPTER 4 : CHARACTERIZATION	107
4.1 Univeral Testing Machine	107
4.2 Microhardness	109
4.3 FTIR	111
4.4 Scanning Electron Microscopy	112
4.5 X-Ray Diffraction	113
4.6 Thermal Gravimetric Analyser	114
CHAPTER 5: RESULTS AND DISCUSSION	117
5.1 Tensile properties	117
5.1.1 Tensile properties of MWCNTs/ABS composites through micro injection moulding	117
5.1.2 Tensile properties of MWCNTs/ABS composites of 3 D printed specimen.	119
5.2 Microhardness of MWCNTs/ABS composite specimens	121
5.3 FTIR Analysis	122
5.3.1 FTIR of MWCNTs/ABS composites by microinjection moulded specimens	122
5.3.2 FTIR of MWCNTs/ABS composites by 3 D printed specimen	124
5.4 TGA Investigation	125
5.4.1 TGA of MWCNTs/ABS composites	125
5.4.2 TGA of 3 D printed materials	126
5.5 XRD Analysis	127
5.5.1 XRD characterization of MWCNTs/ABS composites through Micro Injection moulded specimen	127

5.5.2 XRD characterization of MWCNTs/ABS composites through 3 D printed specimen	128
5.6 Morphology Analysis	129
5.6.1 Morphology analysis of micro injection moulding processed specimens	129
5.6.2 Morphology analysis of 3D printed specimens	131
CHAPTER 6: CONCLUSION AND FUTURE SCOPE	133
6.1 Conclusion	133
6.2 Future Scope	134
References	135
List of Publication	164
Curriculum Vitae	165

LIST OF FIGURES

Figure No	Description	Page No
Figure 1.1	Formation of Acrylonitrile Butadiene Styrene	2
Figure 1.2	Isotactic and Syndiotactic configuration of polymer	3
Figure 1.3	Schematic representation of the three stereoisomers of the polymer chain	4
Figure 1.4	: DEATG-PPV's possible chain shapes in chloroform (a) diluted solutions, methanol (b) diluted solutions, and water (c) diluted solutions, as well as their change into semi-diluted solutions and thin films (right side of a, b, and c). Blue represents the EG side chains and red represents the PPV backbone	5
Figure 1.5	Possible conformations of molecules can be categorised as Anti (Trans), Eclipsed (Cis), and Gauche (+ or -). Additionally, the conformation of butane can be altered by rotating about its two core atoms.	5
Figure 1.6	Schematic representation of Structure of Polymers	7

Figure 1.7 Crystalline and amorphous and semi-crystalline polymers	7
Figure 1.8 Semi-crystalline Polymers	8
Figure 1.9 Behavior of polymers as a function of temperature: (a) degree of crystallinity and (b) crosslinking	9
Figure 1.10 Volume or enthalpy of different material states as a function of temperature	11
Figure 1.11 Different types of nanoparticles	17
Figure 1.12 Polymer nanocomposites made via melt blending, depicted schematically	19
Figure 1.13 Block diagram depicting the in situ polymerization process	20
Figure 1.14 Schematic illustration for the solution mixing method	21
Figure 1.15 The set-up of electrospinning technique	22
Figure 1.16 Schematic model of interphase	24
Figure 1.17 Types of Carbon Nanotubes: (a) SWCNT and (b) MWCNT	31
Figure 1.18 2D sheet of graphene diagram illustrating a vector structure categorization used to characterize the structure of CNT	32
Figure 1.19 Diagram showing the process for producing various chirality configurations in CNTs	34
Figure 1.20 CNTs structure with different chiralities: (A) arm chair structure, (B) zig-zag structure, (C) chiral structure	35
Figure 2.1 Various uses of polymer nanocomposites	52
Figure 2.2 Fused deposition modelling process	55
Figure 2.3 (a) Various fill percentages infill pattern (b) Zero air gap, (c) positive air gap, and (d) Negative air gap [58
Figure 2.4 The concept of layer height, extrusion width, raster angle and air gap for small layer height.	58
Figure 2.5 Stereolithography (SLA) process	60
Figure 2.6 LOM setup	61
Figure 2.7 SLS apparatus	63
Figure 2.8 DED Setup	63

Figure 2.9 The relationship between experiment and computer simulation	67
Figure 2.10 Data-driven multi-scale multi-physics modeling framework	68
Figure 2.11 Meso-scale modeling of EBSM processes from powder spreading to selective melting	70
Figure 3.1 Experimental Setup for preparation of MWCNTs/ABS Nanocomposites, Twin screw extruder (Thermo Scientific Prism Eurolab 16).	100
Figure 3.2 Flow process diagram for preparing the specimen samples of single time extruding and second time extruding by twin screw extruder	101
Figure 3.3 (a) Micro Injection moulding Machine (b) Moulding tool with moulded specimens	102
Figure 3.4 Drawing of prepared sample with proper dimensions by micro injection moulding and 3D printing process	103
Figure 3.5 Schematic diagram of filament extrusion process for preparing the filament for various wt.% of MWCNTs/ABS	103
Figure 3.6 Prepared filaments ready to 3 D print (a) Pure ABS, (b) 1wt. % of MWCNT/ABS, (c) 2wt. % of MWCNT/ABS and (d) 3 wt. % of MWCNT/ABS	104
Figure 3.7 Flashforge Dreamer 3D printer using to preparing specimens	105
Figure 3.8 Process flow diagram of experimental work (a) Model prepared (b) Process for slicing (c) Printing process (d) Specimen for tensile test (e) Sample after tensile test.	106
Figure 4.1 Universal Testing Machine (UTM) makes Tinius Olsen	109
Figure 4.2 Microhardness tester	110
Figure 4.3 FT-IR Setup	111
Figure 4.4 Scanning Electron Microscopy (SEM) makes TESCAN MAGNA GMH	112
Figure 4.5 X-ray Diffractometer makes Bruker D8-Advance	113
Figure 4.6 TGA 4000 Thermogravimetric Analyser	114

Figure 5.1 Comparison stress and strain curve for 1, 2, and 3 wt.% of MWCNT reinforced in ABS a) single-time extruded materials b) second-time extruded materials prepared by microinjection moulding.	119
Figure 5.2 (a) Comparative strain and stress graph of single extruded composite Materials	119
Figure 5.2 (b) Comparative strain and stress graph of double extruded composite Materials	120
Figure 5.3 3 D printed comparative graph of stress and strain for pure ABS and 1, 2, and 3%wt. of MWCNTs reinforced Composites	121
Figure 5.4 Comparative ultimate tensile stress in various nanocomposite materials with pure ABS	121
Figure 5.5 Comparison of pure ABS and 1, 2, and 3 wt.% MWCNT/ABS (a) single extruded composites (b) double extruded composites for microhardness.	122
Figure 5.6 FTIR curves of single extruded composites (a) Pure ABS (b) 1 wt.% of MWCNTs/ABS (c) 2 wt.% of MWCNTs/ABS, and (d) 3 wt.% of MWCNTs/ABS.	123
Figure 5.7 FTIR curves of double extruded MWCNT/ABS composites for (a) 1 wt.% of MWCNTs reinforcement (b) 2 wt.% of MWCNTs reinforcement (c) 3wt.% of MWCNTs reinforcement (d) Pure MWCNTs	124
Figure 5.8 FTIR Results of 3D printed pure ABS and 1, 2, and 3 wt. % MWCNTs reinforced composites.	125
Figure 5.9 (a)TGA of single extruded MWCNTs/ABS nanocomposites of 1, 2, and 3 wt.% of MWCNTs reinforcement and pure ABS(b)) TGA of double extruded MWCNTs/ABS nanocomposites of 1, 2, and 3 wt.% of MWCNTs reinforcement and pure ABS.	126
Figure 5.10 Thermogravimetric analysis curves for materials made of ABS and MWCNT/ABS 3 D printed nanocomposites.	128
Figure 5.11 XRD pattern for single and double extruded MWCNTs/ABS Nanocomposites	129

Figure 5.12 XRD Analysis of 3D printed (a) Pure ABS, (b) 1 wt. % MWCNTs/ ABS, (c) 2 wt. % MWCNTs/ABS (d) 3 wt. MWCNTs/ABS composite	130
Figure 5.13 SEM images of single extruded nanocomposite (a) Pure ABS (b) 1wt.% of MWCNTs/ABS (c) 2 wt.% MWCNTs/ABS (d) 3 wt.% of MWCNTs/ABS composite.	131
Figure 5.14 SEM images of double extruded nanocomposite (a) Pure ABS (b) 1wt.% of MWCNTs/ABS (c) 2 wt.% MWCNTs/ABS (d) 3 wt.% of MWCNTs/ABS composite.	132
Figure 5.15 Scanning Electron Microscopy images of the 3D printed MWCNTs /ABS tensile test specimen fracture surfaces (a) Pure ABS (b) 1% wt. (c) 2% wt. MWCNT loading percentages. d) 3% wt. MWCNT loading showing its agglomeration.	133

LIST OF TABLE	DESCRIPTION	PAGE NO.
Table 2.1	Comparison of different AM techniques	64
Table 3.1	Technical specifications of Thermo Scientific Haake MiniJet II	102
Table 3.2	Specification of filament Extruder Scientific machine.	104
Table 3.3	Production parameters for filaments extruders	104
Table 3.4	The FDM process used for experimental setup of DREAMER FLASH FORGE Specifications	106
Table 4.1	Microhardness tester Data were used in the study	110
Table 4.2	Technical Description and Specifications of the TGA setup:	115
Table 5.1	Enhanced tensile strength of single extruded and double extruded composite materials with respect to pure ABS.	120

List of Abbreviation

AM:	Additive manufacturing
DP:	Degree of polymerisation
WSCP:	Water-soluble conjugated polymer
PET:	Polyethene terephthalate
MMCs:	Metal Metrics Composites
CMCs:	Ceramic Matrix Composites
PMCs:	Polymer Matrix Composites
AACs:	Alkali-Activated Composites
ABS:	Acrylonitrile butadiene styrene
PZC:	Point of zero charge
CB:	Carbon black
CCB:	Conductive carbon black
CNT:	Carbon nanotube
DMMP:	Dimethyl methyl phosphonate
FTIR:	Fourier's transform infrared,
UV-Vis:	Ultraviolet-Visible Spectroscopy
XPS:	X-ray Photoelectron Spectroscopy
TEM:	Transmission Electron Microscopy
AFM:	Atomic Force Microscopy
CLSM:	Confocal Laser Scanning Microscopy
STM:	Scanning Tunneling Microscopy Scanning
FFF:	Fused Filament Fabrication
PLA:	Polylactic Acid
TPU:	Thermoplastic Polyurethane
STL:	Surface Tessellation Language
NFRCs:	Natural Fiber Reinforced Composites
FDM:	Fused deposition modeling
SLA:	Stereolithography
RP:	Rapid prototyping
LOM:	Laminated Object Manufacturing
SLS:	Selective laser sintering
DED:	Direct energy deposition
ALM:	Additive Layer Manufacturing
WAAM:	Wire arc additive manufacturing
DEM:	Discrete element methodology
EBSM:	Electron Beam Selective Melting
FVM:	Finite volume Methods

RVE:	Representative Volume Elements
DNS:	Direct numerical simulations
SCA:	Self-consistent clustering analysis
LENS:	Laser-engineered net shaping
UTS:	Ultimate Tensile Strength
TLCP:	Thermotropic Liquid Crystalline Polymers
LDM:	Liquid deposition modeling
ALD:	Atomic Layer Deposition
PPBAM:	Polymeric Pellet-Based Additive Manufacturing
DSC:	Differential Scanning Calorimetry
PEEK:	Polyether Ether Ketone
DEM:	Discrete Element Methodology
CFRTPCs:	Continuous fiber-reinforced thermoplastic composites
PHA:	Polyhydroxyalkanoate
SSS:	Siliceous Sponge Spicules
GFRP:	Glass fibre-reinforced polymer
MWCNTs:	Multiwall carbon nanotubes
NBR:	Nitrile rubber
NC:	Needle Coke
OPC:	Ordinary Portland Cement
PANI:	Polyaniline
PNC:	Polymeric nanocomposites
PP:	Polypropylene
PSI:	Precipitated silica
PU:	Polyurethane
SEM:	Scanning electron microscopy
SWCNT:	Single-wall carbon nanotube
TGA:	Thermogravimetric analysis)
XRD:	X-ray diffraction
CNC:	Cellulose Nanocrystal
PBT:	polybutylene terephthalate
TPTC:	Thermal Performance Test Coefficient
VOCs:	Volatile Organic Compounds
FGAM:	Functionally Graded Additive Manufacturing
ATR:	Attenuated total reflection
Tg:	Glass transition temperature
Tm:	Melting point

“Preamble”

In recent years, additive manufacturing (AM) has emerged as a revolutionary technique in fabricating complex structures with unparalleled precision and efficiency. Its application spans across various industries, ranging from aerospace to biomedical engineering. Within this realm, the integration of nanotechnology into additive manufacturing processes has opened new avenues for the development of advanced materials with enhanced properties. Among these, polymeric nanocomposites stand out as a promising class of materials, offering a synergistic combination of polymer matrices with nanoscale reinforcements.

This thesis embarks on a comprehensive exploration into the synthesis, characterization, and application of polymeric nanocomposites fabricated through additive manufacturing techniques. The research endeavors to elucidate the intricate interplay between processing parameters, material compositions, and resulting properties, thereby advancing our understanding of these multifaceted materials.

The preamble sets the stage by elucidating the significance of the research topic, highlighting the transformative potential of polymeric nanocomposites and additive manufacturing techniques. It provides a brief overview of the objectives, methodologies, and anticipated contributions of the thesis, laying the groundwork for the subsequent chapters.

Throughout this endeavor, the thesis aims to address key research questions pertaining to the optimization of additive manufacturing parameters, the characterization of nanocomposite structures, and the evaluation of their mechanical, thermal, and functional properties. By elucidating these aspects, this research endeavors to pave the way for the widespread adoption of polymeric nanocomposites in diverse industrial applications, ranging from lightweight structural components to biomedical implants.

Keywords: Additive manufacturing, Polymeric nanocomposites, Nanotechnology, Synthesis, Characterization, Mechanical properties, Thermal properties, Functional properties.

STUDY OF POLYMERIC NANOCOMPOSITES THROUGH ADDITIVE MANUFACTURING PROCESS

ABSTRACT

Polymer are very essential material for additive manufacturing (AM) process. It's have revolutionized the production of complex structures with enhanced design flexibility. This study delves into the realm of polymeric nanocomposites fabricated through additive manufacturing processes, aiming to investigate their mechanical properties and potential applications. The integration of nanomaterials, such as multiwalled carbon nanotubes (MWCNTs) into polymer such as Acrylonitrile Butadiene Styrene (ABS) matrices has shown promise in enhancing mechanical, and thermal, properties.

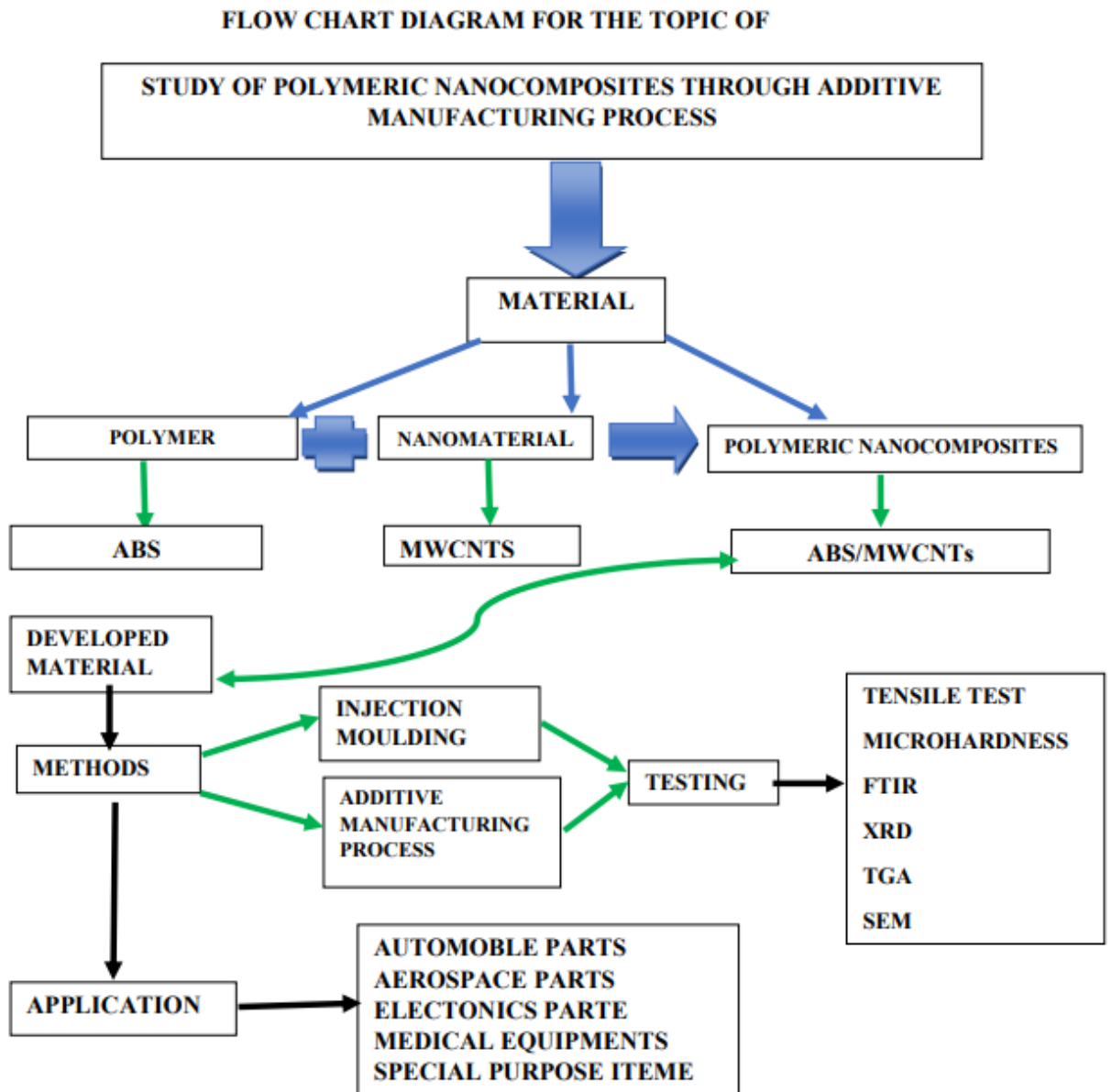
The research begins by elucidating the fundamentals of additive manufacturing techniques, including stereolithography, fused deposition modeling, as well as their compatibility with polymeric nanocomposite fabrication. A systematic analysis of various nanomaterials, such as Multiwalled carbon nanotubes, incorporated into ABS, provides insights into the synergistic effects on material performance.

Furthermore, the study investigates the influence of processing parameters, such as printing speed, layer thickness, and material composition, on the final properties of polymeric nanocomposites. Mechanical testing, thermal analysis, and microstructural characterization techniques are employed to evaluate the resulting materials' structural integrity, thermal stability, and morphological features.

The potential applications of polymeric nanocomposites produced through additive manufacturing are explored across multiple industries, including aerospace, automotive, biomedical, and electronics. The study also addresses challenges and limitations associated with the fabrication process, providing a basis for future advancements in the field.

In conclusion, this comprehensive investigation contributes to the understanding of polymeric nanocomposites synthesized through micro injection moulding and additive manufacturing, offering valuable insights into their (XRD) structural (SEM), thermal

(TGA), mechanical properties (Tensile Strength) and FTIR. The findings of this research have the potential to guide the development of innovative materials with tailored functionalities, paving the way for their widespread adoption in diverse industrial applications. This study would help researchers to find new application of this environmental friendly material in various fields.



CHAPTER 1

INTRODUCTION

This chapter provides the necessary background of polymer nanocomposites and use of multiwall carbon nanotubes as fillers. The scope of the present investigations and organization of thesis are also presented. Different techniques for preparation of polymeric nanocomposites and their effects on composite property are described. Various types of functionalization of MWCNTs and its effect on preparation of polymeric nanocomposites have also been emphasized in this chapter. This chapter has also described composites used in additive manufacturing.

1.1 Polymer

1.1.1 Generalities of Polymer

Polymers are a wide range of materials consisting of several small particles (monomers) linked up to form complex chains. Lengths of these chains in commercial polymers may vary from 1000 to 10,000 units. Polymers have been useful to people for many centuries in the form of fats, tars, resins, and gums. Polymers are called macromolecules because they are incredibly huge. Prior to processing using standard procedures typically utilized in the manufacturing of plastics, cellulose, as an example of a polymeric material, necessitates significant modification. Polyethylene and polyvinyl chloride, which are common plastics, have supplanted more conventional materials such as copper and paper in a wide range of applications. Examples of plastics that can be utilized in the production of fibers include nylon and cellulose acetate.

The phenomenon by which monomers are converted into polymers is referred to as polymerization. Generally, the progenitor compound of the monomers consists of a double-bonded substance that undergoes a single bond formation during the polymerization reaction, resulting in the formation of the polymers. Consider, for instance, the production of acrylonitrile butadiene. Terpolymerized styrene is produced when acrylonitrile and styrene are polymerized in the presence of polybutadiene. This

polymer consists of a 15% to 35% combination of acrylonitrile, 5% to 30% butadiene, and 40% to 60% styrene. A long polybutadiene chain is created by interconnecting smaller poly (styrene-co-acrylonitrile) chains [1].

Polar nitrile groups from adjacent chains form an attractive bond that fuses the chains, thereby enhancing the strength of ABS in comparison to pure polystyrene.

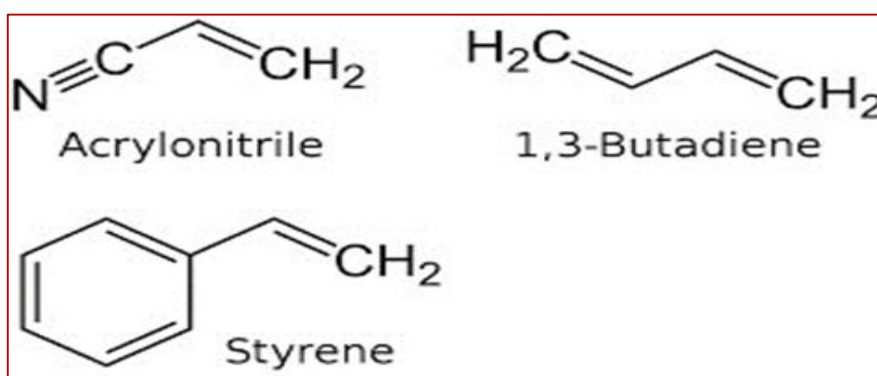


Figure 1.1 Formation of Acrylonitrile Butadiene Styrene [1].

1.1.1.1 Polymerization process:

Polymerization is the process of chemically combining monomer molecules to create either linear chains or a three-dimensional network of polymer chains [2]. The 'degree of polymerization,' or DP, is the quantity of monomer units that repeat along the chain. In polymer chains, DP stands for the average number of monomer units. Polymerization can occur through two distinct methods. [3]:

- (i) **Condensation polymerization:** In condensation polymerization, two ends of each molecule chemically react to progressively build up a long chain of molecule.
- (ii) **Addition polymerization :** Condensation polymerization differs from addition polymerization in that some small molecules are formed as by-products during the reaction. The reactive chemicals that carry out these reactions usually contain functional groups, such as alcoholic beverages and amine, a carboxylic acid (or another carboxylic derivative [5].

1.1.1.2 Polymer Structure:

The physical structure of a polymer chain is a significant component that influences its macroscopic properties. Configuration and conformation are used to characterize a polymer's geometric structure.

Configuration: Configuration refers to the spatial arrangement of atoms within a molecule. A polymer's structure can be altered only by breaking and rebuilding chemical bonds. There are two sorts of polymer configurations: Trans and Cis. These structures cannot be altered physically (e.g., through rotation). The Cis configuration arrangement occurs when substituent groups flank two carbon-carbon double bonds. What we call "trans" substituents are located on the other side of a double bond. [6].

One essential component of a polymer chain is its physical structure, which significantly impacts its macroscopic properties. A polymer's conformation and configuration explain its geometric structure [7].

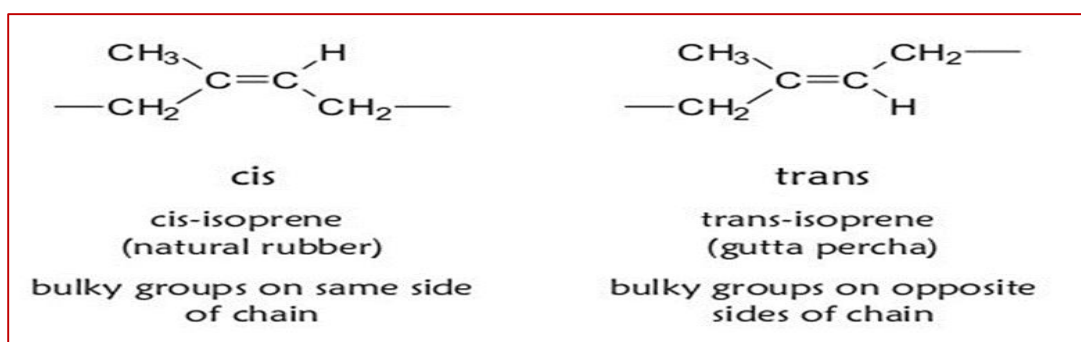


Figure 1.2 Isotactic and Syndiotactic configuration of polymer [6].

The configuration of polymer chains is referred to as stereoregularity. It is possible to obtain three different structures. A polymer is said to be "atactic" if the monomers have joined the chain randomly, such as in the case of polypropylene. When every side group is arranged in a cis fashion on one side of the chain, a polymer is said to be "isotactic," such as natural rubber. A polymer is referred to as "syndiotactic" if the side groups are arranged in an alternating manner (trans arrangement), as in the case of Gutta-percha, as seen in Fig. 1.2.

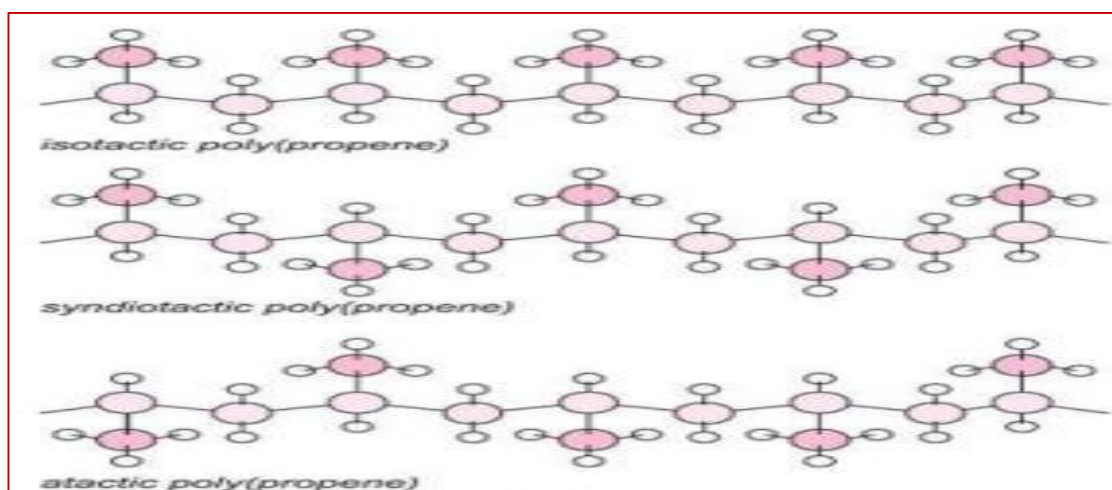


Figure 1.3 Schematic representation of the three stereoisomers of the polymer chain [8].

1.1.1.3 Conformation: The order that results from molecules rotating around their solitary bonds is referred to as conformation. As a result, a polymer's conformation can alter without covalent connections breaking or rearranging. It is possible to rotate around a single bond rather than a double bond because doing so does not necessitate breaking the bond. A change in the torsional angle indicates an atom's capacity to spin in this manner regarding the bonds of atoms. Fig. 1.3 represents the stereoisomers of the polymer chain of propene. Conformations are arrangements of two atoms joined by other atoms or groups that have different torsional angles [8].

Polymer-based materials are used in almost every aspect of contemporary life because they are inexpensive, simple to manufacture, and can change their material properties chemically. Poly [2,5 bis (diethylaminetetraethylene glycol) phenylenevinylene] (DEATG-PPV) a non-ionic, water-soluble conjugated polymer (WSCP), can have its optical characteristics, chain conformation, and film morphology altered by altering the solvent's polarity, according to Zhihua Xu et al , Figure 1.4 shows that interactions between the polymer and solvent significantly affect the chain conformation of this non-ionic WSCP. It controls how drop-cast thin films turn out regarding their structure and optical characteristics. [9]. The distances between atoms or groups revolving around a bond determine the sort and quantity of interaction between them and the different conformations that result from these distances. Therefore, various conformations can correspond to distinct molecular potential energies. There are a few conceivable

generalized conformations: Figure 1.5 illustrates Anti (Trans), Eclipsed (Cis), and Gauche (+ or -).

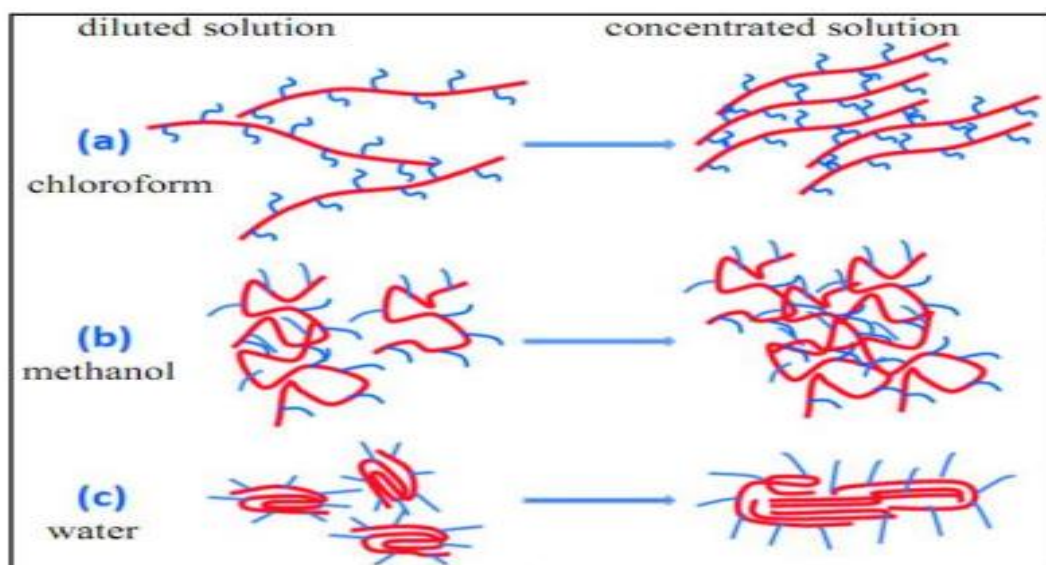


Figure 1.4 DEATG-PPV's possible chain shapes in chloroform (a) diluted solutions, methanol (b) diluted solutions, and water (c) diluted solutions, as well as their change into semi-diluted solutions and thin films (right side of a, b, and c). Blue represents the EG side chains and red represents the PPV backbone [9].

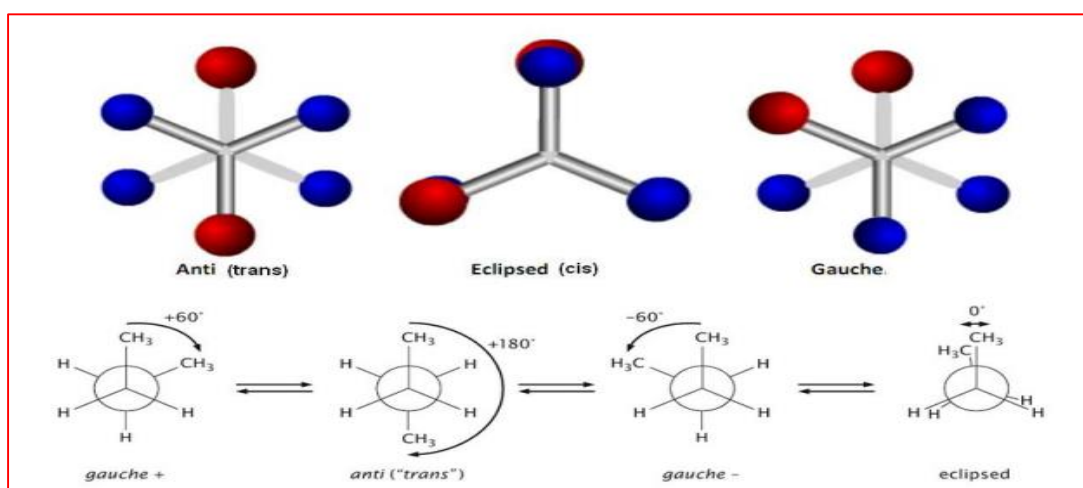


Figure 1.5 Possible conformations of molecules can be categorised as Anti (Trans), Eclipsed (Cis), and Gauche (+ or -). Additionally, the conformation of butane can be altered by rotating about its two core atoms.

Huang et al. [10] emphasise the significance of the trans conformer in annealing-induced crystallisation in polyethene terephthalate (PET). The researchers investigated the trans-gauche ratio, mobility in various domains, and crystallisation growth at the annealing temperature. The trans conformer rose continually as the annealing temperature increased, whereas the degree of crystallinity decreased in the final annealing stages. Koenig et al. [11] analyse the creation of the "Trans" component during the isothermal crystallisation of PET at low temperatures. The crystallisation process was categorised into two distinct stages: primary and secondary. The conclusion in this example was that the trans isomer fraction grows linearly with annealing time, altering the physical properties of the polymer.

Polymer molecules can have a variety of topologies, depending on the structure of the monomer(s) and the polymerization process used. The most prevalent structures are linear, branching, and network.

[i] Linear Polymer: Linear polymers are substances with long, straight chains. Examples include high-density polyethylene and polyvinyl chloride. [ii] Branched Polymers: These polymers have linear chains with some branches, such as low-density polythene. [iii] Cross-linked polymers are usually made up of monomers with two or three functions. They have strong covalent bonds between linear polymer chains, like urea-formaldehyde resins and vulcanized rubber. [iv] Polymers that form a three-dimensional network through intricate linking are called "networked polymers." Thermosetting describes these polymers because they cannot be softened when heated without destroying the underlying polymer structure. Figure 1.6 depicts polymers' structures of linear, branching, and cross-linked network architecture [12].

1.1.1.4 Polymer Morphology: The microscale organisation and spatial arrangement of polymer chains are included in polymer morphology. In the solid state, polymers display two forms of morphology: amorphous crystalline and semi-crystalline, as illustrated in Fig. 1.7 [13]. The arrangement of molecules within a solid and their shape play a critical role in defining polymer's characteristics. Polymer's molecular forms conformation, and orientation can all substantially impact its macroscopic properties.

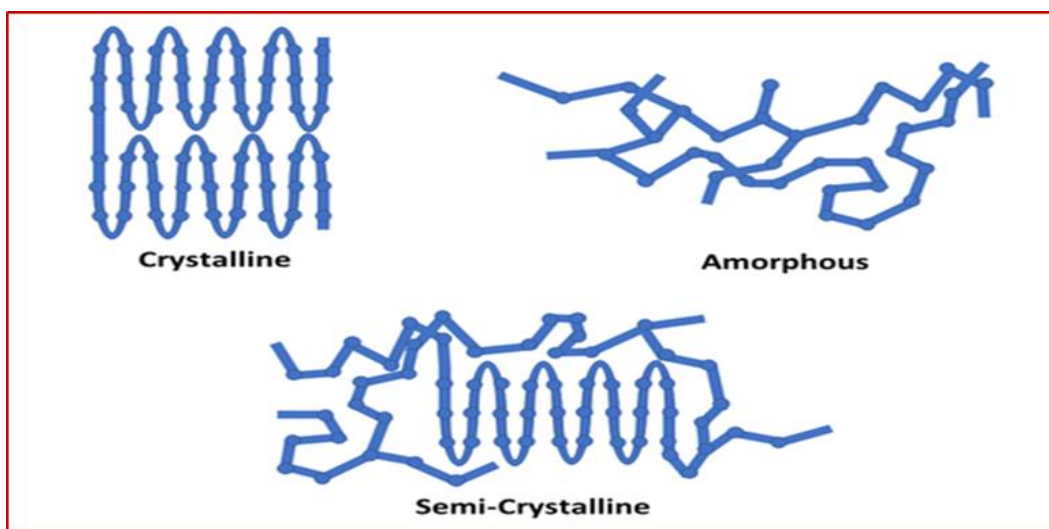


Figure 1.6 Schematic representation of Structure of Polymers [12].

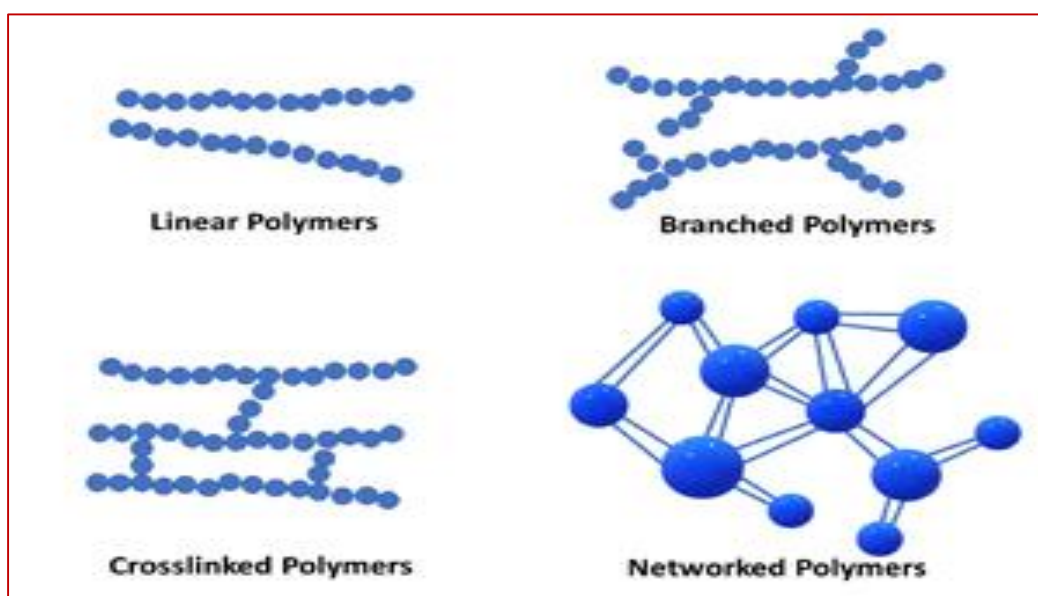


Figure 1.7 Crystalline and amorphous and semi-crystalline polymers [13].

Most polymers have a semi-crystalline shape. Instead of producing a single melting point, they produce mixtures of microscopic crystals and amorphous material that melt at different temperatures. The polymer chains are folded and stacked to form the crystalline substance, which has excellent order. The structure appears amorphous or glassy, with no long-range organisation and entangled chains (Figure 1.8). Specific

polymers lack structure. Nonetheless, most mix the tangled and disorganized zones surrounding the crystalline portions [14].

The state of an amorphous substance is contingent upon its composition, temperature, and duration. Amorphous materials transition from a glassy state to a rubbery state when temperature, relative humidity, or moisture content increases. Molecular mobility and mechanical and dielectric properties change [15]]. Due to the robust intermolecular interactions among molecules that are closely packed in the crystallites, semi-crystalline polymers make very long plastics. Drawing is a method of stretching polymers to align the molecules and produce crystallinity. The extent of the polymer's crystalline structure determines its degree of crystallinity. It can be zero for completely amorphous polymers and one for hypothetically completely crystalline ones. Polymers with microcrystalline regions tend to exhibit greater strength (they can withstand more bending without fracturing) and higher resistance to impact than entirely amorphous polymers. [16].

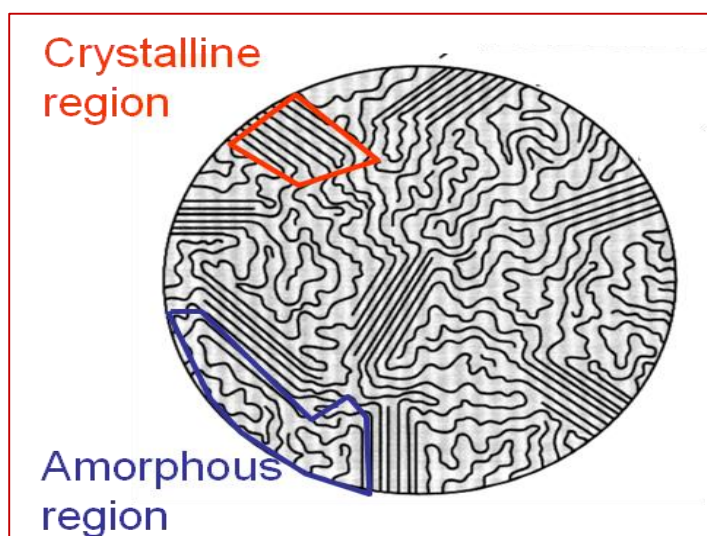


Figure 1.8 Semi-crystalline Polymers [14].

At low temperatures, the molecules of an amorphous or semi-crystalline polymer exhibit minimal movement due to their low energy, resulting in a solid form called the glassy state. As the temperature of the polymer increases, the molecules experience increased vibrational energy, causing them to transition from a solid, glassy state to a more

flexible, rubbery state [17]. Amorphous polymers undergo a gradual phase shift-free transition from solid to liquid, passing through a "rubbery" state within a minimal temperature range known as the glass transition temperature. Glass changes from its complex and brittle state to a softer and more flexible one. This change occurs in a partly crystalline polymer where there is yet to be a complete crystalline structure. The crystalline regions remain undamaged and serve as strengthening components, resulting in a high hardness level in the sample. If continuous heating is maintained, the crystalline regions will undergo melting. The temperature at which the last crystallite begins to melt is called a polymer's equilibrium crystalline melting point (T_m). T_m is not a function of basic material properties but rather of crystallinity and crystallite size distribution, as shown in Figure 1.9 [18].

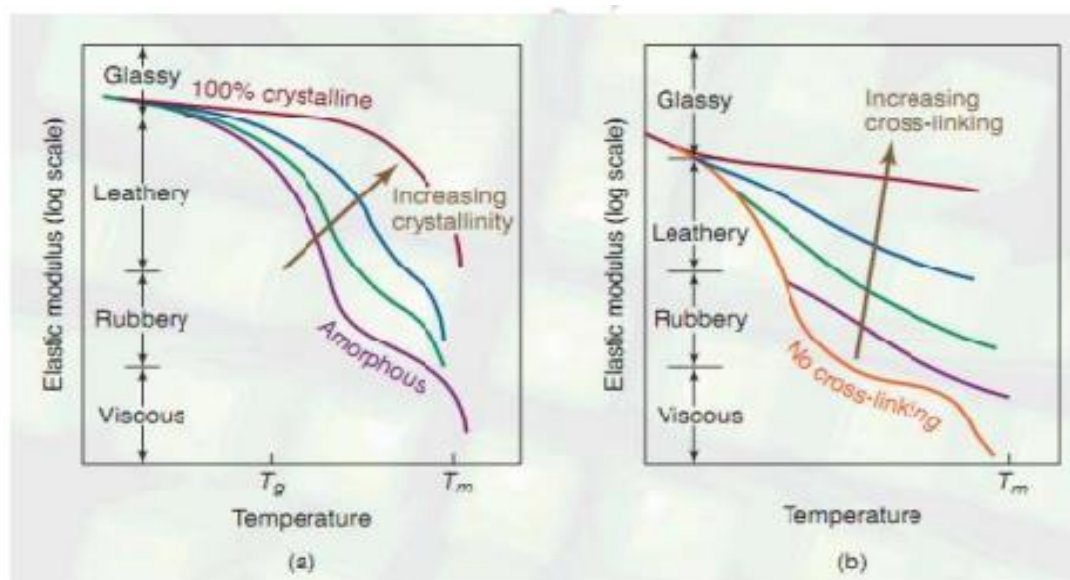


Figure 1.9 Polymer behaviour as a function of temperature, (a) degree of crystallinity, and (b) cross-linking [19].

Polymers must be heated to the glass transition temperature (T_g) or higher before moulding. If the temperature is raised above T_g , the polymer melts. In polymers, the term "melting point" (T_m) refers to the specific temperature at which a transition occurs from a structured crystalline or semi-crystalline state to a disordered solid amorphous state. While commonly referred to as T_m , the specific characteristic is more accurately

known as the crystalline melting temperature. Crystalline melting is only observed in thermoplastics, as thermosetting polymers break down at high temperatures instead of undergoing a melting process. Polymers can undergo the process of spinning to form fibres while they are in a liquid state[19].

The two characteristics defining the glass transition are the absence of latent heat and a particular temperature at which liquid/rubbery-like and solid/glassy-like phases coexist. The kinetic, thermodynamic, entropic, and free-volume theories are among the many hypotheses that attempt to explain the glass transition phenomenon. The kinetics of the glass-making process and measurements of thermodynamic quantities such as entropy, volume, and enthalpy serve as the foundation for these theories. The glass transition is a second-order phase transition according to thermodynamic or entropic theories. Figure 1.10 shows how a material's enthalpy changes with temperature in the glassy and rubbery-like phases. The values for the thermal expansion coefficient and heat capacity show changes [20–23]. This finding suggests that the change in heat capacity is a hallmark of the glass transition. Inducing a condition, such as an increase in temperature or moisture level, that results in the system temperature above T_g leads to the system transitioning from a glassy to a rubbery state. T_g expands the available space, enabling more freedom of movement for molecules in both rotational and translational motion. Since viscosity and volume expansion in polymer systems depend on the system's free volume, kinetic models have been developed to explain the glass transition. The foci of the kinetic theory of the glass transition are how the transition evolves through time and how molecules unwind within the temperature window when it occurs [24].

Molecular symmetry significantly impacts the melting characteristics and solubility of organic molecules. The solubility and melting point of crystalline compounds with symmetrical structures are generally lower than those of molecules with less symmetry, although they share similar structures. Symmetry in a molecule increases residual entropy while the molecule is in the solid phase. It means that a crystal of symmetric molecules has a higher entropy than a crystal of a similar but non-symmetric molecule [25]. Furthermore, temperature affects the enthalpy of various material states, as shown in Fig. 1.10.

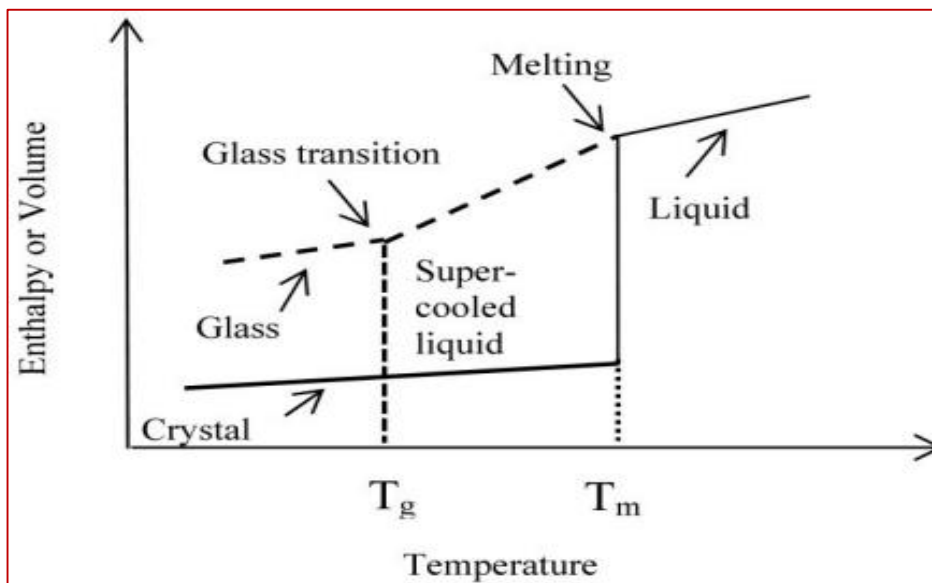


Figure 1.10 Volume or enthalpy of different material states as a function of temperature [26].

When there is no long-range ordering among the chains in the bulk polymer, it forms an amorphous solid. The glass transition temperature (T_g) indicates when the polymer hardens into an amorphous solid. During crystallization, shorter chains are more likely than longer molecules to self-assemble into crystalline structures.. As a result, the degree of polymerization (DP) plays a crucial role in defining the crystallinity of a polymer. Low-molecular-weight polymers (short chains) have lower strength. Despite the lattice's crystal composition, weak Van der Waals forces are primarily responsible for maintaining its cohesion. The phenomenon induces the displacement of the crystalline layers, resulting in the formation of a fracture inside the substance.

Due to their tangling tendency, polymers with a high DP have trouble organising into layers. However, high DP (amorphous) polymers are more robust because the molecules intertwine between layers. Polymers typically incorporate crystalline and amorphous structures to produce a material that possesses strength and stiffness. Under conditions when the polymer's temperature drops below its glass transition temperature (T_g), it gradually becomes more prone to breaking, and when the temperature exceeds T_g , the

polymer becomes more elastic. When heated beyond its glass transition temperature (T_g), the polymer takes on a rubbery texture. Consequently, knowing T_g is essential when choosing materials for various applications. Elastomers have T_g values significantly below room temperature, whereas rugged, structural polymers have T_g values above room temperature. This behaviour can be explained by looking at the structure of glassy materials, which often include components like lengthy chains, networks of linked atoms, or complicated chemical structures. Usually, such materials have a high viscosity in liquid form. Polymer structure and morphology can be adjusted using various processing techniques and pre- and post-treatment options. It has been shown that polymers that can crystallise when they come together from their molecular complexes have semicrystalline properties that are different from samples that concentrate from completely disordered melts or liquids [26–28]. Another essential attribute of polymers, which is strongly reliant on polymer morphology and temperature, is their response to force, which can be classified into two types: elastic and plastic. Tensile strength is an essential attribute of polymers formed by stretching polymer films. Fibers, for instance, must have good tensile strength.

1.1.1.5 Classes of Polymers

There are three major polymer classes:

i. Thermoplastic polymers:

In thermoplastics, intermolecular bonding rather than covalent bonds holds the molecules together. Molecules in a thermoplastic have strong intramolecular bonds but modest intermolecular forces. The chains may be straight or branched. Their semi-crystalline or amorphous form allows them to be moulded by applying heat and pressure. They can be heated, loosened, and moulded several times. These materials include polycarbonate, nylons, polysulfone, polyamide-imides, polyether ether ketone, polypropylene, polystyrene, and polyethene.

ii. Thermosetting polymers:

Thermosets, conversely, have several covalent links between their chains, resulting in a three-dimensional structure that can be viewed as a single molecule. Thermosets possess

cross-linked or network structures that establish covalent bonds with every molecule. When heated, they undergo decomposition rather than softening. They can be moulded using heat and pressure, but they cannot be remoulded once formed. Examples include epoxies, phenolics, ureas, melamine, silicone, and polyimides.

iii. Elastomers:

Elastomers or rubbery materials have very weak intermolecular forces and consist of a loose cross-linked structure. Elastomers are a wide variety of materials. These include natural, synthetic polyisoprene, rubber, chloroprene, polybutadiene, butyl, silicone, ethylene propylene, thermoplastic, polysulfide, fluoroelastomers, and more.

1.1.2 Composites:

Composites are materials with very varied chemical or physical characteristics combined from two or more different types of materials. When these elements are combined, a substance with properties different from those of its constituent parts forms; some may favour the new material over the old for different reasons. Some examples are more cost-effective, lighter, or longer-lasting materials than conventional options. Composites can be categorised into three distinct categories based on the matrix phase [29]:

(i) Metal matrix composites (MMCs):

Composites containing at least two components, at least one of which is a metal, are called metal matrix composites. The second part could be an organic molecule, ceramic, or metal. An item is referred to as a hybrid composite when it has at least three different types of materials. This process involves distributing a reinforcing material into a metal matrix to produce MMCs. One option for preventing a chemical reaction with the matrix is to apply a coating to the surface of the reinforcement. As an illustration, carbon fibres are frequently utilized in aluminium matrices to produce composites that exhibit low density and high strength throughout manufacturing [30].

(ii) Ceramic matrix composites (CMCs):

CMCs represent a subset of both composite and ceramic materials. They are composed of an embedded matrix of ceramic filaments. Since carbon and carbon fibres are ceramic

substances, they can be incorporated into the matrix and fibres. The development of CMCs was driven by the desire to address the drawbacks of traditional technical ceramics such as zirconia, alumina, silicon carbide, aluminium nitride, and silicon nitride, which fractured quickly when subjected to thermo-mechanical or mechanical loads due to the initiation of cracks by minute defects or scratches [31].

(iii) Polymer matrix composites (PMCs):

PMCs are composite materials composed of polymers as at least one component. A composite is fundamentally composed of reinforcing material encased in matrix material. The synthesis of polymer-matrix composites involves the combination of inorganic filler materials with polymers. These filler materials may comprise particulate solids, carbon black, silica, glass, aramid, or reinforcement fibres. PMCs provide wide range of application and improved properties as compared to MMCs and CMCs.

The application predetermines the design of the suitable composite system. These composites demonstrate physical properties synergistically derived from their organic and inorganic components. For instance, they retain their process ability while exhibiting superior mechanical properties and a higher heat deflection temperature than pure polymers [32]. Extremely popular are polymer composites owing to their low cost and straightforward fabrication processes. By incorporating diverse inorganic additives into polymers, it is possible to modify their electrical, mechanical, and other operational characteristics [33]. The degree to which these properties alter depends on the filler's characteristics, composition, morphology, and concentration.

Additionally, co-monomers such as isophthalate, phthalate, or naphthalate have been incorporated into polymer composites to reduce permeability progressively [34]. A new class of polymer composites has also been prepared by using treated polymers as filler. The dissolved granules of PET in a solvent and precipitated the solution in an antisolvent to obtain precipitated PET (p-PET). They also prepared composites using this 5% p-PET (weight basis relative to PET) [35]. The results showed that p-PET can be used effectively in small amounts to control the bulk semicrystalline morphology of melt-processed PET as an agent that creates itself. The nucleated polymer could be used for

various applications in textiles and food packaging, with a significant advantage over those obtained with normal received PET. They also prepared composites using this 5% p-PET (weight basis relative to PET) [36]. They found that p-PET could be used in small amounts to control the bulk semicrystalline shape of PET that had been melted down and used as a substance to make nuclei.

(iv) Polymer nanocomposites:

The fabrication process of polymer nanocomposites involves the dispersion of fillers into the polymer matrices, with each filler having a minimum dimension of one nanometre [18]. The proliferation of national programs devoted to nanoscience and nanotechnology has spurred numerous endeavours toward polymer nanocomposites' development and comprehension. With its unique and unconventional properties, it has the potential to redefine the methods used to develop high-performance structures and processes that are lighter, stronger, and more efficient. Over the past decade, nanocomposite materials have gained scientific, industrial, and academic attention due to their enhanced properties, improved performance, and reduced costs. These materials are composed of polymeric matrix materials and nanofillers/nanoparticles. Critical attributes of organo-inorganic nanocomposites [37, 38] include strength, stiffness, and durability enhancements. Polymer nanocomposites consist of thermoplastics, thermosets, or elastomers that have undergone reinforcing with nanoparticles in minute quantities. Making nanocomposites by adding carbon nanotubes, nanoparticles, or intercalated layers to thermoplastics or thermoset supports is an exciting and active area of research. In the realm of polymer/layered nanocomposites, three distinct varieties stand out: (i) nanocomposites that are intercalated, (ii) nanocomposites that form flocculation, and (iii) nanocomposites that peel off [20, 21].

For enhancing polymer composites' mechanical and physical properties, nanoparticles are currently regarded as infill materials with great potential [23]. Now, a substantial amount of research and investigation is being devoted to the development of nanocomposites with additives of various kinds. Nanoscale fillers are usually free of flaws, so they can be used in the polymer composite area setup field. It means that new trends can go beyond the limits of microscale fillers. It would be possible to manipulate

the mechanical, electrical, magnetic, and other properties of hybrid nanomaterials manufactured by incorporating inorganic nanoparticles into polymers and adjusting their concentration, size, and composition. Among the several nanofillers used in nanocomposite production, those with a larger aspect ratio, the ratio of the biggest to the smallest dimension, offer better reinforcement. Integrating nanofillers into nanocomposite development typically occurs on a weight basis [24–27]. Clay and carbon nanotubes (CNT) are examples of these nanofillers [36].

As depicted in Figure 1.11 [22], three distinct varieties of nanoparticles are typically employed to fabricate polymer nanocomposites. The structure of the first form of nanoparticles resembles that of platelets and has a single dimension on the nanometer scale. Larval dimensions can vary from a few hundred nanometers to microns, whereas thickness is typically limited to a few nanometers. Layered nanographites and clay serve as notable illustrations of this category of nanoparticles. Two dimensions of the second form of nanoparticles are measured in nanometers, whereas the third is significantly larger.

Consequently, these particles possess an elongated morphology. Nanofibers and nanotubes are members of this category. The dimensions of the third category of nanoparticles are all measured in nanometers. Spherical silica particles, gold nanocrystals, and additional metal nanoparticles are all excellent examples of these nanoparticles. Using fibre-based polymer nanocomposites in technological applications is experiencing significant growth and expansion across various global markets. Different textile materials find integration into automotive systems, serving multiple functions in critical domains such as lightweight construction, comfort, and safety.

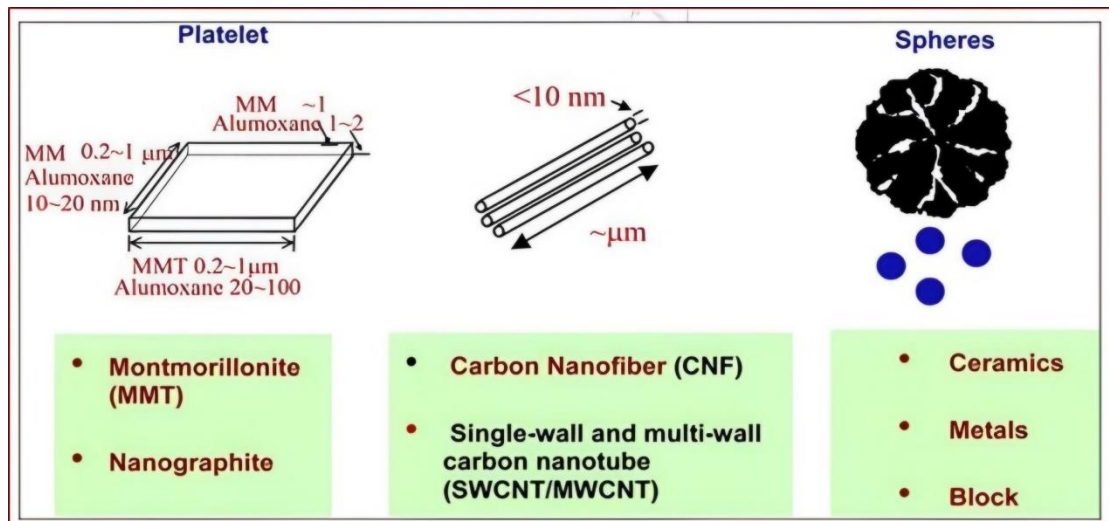


Figure 1.11 Different types of nanoparticles [22]

1.1.3 Process for the Preparation of Nanocomposites

Generally, three techniques exist for producing polymer nanocomposites. Solvent blending, melt blending, and in-situ polymerization are these processes. Each method has merits and demerits, in addition to specific limitations concerning the development of polymer composites and the uniform distribution of nanotubes within a polymer matrix.

As mentioned above, a well-dispersed system is generally required for each of the fabrications. Ultrasonication is one of the methods that is extensively operational. Ultrasonication generates localized shear rate packets encircling the nanotube bundle. Nevertheless, this approach is exclusively viable for matrix materials with exceedingly low viscosity and small volumes, as ultrasonic devices generate negligible shear forces despite their high energy impact. In addition, the dispersion is limited because introducing energy locally breaks and damages the CNTs, which lowers the overall aspect ratio [39]. Carbon nanotubes (CNTs) must be dissolved in a suitable solvent (like chloroform, toluene, etc.) for the sonication method to work well. It makes it easier to separate agglomerates using vibrational energy. Following this, the suspension and polymer can be combined while the solvent is evaporated. Each method is succinctly discussed:

1.1.3.1 Solvent Blending:

During solvent blending, the polymers are dissolved in a co-solvent and processed to create the final product. Afterwards, the solvent is allowed to evaporate. There are different methods to use solutions of polymers, such as electrospinning, wet or dry spinning, rolling into films, and undergoing articulating techniques to produce particles with different diameters (for example, spray-drying, emulsion-diffusion-evaporation, and emulsion-diffusion-evaporation). Compression molding is unsuitable for solution blending due to the solvated state of the polymers and the high concentration of solvent [40]. Subsequently, nanoparticles are incorporated into the polymer solution, a process commonly carried out using ultra sonication. Improving the interactions between the solvent and the nanotubes is possible by lowering the Vander Waals force between them. It makes it easier for polymer chains to move into the spaces between the nanotubes. One notable benefit of this approach is its ability to disperse carbon nanotubes (CNTs) within polymer matrices while preserving the aspect ratio of the initial nanotubes. Furthermore, the orientation of the anisotropic nanotubes can be achieved by applying an electric or magnetic field. However, a significant drawback of this approach is the substantial quantity of solvent required, leading to increased purification expenses.

1.1.3.2 Melt Blending:

The melt blending procedure shown in figure 1.12, entails the direct merging of molten polymers and nanoparticles. Mixing may take place statistically or as a result of excessive shear. This method is currently the most prevalent approach for synthesising polymer composites and can be used to manufacture them on a large scale. A single-screw or twin-screw extruder is the most frequently used apparatus when combining particles and polymers. It has been observed that the residence time and fastener design impact the nanopillars' dispersion. Poor blending, on the other hand, results from back mixing or excessive shear intensity. This phenomenon is currently obscure. The intricacy of the process exacerbates the difficulties associated with investigating the impact of process conditions on nanocomposites' formation. Although the ease of use related to melting blending as a method for synthesising nanocomposites is not advantageous, this technique does manage to attain a dispersion of particles on the

nanoscale for composite components made up of a substantial volume of nano-elements and high-molecular-weight polymers [41].

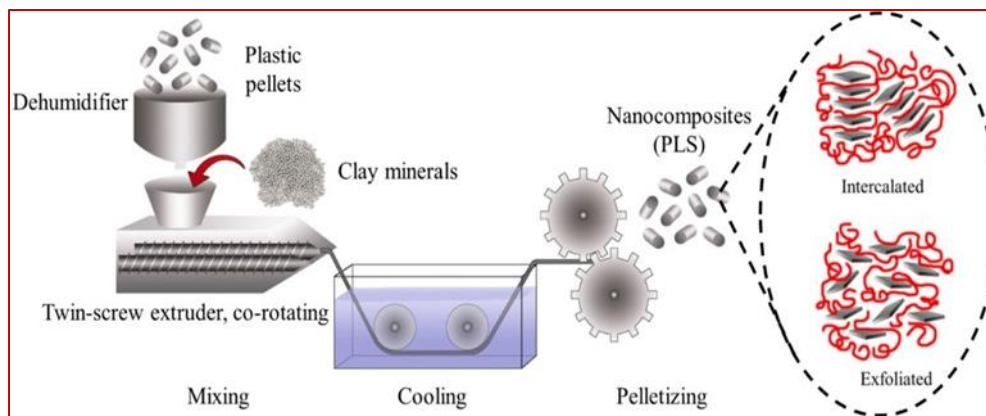


Figure 1.12 Polymer nanocomposites made via melt blending, depicted schematically [41]

1.1.3.3 In-situ polymerization:

In situ, PNC synthesis involves multiple processes. The nanomaterial is synthesised with polymer initially. Figure 1.13 shows the polymerization of monomers with the produced nanomaterial to synthesise the PNC. Polymer and nanomaterial synthesis is the third phase. In situ, PNC synthesis increases compatibility and surface contact by uniformly dispersing nanofillers throughout the polymer matrix [42,43]. The monomer has a low viscosity compared to polymer melt or polymer solution. This makes breaking up the clumped particles easy using sonication or high-shear mixing. Additionally, the diffusion of monomers into the nanoparticles leads to the growth of the polymer chains, which in turn causes the expansion of the inter-particle space. Furthermore, appropriately adjusting the surface chemistry allows for the generation of polymer chains straight from the nanoparticles' surfaces. As a consequence, particle dispersion and interfacial contact with the polymer are greatly enhanced. The method mentioned above is of the utmost importance when handling thermally unstable or insoluble polymers beyond the capabilities of solution or melt processing. It makes these polymers ready for use. Some polymerizations that can be used for in-situ polymerization processing are radical, cationic, ring-opening, and chain transfer. The molecular weight

distribution of the target polymers determines the best polymerization technique to use [44].

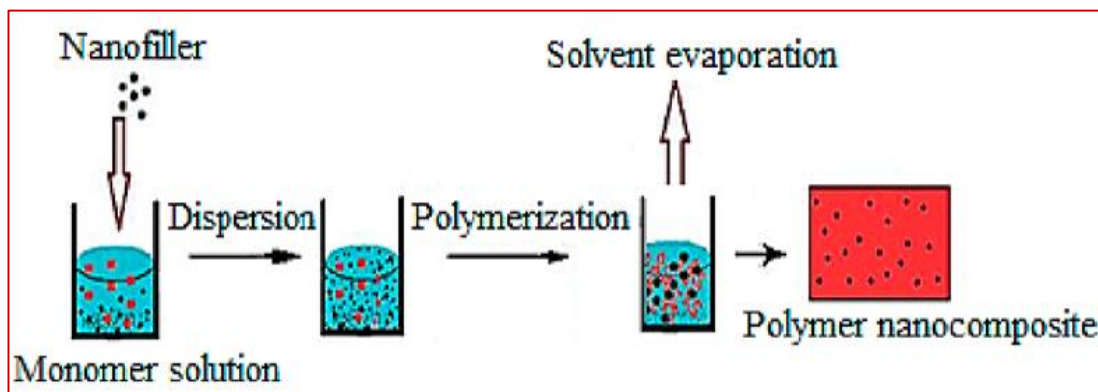


Figure 1.13. Block diagram depicting the in situ polymerization process [43]

1.1.3.4 Solution Mixing

Figure 1.14 shows the process of solution mixing for PNCs evaporating the solvent [45]. The nanoparticles are sonicated into the solution after the polymer has been dissolved in a volatile solvent. PNCs are formed when a solvent is rapidly evaporated [46]. A simple design and few chemicals are needed for the solution mixing procedure [47]. PNCs are created quickly and without additional energy. Many studies have prepared PNCs by solution mixing.. Increased antibacterial activity was shown against *S. aureus* and *E. coli* in starch nanocomposite films with clay nanolayers made by solution mixing [48]. TiO₂ nanoparticles and Ct were generated through solution mixing. This preparation is explained by the point of zero charge (PZC) pH, which is reached when the total of all surface charges, positive and negative, are equal. Positively charged TiO₂ nanoparticles are created by the solution's pH below PZC. When the solution pH exceeds PZC, the surface becomes negatively charged. The electrostatic interaction between the charged surfaces of the nanoparticles and the Ct chains causes the flexible Ct chains to fully stretch and disperse the nanoparticles into the Ct matrix in solutions with a pH lower than the pH at PZC of TiO₂ nanoparticles and the pK_a of Ct [49].

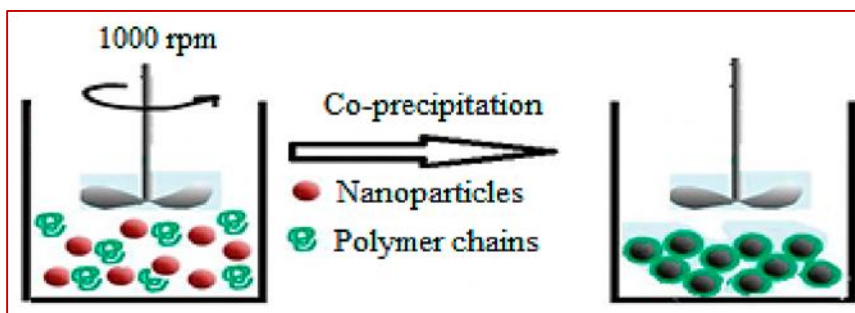


Figure 1.14. Schematic illustration for the solution mixing method (taken from [45]).

1.1.3.5 Electrospinning

The process of electrospinning has proven effective in creating nanofibers. Many variables, including flow velocity, polymer concentration, liquid viscosity, air humidity, and electric field strength, can affect the electrospinning process [50]. Figure 1.15 depicts the electrospinning device. A polymer matrix is enhanced by adding nanomaterials such as clay nanolayers, carbon-based nanomaterials, metal oxide nanoparticles, and metallic nanoparticles to do this. Electrospinning is a flexible method employed in the synthesis of PNCs [51, 52]. For instance, cellulose and organically modified montomotrille electro spun nanofiber mats have been utilised to successfully remove Cr^{6+} ions from aqueous solutions [53]. Multi-walled carbon nanotube (Ct) nanocomposite fibres have been prepared via electrospinning [54]. Electrospinning was also used to create PHBV nanocomposite fibres containing multi-walled carbon nanotubes. In order to coordinate the nanomaterial with the electrospun fibres and stretch it, the rotating disc collector is used [55-57]. Moreover, a cellulose/multi-walled carbon nanotubes nanocomposite was generated by electrospinning at 27 C with a relative humidity of 34% and a DC voltage of 14.25 kV using a horizontally positioned metal needle [56].

Several extrusion or compounding procedures, such as in-situ polymerization, melt blending, and solution mixing, are popular ways of creating polymeric nanocomposites. The choice of nanofiller and processing method depends on the desired properties and the compatibility of the polymer with the nanofiller.

to scratches, are advantageous for applications where surface quality is critical. Nanocomposites can decrease the permeability of gases and liquids in packaging materials, enhancing product protection and extending the expiration life.

The enhanced qualities of these materials can benefit the aerospace, automotive, electronics, packaging, and construction industries, allowing for higher performance and more efficient products. However, it's important to note that the dispersion of nanofillers within the polymer matrix and their interactions with the polymer are critical factors in achieving the desired properties of polymeric nanocomposites.

1.1.4 Factors Affecting Properties of Polymer Nanocomposites

1.1.4.1 Properties of the Matrix

An application's suitability is evaluated based on the characteristics displayed by different polymers. The primary benefits of polymers as matrices are their low specific gravity, exceptional chemical resistance, and straightforward processing. However, their modulus, tensile strength, and operating conditions determine their applications [58].

1.1.4.2 Particle, flakes, fibre, and laminate shape and orientation of dispersed phase inclusions

Although they can improve or decrease the price of isotropic materials, particles do not have any optimal orientations [59]. Reinforcing particles can have any number of geometric shapes, including spherical, cubic, platelet, regular, or irregular. Particle reinforcements are nearly homogenous in size across all directions. There are two subclasses of particle-reinforced composites: dispersion-strengthened and big particle-reinforced composites. Laminar composites are composed of two-dimensional panels or sheets that, like wood, have a specific direction of maximum strength. Stacking and cementitiously adhering the layers together alters the direction of high strength with each succeeding stratum [60].

1.1.4.3 Interfacial Adhesion

The behaviour of composite material can be understood by looking at how the fiber/matrix interface, the reinforcing element, and the polymer matrix all work together shown in Figure 1.16. For superior mechanical properties to be achieved, interfacial adhesion must be robust. The chemical reaction or adsorption by which matrix molecules become anchored to the fiber surface determines the degree of interfacial adhesion. The advanced technological developments in instrumentation and characterization have facilitated the investigation of the interface in more detailed manner [61].

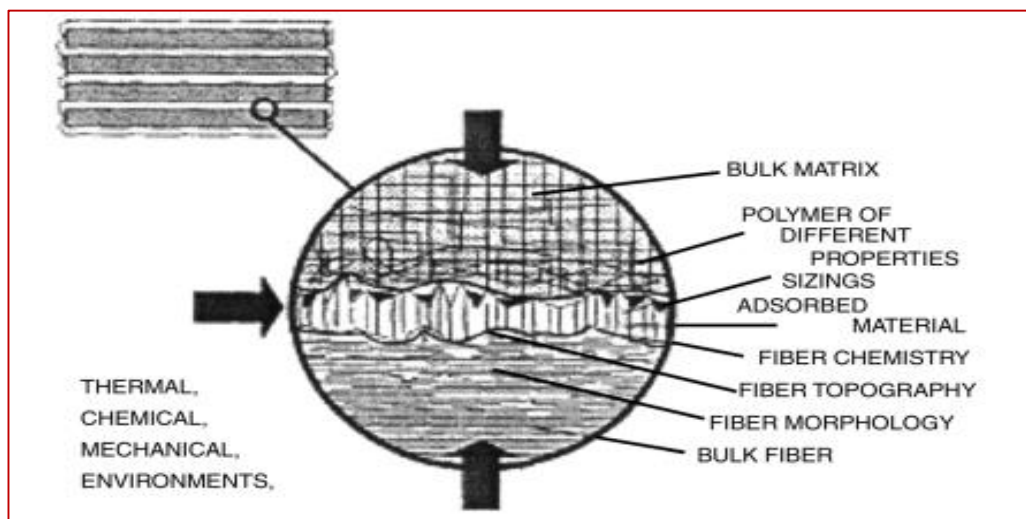


Figure 1.16 Schematic model of interphase[61]

1.1.5 Characterization of Polymer Nanocomposites

Characterizing the interface provides pertinent insights into the dynamics between the matrix and fiber. The stability of the interfacial area dictates the mechanical properties of composites reinforced with fibres. Therefore, the characterization of the interface is critical. The following are the diverse methodologies that can be employed to characterize the interface [62].

1.1.5.1 Spectroscopic Tests

Analytical methods may incorporate spectroscopic testing into their procedures to investigate the relationship between matter and electromagnetic radiation.. These tests

provide valuable information about the composition, structure, and properties of materials. Here are some common types of spectroscopic tests:

Fourier Transform Infrared Spectroscopy: Fourier transform infrared spectroscopy can be employed to better understand the chemical makeup and bonding interactions of polymer nanocomposites. It can provide information about functional groups present in both the polymer matrix and the nanofillers, as well as any chemical changes occurring upon the incorporation of nanofillers.

Raman Spectroscopy: Raman spectroscopy is valuable for studying the molecular structure and vibrational modes of polymer nanocomposites. It can identify different phases within the nanocomposite, detect chemical changes, and assess the dispersion of nanofillers in the polymer matrix.

UV-Vis Spectroscopy (Ultraviolet-Visible Spectroscopy): UV-Vis spectroscopy is used to investigate the optical properties of polymer nanocomposites, including absorption and transmission characteristics. It can provide insights into the dispersion and aggregation of nanofillers, as well as the influence of nanofillers on the optical behaviour of the nanocomposite. **Nuclear Magnetic Resonance Spectroscopy:** NMR spectroscopy is particularly useful for studying the dynamics and mobility of polymer chains in nanocomposites. It can provide information about the polymer chain conformation, segmental mobility, and interactions between the polymer matrix and nanofillers.

X-ray Photoelectron Spectroscopy (XPS): XPS can be used to study the elemental makeup and surface chemistry of polymer nanocomposites. It can evaluate the interactions between the polymer matrix and nanofillers at the interface and detect changes in their chemical environments.

Transmission Electron Microscopy (TEM): Although not strictly a spectroscopic technique, TEM is often used in conjunction with spectroscopy to characterize the morphology and dispersion of nanofillers within the polymer matrix. TEM can provide direct visualization of the nanoscale structure and distribution of nanofillers, complementing spectroscopic analysis.

1.1.5.2 Micromechanical Technique

The micromechanical technique is a valuable method for characterizing the mechanical properties of polymer nanocomposites at the microscale. This technique involves

manipulating and analyzing individual constituents within the nanocomposite material to understand their contributions to the overall mechanical behavior. Here's an overview of the micromechanical technique applied to polymer nanocomposites:

Micro indentation: Applying a controlled load or force to a material's surface using a sharp indenter, usually with a diameter in the micrometre range, is called micro indentation. The polymer nanocomposite's mechanical properties, including modulus and hardness, can be ascertained by observing the indentation depth and load. This technique can reveal information about the reinforcement effect of nanofillers on the polymer matrix.

Atomic Force Microscopy (AFM): AFM is a multipurpose instrument for characterising nanoscale mechanical properties and surface topography. When studying polymer nanocomposites, AFM can be employed to examine the interfaces, nanofillers, and individual polymer chains for their mechanical properties at the local level. It can also provide insights into the distribution and alignment of nanofillers within the polymer matrix.

Nano indentation: Nanoindentation is similar to microindentation but operates at even smaller length scales, typically in the nanometer range. It allows for precise measurements of mechanical properties such as hardness, modulus, and elastic/plastic deformation behavior at the nanoscale. Nanoindentation can be used to assess the nanofiller-matrix interactions and quantify the reinforcement effect of nanofillers in polymer nanocomposites.

Micropillar Compression: Micropillar compression involves fabricating miniature pillars from the polymer nanocomposite material and subjecting them to compressive loading using a micromanipulator or nanoindenter. By measuring the deformation response of the micropillars, it is possible to extract mechanical properties such as yield strength, strain hardening, and deformation mechanisms at the microscale. This technique provides insights into the strength and toughness of the nanocomposite material.

Microtensile Testing: Microtensile testing involves fabricating microscale specimens from the polymer nanocomposite material and subjecting them to tensile loading using specialized microscale testing equipment. Microscale specimens' stress-strain responses allow determining mechanical parameters like modulus, elongation at break, and tensile

strength. Microtensile testing allows for the evaluation of the nanofiller-induced enhancements in mechanical properties and the influence of processing conditions on the nanocomposite performance.

1.1.5.3 Microscopic Techniques

Microscopic techniques play a crucial role in the characterization and analysis of materials at the micro- and nanoscale. These techniques offer essential information about the morphology, structure, composition, and properties of many materials, such as polymers, nanomaterials, and biological specimens. Here are some commonly used microscopic techniques:

Optical Microscopy: Optical microscopy utilizes visible light to view and amplify specimens. It provides low to moderate magnification (up to about 1000x) and is widely used for routine inspection and analysis of biological samples, materials, and surfaces. Bright-field, dark-field, phase-contrast, and fluorescence microscopy are methods that increase contrast and illuminate particular characteristics of the sample.

Scanning Electron Microscopy (SEM): SEM scans the surface of a specimen using a concentrated beam of electrons. Surface topography, morphology, and elemental composition can be examined in detail using high-resolution photographs obtained at magnifications ranging from 10x to 100,000x. Metals, ceramics, semiconductors, and biological samples are some of the materials that lend themselves well to scanning electron microscopy (SEM).

Transmission Electron Microscopy (TEM): TEM is a technique that uses a stream of electrons to make high-resolution images by passing them through a fragile specimen. It provides atomic-scale resolution and is used to study the internal structure, crystallography, defects, and interfaces of materials. TEM is indispensable for investigating nanomaterials, nanoparticles, polymers, biological specimens, and semiconductor devices.

Atomic Force Microscopy (AFM): AFM measures the forces that are applied to the surface of a specimen during the scanning motion of a sharp tip. It provides topographic images with nanometer-scale resolution, as well as information about surface roughness, mechanical properties, and molecular interactions. AFM is widely used in nanotechnology, materials science, and biology for imaging and characterization of surfaces and nanostructures.

Confocal Laser Scanning Microscopy (CLSM): CLSM utilizes a laser beam to scan successive optical sections of a specimen at different depths. It provides three-dimensional images with high spatial resolution and optical sectioning capabilities. CLSM is valuable for studying the three-dimensional structure and distribution of fluorescently labeled molecules, cells, and tissues in biological samples.

Scanning Probe Microscopy: Scanning probe microscopy (SPM) comprise selected methods for examining the molecular or atomic surface characteristics of substances. Examples of such methods include atomic force microscopy (AFM) and scanning tunnelling microscopy (STM). These techniques enable imaging, manipulation, and characterization of surfaces with unprecedented resolution and precision, making them indispensable tools for nanoscience and nanotechnology research.

X-ray Microscopy: X-ray microscopy utilizes X-rays to image samples with high resolution and contrast, allowing for the visualization of internal structures and elemental composition. Differential three-dimensional imaging and elemental mapping of materials are accomplished using techniques like X-ray fluorescence microscopy (XRF) and X-ray microtomography (micro-CT).

1.1.5.4 Thermodynamic Methods.

Thermodynamic methods are analytical approaches used to study and analyze the thermodynamic properties of materials, chemical reactions, and processes. These methods provide insights into the energy changes, equilibrium conditions, and spontaneity of reactions based on the laws of thermodynamics. Here are some common thermodynamic methods:

Calorimetry: Calorimetry is the practice of quantifying the heat changes that occur during reactions involving chemicals or physical operations. Differential scanning calorimetry (DSC) and isothermal titration calorimetry (ITC) are two well-known methods. Differential scanning calorimetry (DSC), which monitors heat flow vs temperature, can learn phase transitions, enthalpy changes, and heat capacity. Using ITC, one can determine changes in thermodynamic parameters such as enthalpy, entropy, and Gibbs free energy by monitoring the rate of heat change during titration.

Thermogravimetric Analysis (TGA): TGA is a controlled-environment method for determining how much a sample's weight varies over time or as a function of temperature. It is used to study decomposition, oxidation, and stability of materials by monitoring mass loss or gain. TGA can provide information about decomposition kinetics, activation energies, and thermal stability of materials.

Phase Diagram Analysis: Phase diagrams depict the thermodynamic phases and equilibrium conditions of a system as a function of temperature, pressure, and composition. Constructing and analyzing phase diagrams provide insights into phase transitions, phase equilibria, and phase stability of materials. When studying phase transitions, combining phase diagram analysis with other techniques, such as differential scanning calorimetry (DSC) and differential thermal analysis (DTA), is standard practice.

Equilibrium Thermodynamics: Equilibrium thermodynamics deals with the study of thermodynamic properties at equilibrium states. It includes the analysis of equilibrium constants, chemical potential, Gibbs free energy, and entropy changes for chemical reactions and phase transitions. Thermodynamic modeling and simulations, such as using the Gibbs-Duhem equation or activity coefficient models, are employed to predict and interpret experimental data.

Statistical Thermodynamics: Statistical thermodynamics provides a microscopic interpretation of thermodynamic properties based on the statistical behavior of atoms and molecules. It involves concepts such as partition functions, Boltzmann distribution, and ensemble theory to describe the thermodynamic properties of systems at the molecular level. Statistical thermodynamics is particularly useful for understanding phenomena such as entropy, heat capacity, and molecular interactions in gases, liquids, and solids.

Non-equilibrium Thermodynamics: Non-equilibrium thermodynamics deals with systems that are not in thermodynamic equilibrium, such as processes involving heat transfer, mass transfer, and chemical reactions. It includes the analysis of kinetic processes, transport phenomena, and irreversible thermodynamic processes. Non-equilibrium thermodynamics provides insights into the behavior of systems far from equilibrium and is essential for understanding phenomena such as phase transformations, diffusion, and reaction kinetics.

1.1.6 Carbon Nanotubes

Carbon nanotubes (CNT) based materials have emerged as an active and rapidly advancing area of research. The large surface area, high modulus and high conductivity of CNT make them efficient fillers for engineering polymer. The material properties of carbon nanotube-incorporated polymer composites are enhanced, as usual mechanical strength, electrical conductivity, and electromagnetic shielding [28-33]. In hollow tubes, CNTs are rolled using single or multiple layers of graphite. These cylinders, which have diameters as tiny as 0.7 nanometers and lengths in the tens of microns, are sealed at both extremities with caps resembling fullerene. These structures generally comprise two end caps and a benzene ring side wall; the end caps resemble fullerenes.

1.1.6.1 Types of Carbon Nanotubes

SWCNTs refer to carbon nanotubes with a wall thickness equivalent to a single carbon sheet. The Vander Waals forces between nanotubes often cause large strands to form. These are ordered arrays of SWCNTs arranged in a triangular lattice. Carbon nanotubes with increasing diameters that include the coaxial array MWCNTs are composed of SWCNTs. MWCNTs are composed of SWCNTs as their building elements. Typically measuring several microns in length, MWCNTs have structures with extraordinarily high aspect ratios and an exterior diameter ranging from two to several tens of nanometers. Figure 1.17 shows two primary varieties of carbon nanotubes (CNTs): SWCNTs, or single-walled carbon nanotubes, and MWCNTs, or multi-walled carbon nanotubes [63].

(i) *Single-walled carbon nanotubes (SWCNT):*

An SWCNT can be imagined as a seamless cylinder made of long-wrapped graphene sheets formed by moulding a single layer of graphite, or graphene. The diameter of most SWCNTs is close to 1 nanometre. To be more precise, a SWCNT is divided into two distinct regions that possess unique physical and chemical characteristics. The initial component is the sidewall, while the subsequent component is the end cap. Production of SWCNTs is relatively inexpensive.

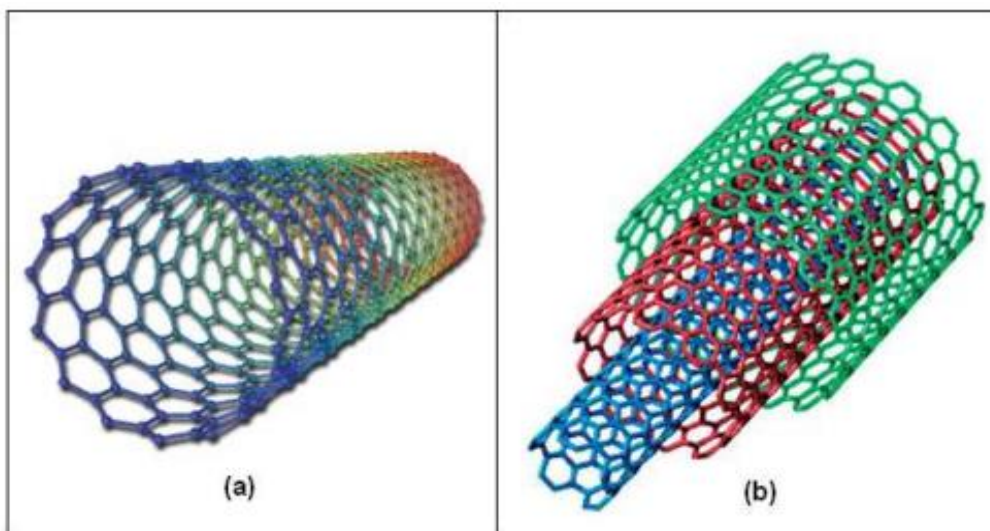


Figure 1.17 Types of Carbon Nanotubes: (a) SWCNT and (b) MWCNT[63].

(ii) *Multi-walled carbon nanotubes (MWCNT)*

"Multi-walled carbon nanotubes" (MWCNTs) refer to a group of carbon nanotubes with different wall thicknesses arranged in a tube shape. In addition to their length and diameter being significantly different from those of SWCNTs, these structures also possess distinct properties. Similar to the gap between graphite's graphene layers, the interlayer distance in MWCNTs is around 3.3 Å. In addition to MWCNTs, other manufactured carbon nanotubes with morphology and characteristics very similar to SWCNTs are double-walled carbon nanotubes (DWCNTs). There are two main reasons why MWCNTs are better than SWCNTs:

- (i) MWCNTs are less expensive than SWCNTs.
- (ii) MWCNTs are more chemical resistant than SMCNT.

This becomes crucial in cases where the CNT needs to be fictionalized to acquire new assets. Some C=C double bonds will be broken during the covalent functionalization of SWCNTs. It will create "holes" in the structure of the nanotube, which will change its electrical and mechanical properties.

1.1.6.2 *Structure of Carbon Nanotubes*

Crystalline carbon exists in its most stable form as graphite. Graphite is composed of carbon atoms piled in strata. Atoms are organized in the strata at the apex of hexagons

that envelop the entire plane. A robust covalent bond exists between the carbon atoms, with a carbon-carbon distance of approximately 0.14 nanometers. With an interlayer distance of ~ 0.34 nm and feeble long-range Van der Waals interactions, the layers are only loosely bound. Weak interlayer coupling imparts graphite with the appearance of an exceptionally flexible substance. Carbon nanotubes are conceptualized as graphene

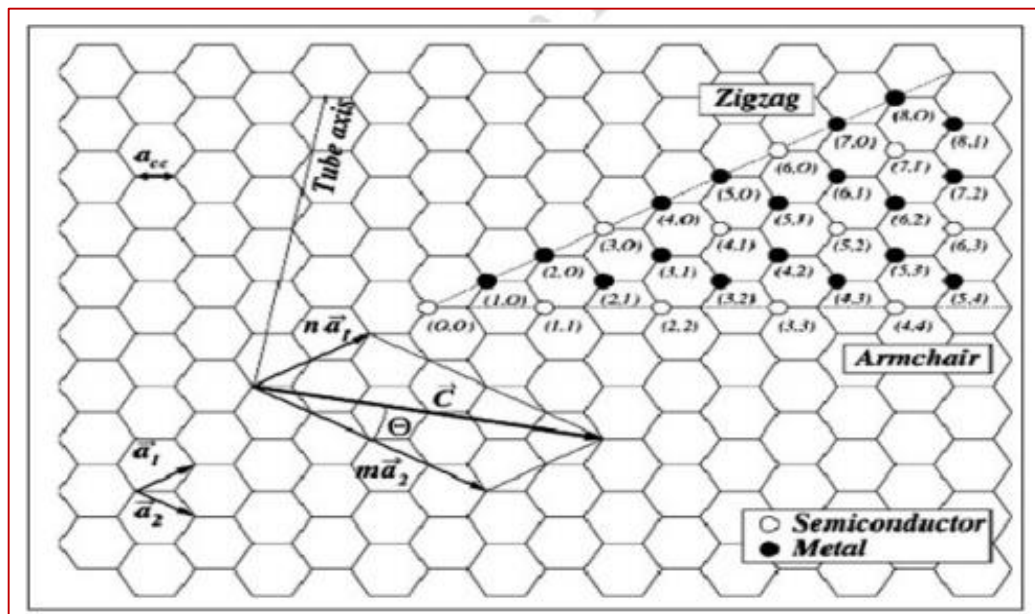


Figure 1.18 2D sheet of graphene diagram illustrating a vector structure categorization used to characterize the structure of CNT [64].

sheets that have been curved. A honeycomb lattice gives rise to graphene sheets, continuous cylinders of a single atomic layer of crystalline graphite. The orientation of the graphene sheet during rolling determines the type of CNT. The tube chirality delineates how graphene is rolled into tubes, which signifies the angle at which the graphene sheet's orientation concerns the tube's axis. The chiral vector, which denotes how the graphene sheet rolls, delineates this. As depicted in Figure 1.18, a CNT is formed by rolling a hexagonal graphite sheet according to a vector structure classification.

The vector (n, m) constitutes its determination. One of two selected atoms from a planar graphene sheet is designated as the origin. The chiral vector \vec{C} is defined as follows [65]: it is directed from the initial atom to the subsequent one.

$$\vec{C} = n\vec{a}_1 + m\vec{a}_2$$

The unit vectors \vec{a}_1 and \vec{a}_2 are the principal lattice vectors for the graphene sheet's honeycomb lattice, with integers n and m . The result is a type of nanotube known as a (n, m) nanotube. This chiral vector runs perpendicular to the CNT axis. The following equation can be used to determine the length of the chiral vector C , which stands for the circumference of the CNT:

$$c = |\vec{C}| = a\sqrt{n^2 + nm + m^2}$$

The value a represents the length of the unit cell vectors \vec{a}_1 and \vec{a}_2 .

The length of a carbon-carbon bond, denoted as a_{cc} , is related to this length in the following way:

$$a = |\vec{a}_1| = |\vec{a}_2| = a_{cc}\sqrt{3}$$

The relation that gives the diameter of the CNT using the circumferential length c is thus:

$$d = c/\pi$$

Here is a description of the chiral angle, which is created by the chiral vector and the nanotube's zigzag axis:

$$\theta = \tan^{-1} (m\sqrt{3} / (n + 2m))$$

The only variables that can be used to describe carbon nanotubes are the integers (n, m) and their relationship to the chiral vector. These data reveal three types of CNTs, as shown in Figure 1.18:

- (i) With a zigzag angle of 30° , $m = 0$;
- (ii) With a chair angle of 0° , $n = 1$;
- (iii) In this absence n , and m , are chiral tubes as $(0^\circ < \theta < 30^\circ)$ are used

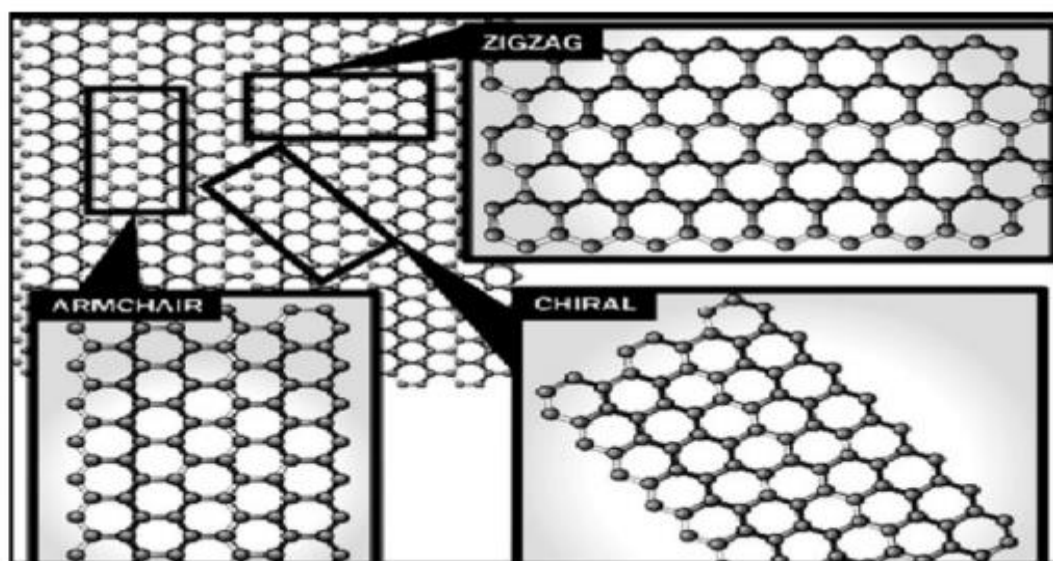


Figure 1.19 Diagram showing the process for producing various chirality configurations in CNTs [66].

The optical, mechanical, and electrical properties of the CNT are affected by the value of (n, m) , which in turn dictates its chirality [66]. The $(10, 10)$ tube is semiconducting, similar to CNTs with $|n - m| = 3j \pm 1$, and CNTs with $|n - m| = 3j$ are metallic, identical to CNTs with $|n - m| = 3j$, which are an integer [66]. The constructions of the armchair and the zigzag tubes are very symmetrical. These words refer to the arrangement of hexagons around a circle. Figure 1.19 shows three different ways to roll a graphene sheet into a tube, and Figure 1.20 shows the several structural variants of carbon nanotubes. The open ends of the tubes show the difference in construction.

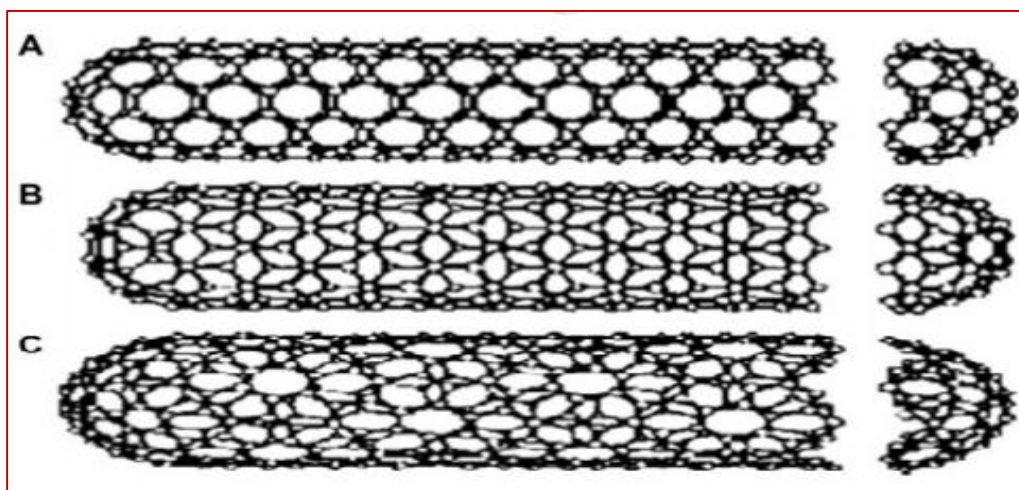


Figure 1.20 CNTs structure with different chiralities: (A) arm chair structure, (B) zig-zag structure, (C) chiral structure [67].

1.1.6.3 Properties of Carbon Nanotubes

CNTs have unique properties that depend on many things, such as how they were made, how much they are graphitized, whether they have defects, their chirality, diameter, degree of crystallinity, and entanglements. Due to the ternary coordination of every carbon atom within a nanotube, the nanotubes are conjugated aromatic systems. This structure features localized C-C σ -bonds formed by three of every four valence electrons in the carbon atom, which are part of the sp^2 hybrid orbitals. The delocalized π -system is formed with the help of the remaining electron. Due to the feeble bonds between these π -electrons and their atoms, they participate in charge transport. A high conductivity is observed in metals when no energy gap separates occupied π -states from vacant π -states. A carbon nanotube is classified as a semiconductor if the energy gap is relatively narrow and this condition is unmet. Conversely, the CNT functions as an insulator if the gap is wide. Because conduction occurs within the nanotube, CNTs serve as functional quantum conductors.

CNTs possess chemical bonds consisting exclusively of sp^2 pairs, which resemble the bonds found in graphite. This bonding arrangement, which is more robust than diamond sp^3 bonds, imparts the molecules' distinctive strength. Carbon nanotubes have the most excellent elastic modulus and tensile strength compared to all other materials. On top of that, they're the stiffest. The strand-like organisation of carbon nanotubes (CNTs) results

from Van der Waals forces. Pressure causes carbon nanotubes to connect, allowing for the substitution of sp^2 bonds for sp^3 bonds. High-pressure CNT connecting is an excellent method for creating long, robust conductors [69].

By making polymer nanocomposites, the exceptionally high electrical conductivity of CNTs has been used to make materials that are typically very insulating, like polymers, conduct electricity. Particularly noteworthy is that, depending on their structure, nanotubes may be metallic or semiconducting. Consequently, specific nanotubes exhibit conductivities surpassing those of copper, whereas others resemble silicon in behaviour. Considerable attention is being devoted to the feasibility of fabricating nanoscale electronic devices using nanotubes, and modest advancements are being achieved.

1.1.6.4 Carbon Nanotube-based Polymer Nanocomposites

Considerable research attention has been consistently drawn to the extraordinary properties of carbon nanotubes (CNTs), including but not limited to fire retardancy, high electrical conductivity, UV protection, enhanced garment comfort, high stiffness, and high strength when incorporated into polymeric nanocomposites. Various obstacles must be addressed to achieve optimal carbon nanotube-polymer nanocomposite performance. Consider this: purifying nanotubes involves a crucial process of eliminating metallic and amorphous carbon impurities without causing harm to the nanotubes [39]. How carbon nanotubes are spread throughout the polymer matrix significantly impacts the performance of the nanocomposite. Getting the best dispersion is a complex task that involves thorough research at various levels.

One of the primary techniques for creating CNT/polymer nanocomposites is by blending CNT and polymer in an appropriate solvent. Solution blending can disperse and de-aggregate nanotubes by thoroughly mixing them with polymers in a solvent. In this procedure, there are primarily three stages: Dispersing nanotubes in a solvent. They can be mixed with the polymer at room or higher temperatures. Casting a film or precipitating the nanocomposite to retrieve it.

Although solution processing is a highly effective method for dispersing nanotubes and forming nanocomposites, it needs to be better suited for processing on an industrial

scale. Melt processing is the method of choice for industrial applications due to its simplicity and low cost, which enable it to facilitate mass production for industrial or business purposes. Melt methods usually involves spreading nanofillers like CNTs using a lot of shear force and melting polymer granules to make a thick liquid.

Furthermore, in situ polymerization is a very effective method that makes it easier for carbon-based fillers to distribute evenly within the matrix. As a result, the filler and matrix are firmly bound together.

This method works well because it mixes additives with monomers or prepolymers in a solvent until a smooth mixture forms. Then, the temperature and time are controlled to complete polymerization [70]. This method permits the transplantation of polymer macromolecules onto the walls of CNTs, which is its primary benefit.

Furthermore, this processing method is efficient as it enables the fabrication of nanocomposites featuring a substantial concentration of nanotubes and exceptional miscibility with virtually every polymer matrix. The scope of in-situ polymerization reactions may be limited by the reaction medium's viscosity, which must be acknowledged as the polymerization process progresses. Fundamentally, in-situ polymerization can fabricate polymer nanocomposites comprising carbon nanotubes (CNTs) covalently or non-covalently bonded to the polymer matrix. There are n-n and Van der Waals forces that make the polymer and nanotube interact without being covalent. These forces cause the polymer molecules to stick to the nanotube and wrap around it physically.

1.1.7 General Background of Functionalization of CNT

To make composites using this CNT for some possible uses, you need a pure material chemically compatible with the graphitic network. [71]. In addition to varying in diameter and wall number, as-synthesized CNTs contain impurities such as amorphous carbon and metal catalyst particles [72]. Moreover, achieving robust interfacial bonding is essential for ensuring effective load transfer between the polymer and CNT interface. Yet, the powerful intrinsic Van der Waals forces among CNTs cause them to remain closely intertwined, making it challenging to achieve a consistent dispersion. In addition, the CNTs and polymer matrix cannot form an interfacial bond due to the

remarkably smooth and non-reactive surface. Several studies have shown that attaining optimal nanotube dispersion and enhancing bonding between nanotubes and polymer matrix is feasible with the right surface chemistry design.

To improve the efficiency and compatibility of CNTs, it is very important to remove impurities and modify its surface chemistry by functionalization. These surface modification techniques, often referred to as functionalization, plays an important role in facilitating the attachment of different functional groups such as silane, and others and bio-molecules such as proteins or DNA making its useful as functional materials and sensors [73]. Reports indicate that the end caps of nanotubes are more reactive than the sidewalls. There might be sp^3 -hybridized flaws, Stone-Wales flaws, or vacancies in the nanotube lattice on the sidewalls. This inherent flaw allows for the attachment of various chemical groups to the defect sites, which can then be used to customize the polymer/CNT interface. Furthermore, the delocalized ' π -electron cloud' can aid in the adsorption of various moieties onto the CNT surface.

The oxidative treatment of metal nanoparticles or carbonaceous impurities from nanotubes is an effective method [71–73]. Oxidation of nanotubes can be accomplished in two general ways: chemical treatment utilizing diverse mixtures of inorganic acids [74, 75] or subjecting them to air oxidation at elevated temperatures [76]. One significant drawback of oxidation is that many nanotubes are eradicated in addition to eliminating impurities. Furthermore, carboxylic functionalities are produced on the sidewalls and extremities. Numerous variables affect the efficacy and yield of the resulting pure material, including metal concentration, oxidation time, oxidizing agent, and temperature. In an inorganic acid solution, sonication can help remove metal impurities from a suspension of unprocessed carbon nanotubes [75]. The cutting that results from this treatment reduces SWCNTs to short "fullerene pipes." When the ends of pipelines are exposed, dangling bonds easily change into oxygenated functional groups, such as esters, quinones, carboxylic acids, and anhydrides. These functionalities are notably concentrated at defect locations along the sidewall of carbon nanotubes. Even with their exceptional characteristics, the utilization of CNTs remains severely limited due to their challenging dispersion and stabilization in common solvents.

1.2 Additive Manufacturing Process

Additive manufacturing is often considered a crucial component of this emerging

paradigm [77]. Industry 4.0 focuses on the digital manufacturing of personalized, precise, and valuable products. A high-speed additive manufacturing technology offers rapid and precise production with superior surface finish, and appropriate functional properties [78]. The Spartech analysis of Wohlers 2024 report indicated that the growth rate for various components of 3D printing, including materials, software, hardware, and services, have raised to 24.4% by the year 2024 (New report April 2024) [79]. AM allows design freedom, mass customization, waste reduction, complicated structures, and quick prototyping [80]. MWCNT-loaded samples have much higher mechanical strength than ABS-filled samples. The only way to improve mechanical strength is with MWCNTs and polymers to improve matrix/filler bonding [81]. In aviation industry, maintenance is a crucial aspect of guaranteeing flight safety in civil aviation. Due to increasing growth of civil aviation in China, the maintenance field within the civil aviation industry has garnered significant attention from industry stakeholders [82]. This technology has witnessed a notable rise in its application for mass customization and the fabrication of various open-source designs across several sectors, including agriculture, healthcare, the automobile, locomotive, and aviation industries [83]. The potential of AM processes, which revolutionized the production of optical equipment currently dependent on laborious and expensive polishing and grinding procedures, subject to significant interest and exploration. However, the inherent trade-off between speed and precision significantly restricts the practical applications of 3D printing technology in the optical domain [84]. In rapid prototyping (RP), fused deposition modelling (FDM) is also a rapidly developing technology [85]. The hollow-section products can be produced easily through AM technique. Proper robustness and freedom of shape can be ensured by for a 3D printed product [86, 87]. The particular collection of surface and dimensional flaws caused by FDM impedes quick tooling and casting. A larger framework includes multiple FDM part surface finishing methods [88]. Material reflow, which fills up porosity gaps and staircase effects within layers, produces a better surface quality and higher mechanical properties [89]. The significant capillary action of irregular grooves and cracks in BF improves mechanical characteristics by infiltrating the polymer into the fibre [90]. The size accuracy and compressive strength of FDM-made ABS specimens was studied. The number of shells, nozzle temperature, bed temperature, and layer height influenced dimensional accuracy, while printing speed

and nozzle temperature affected compressive strength. The horizontal specimen had higher compressive yield stresses and wider nozzle and bed temperature processing ranges than the vertical specimen. It was observed that the compressive strength and dimensional accuracy were unaffected by shell number [91].

1.3 Challenges in existing polymeric nanocomposites

Polymeric nanocomposites, made of polymers reinforced with nanoscale fillers, show much promise in many areas because they have better thermal, mechanical, and barrier properties. Every transaction can be seen using the transaction identity on the Block Explorer. However, there are several challenges associated with existing polymeric nanocomposites [92]. Some of these challenges are:

Uniform dispersion of nanoparticles: The key to achieving the best properties is evenly distributing the nanoparticles throughout the polymer matrix. When nanoparticles clump together, they can affect the nanocomposite's performance and cause the material's properties to be uneven.

Interfacial adhesion: The nanocomposite's overall performance determines how well the nanoparticles and polymer matrix interact at the interface. Weak interfaces that need better adhesion can limit the stress transmission between the nanoparticles and the polymer matrix and impact mechanical qualities.

Printability: Not all polymeric nanocomposites are easily printable using common AM techniques like FDM or Stereolithography (SLA). Factors such as viscosity, rheological properties, and thermal stability need to be carefully optimized to ensure proper extrusion, layer adhesion, and dimensional accuracy during printing.

Nanoparticle Agglomeration: Nanoparticle agglomeration can occur during the processing of nanocomposite materials, leading to inconsistencies in material properties and compromising the final part quality. Strategies to prevent or minimize agglomeration, such as surface modification of nanoparticles or using dispersing agents, are essential.

Interfacial Bonding: Achieving interfacial solid interaction between nanoparticles and the polymer matrix is essential to improve mechanical properties, such as tensile

strength and toughness. Poor interfacial bonding can lead to delamination or weak interfaces between printed layers, compromising the structural integrity of the final part.

Optimized Nanoparticle Loading: Determining the optimal loading of nanoparticles within the polymer matrix is essential for achieving the desired balance of properties such as mechanical strength, thermal stability, and electrical conductivity. However, excessive nanoparticle loading can lead to processing difficulties, increased material cost, and potential degradation of print quality.

Material Compatibility: Compatibility between nanoparticles and polymer matrix is crucial to avoid phase separation, degradation, or adverse reactions during processing or post-processing treatments. Incompatibility can lead to reduced mechanical properties, poor print quality, or even material failure.

Post-Processing Challenges: Post-processing steps such as surface finishing, machining, or heat treatment can pose challenges for polymeric nanocomposites. Nanoparticles may alter the response of the material to these processes, requiring careful optimization to achieve the desired surface finish, dimensional accuracy, and mechanical properties.

Materials scientists, chemists, engineers, and manufacturing process experts must collaborate to solve these problems. Polymeric nanocomposites could forever change additive manufacturing by removing these limitations and paving the way for the mass creation of high-performance components with precisely engineered characteristic

1.4 Need for new materials for additive manufacturing processes

The demand for new polymeric nanomaterials in additive manufacturing processes, often referred to as 3D printing, is driven by the need to enhance the capabilities and address the limitations of current materials. Here are several reasons highlighting the need for the development and integration of new polymeric nanomaterials in additive manufacturing:

Improved Mechanical Properties: Polymeric nanocomposites can offer enhanced mechanical strength, stiffness, and toughness compared to traditional polymers. These

properties are crucial for manufacturing components with high structural integrity, especially in industries like aerospace and automotive.

Enhanced Thermal Stability: New polymeric nanomaterials with improved thermal stability can withstand higher temperatures during the 3D printing process. This is particularly important in applications where elevated temperatures are required for proper material deposition and layer bonding.

Increased Print Speeds: Some polymeric nanomaterials exhibit better melt flow characteristics, allowing for faster printing speeds. This can lead to increased efficiency and productivity in additive manufacturing processes, reducing the time required to produce complex parts.

Light weighting: The combination of nanomaterials with low density and high strength is advantageous for additive manufacturing in industries that prioritize lightweight structures, such as aerospace and automotive. This contributes to improved fuel efficiency and overall energy savings.

Improved Resolution and Detail: Nanomaterials can enhance the resolution and detail achievable in 3D printing. This is particularly relevant for applications in electronics, microfabrication, and medical devices where intricate features and fine structures are essential.

Conductive and Semi-Conductive Properties: Polymeric nanomaterials with conductive or semiconductive properties are crucial for the development of 3D-printed electronics. These materials enable the fabrication of components like sensors, antennas, and flexible circuits directly through additive manufacturing.

Biocompatibility: In the field of biomedical 3D printing, the development of polymeric nanomaterials with high biocompatibility is essential. These materials can be used for printing customized implants, tissue scaffolds, and drug delivery devices.

Smart and Functional Materials: Polymeric nanocomposites can be designed to exhibit smart functionalities, such as shape memory, self-healing, or stimuli-responsive behaviour. These properties expand the range of applications for 3D-printed objects in various industries.

Chemical Resistance: Nanocomposites with improved chemical resistance are valuable for applications where 3D-printed objects may be exposed to harsh chemicals or corrosive environments.

Reduced Warping and Shrinkage: Certain nanomaterials can help mitigate common issues like warping and shrinkage during the 3D printing process, leading to improved dimensional accuracy and part quality.

Sustainability: The development of sustainable nanomaterials for additive manufacturing contributes to environmentally friendly practices. This may involve the use of biodegradable polymers or materials derived from renewable resources.

Improved Printability: New polymeric nanomaterials can be engineered to have better printability characteristics, such as improved followability, adhesion between layers, and reduced nozzle clogging. These improvements facilitate smoother and more reliable 3D printing processes.

It is concluded that the integration of new polymeric nanomaterials in additive manufacturing processes is driven by the desire to advance the capabilities of 3D printing technology. These materials offer opportunities to enhance mechanical properties, increase print speeds, achieve finer details, and enable new applications across a range of industries. Ongoing research in materials science and additive manufacturing is crucial for unlocking the full potential of these advanced materials.

1.5 Research Objectives:

The main objectives of this research work are listed below:

1. Study of material and characterization of polymeric nanocomposites.
2. Development of new polymeric nanocomposites material.
3. Study of Mechanical Properties of the developed material.
4. Application of developed material with Additive manufacturing process.

(1) Study of material and characterization of polymeric nanocomposites.

i *Importance:* Understanding the properties and behaviour of polymeric nanocomposites is fundamental for optimizing their performance in specific

applications. Characterization involves analysing factors such as dispersion, interfacial adhesion, and structural integrity.

ii *Potential Impact:* Accurate material characterization guides the selection of appropriate nanofillers and polymer matrices, leading to improved processing techniques and enhanced properties. This knowledge is essential for ensuring the reliability and predictability of the material's behaviour in real-world applications.

(2) Development of New Polymeric Nanocomposite Materials:

i *Importance:* The creation of novel polymeric nanocomposites expands the range of materials available for various industries. Tailoring these materials allows for the optimization of specific properties, leading to advancements in performance, functionality, and sustainability.

ii *Potential Impact:* New materials can revolutionize industries by offering improved mechanical, thermal, electrical, and chemical properties. They can address specific challenges, provide solutions for niche applications, and contribute to the development of more efficient and environmentally friendly products.

(3) Study of Mechanical Properties of the Developed Material:

i *Importance:* Mechanical properties, including strength, stiffness, and toughness, are critical for determining a material's suitability for structural applications. Understanding these properties ensures that the material meets the requirements of specific industries and applications.

ii *Potential Impact:* A comprehensive study of mechanical properties informs the material's potential applications, such as in automotive, aerospace, construction, or consumer goods. Materials with enhanced mechanical properties can lead to more durable and reliable products.

(4) Application of Developed Material with Additive Manufacturing Process:

i *Importance:* Integrating new materials into additive manufacturing processes allows for the creation of complex and customized components. This aligns with the growing demand for lightweight, functional, and intricately designed parts.

- ii *Potential Impact:* The application of developed materials in additive manufacturing opens up new possibilities for rapid prototyping, customized production, and creating parts with intricate geometries. This can impact healthcare (biomedical 3D printing), electronics, automotive, and more industries.

In summary, achieving these objectives can significantly impact various industries by advancing material science, enabling the development of high-performance materials, improving manufacturing processes, and facilitating the production of innovative and customized products. The outcomes of these objectives can lead to enhanced product functionality, increased efficiency, and the exploration of new applications across a wide range of sectors.

1.6 Contribution to the Field of Materials Science

- (i) The study significantly advances our understanding of nanocomposites, specifically their fabrication through additive manufacturing processes. This contributes valuable insights to the broader field of materials science, offering new perspectives on the interactions between nanomaterials and the additive manufacturing environment.
- (ii) By exploring the synergistic effects and optimization strategies, the research contributes knowledge that can be applied to enhance the design and development of a wide range of advanced materials beyond nanocomposites.

1.7 Advancements in Additive Manufacturing

- (i) The research investigates the unique role of additive manufacturing in shaping the properties of nanocomposites. Understanding the influence of various parameters during the manufacturing process contributes to the refinement of additive manufacturing techniques.
- (ii) Insights gained from this study could potentially lead to the development of improved additive manufacturing methodologies, optimizing the production of complex structures with enhanced mechanical, thermal, and electrical properties.

1.8 Potential Applications

- i. The findings of the study have direct implications for diverse industries, including aerospace, automotive, biomedical, and electronics. The tailored properties of

nanocomposites produced through additive manufacturing make them suitable for a wide range of applications.

- ii. The research identifies and discusses specific applications where these advanced materials could be employed, such as lightweight components in aerospace, biocompatible implants in healthcare, or high-performance electronic devices..

1.9 Technological Advancements:

The study contributes to technological advancements by providing a foundation for the development of innovative materials with customizable properties. This has the potential to revolutionize existing technologies and create opportunities for the design of new, more efficient systems. Optimized nanocomposites may pave the way for the creation of advanced functional materials with improved strength, thermal stability, and conductivity, thereby influencing the development of cutting-edge technologies in various sectors. In conclusion, the study advances materials science, additive manufacturing, and nanocomposites' practical applicability across sectors. This research could advance technology by solving problems and developing new materials and technologies.

1.10 Overview of the Thesis: The studies reported in this thesis are concentrated on fabrication of polymeric nanocomposites using Multiwalled carbon nanotubes and Polymer as ABS. These composites material have used for Additive Manufacturing process as fused deposition modelling technique. The entire, thesis is presented in six chapters, the contents of which are spread in such a manner so as to gather an understanding of the microstructure–property relationships in these nanocomposites.

Chapter 1: Introduction :

This chapter provides the necessary background relevant to the thesis's contents, the motivation behind this work, and its objectives. It provides an overview of polymer and MWCNT and the modification and fabrication of polymeric nanocomposites. It also describes methods for fabricating polymeric nanocomposites, such as injection moulding and additive manufacturing, and their applications. This chapter also discusses the present work's objectives and the thesis's structure.

Chapter 2: Literature Review:

This chapter presents the literature survey carried out in this study to evaluate polymeric nanocomposites, various nanocomposites, MWCNT, and functionalized MWCNT. Its significance in multiple industries like Automotive, Aerospace and aviation, electronics and semiconductor, medical & health, and energy sectors. Introduce the various types of additive manufacturing, such as FDM, SLA, LOM, SLS, and DED. Detailed information on work carried out by researchers and groups has been discussed. Modelling and simulation of additive manufacturing were also described. The detailed survey of the literature review also pointed out motivation and research gaps were discussed.

Chapter 3: Material and Methods

This chapter deals with the raw ingredients, experimental setups and processing processes used to prepare the polymeric nanocomposite. It also covers the procedures for developing the material. The prepared materials are used to fabricate specimens through micro injection moulding machines and 3D printings. The study begins with a discussion of the specific polymer and polymeric nanocomposite materials, followed by examining the processing processes and characterization methods utilized for identification and analysis.

CHAPTER 4: CHARACTERIZATION

This chapter details the investigation, which involved numerous characterization techniques to analyse the functional group. It discusses equipment characterisation for mechanical characteristics, structural properties, thermal behaviour, crystallographic nature, and morphological properties of the obtained specimens.

CHAPTER 5: RESULTS AND DISCUSSION

This chapter discusses the details for finding the optimum process parameter and the effect of process parameters for obtaining the maximum tensile properties and microhardness of the fabricated polymeric nanocomposite through microinjection

moulding and 3-D printing. The microhardness was tested only in injection moulded samples due to the very good finished surfaces. The 3D printed samples were not fusible to take this analysis. And other properties are also covered in this chapter like XRD, FTIR, TGA and SEM.

CHAPTER 6: CONCLUSION AND FUTURE SCOPE

This chapter presents the concluding results for various properties, such as mechanical and thermal properties, and discusses the future scope. In summary, it can be inferred that incorporation of MWCNT in a reorganized polymer matrix would lead to better dispersion of MWCNT. This chapter shows the improvement of mechanical and thermal properties.

CHAPTER 2

LITERATURE REVIEW

This chapter presents the literature survey carried out in this study to evaluate polymeric nanocomposites, various nanocomposites, MWCNT, and functionalized MWCNT. Its significance in multiple industries like Automotive, Aerospace and aviation, electronics and semiconductor, medical & health, and energy sectors. Introduce the various types of additive manufacturing, such as FDM, SLA, LOM, SLS, and DED. Detailed information on work carried out by researchers and groups has been discussed. Modelling and simulation of additive manufacturing were also described. The detailed survey of the literature review also pointed out motivation and research gaps were discussed.

2.1 Overview of polymeric nanocomposites:

Khan, Idrees, et al. [2022] described A new type of composite material called polymer nanocomposites is being developed. They improve the performance of organic polymer matrices by mixing in inorganic nanoparticles. The constituents of polymer nanocomposites are polymers and Nanofillers. By combining the two components, the polymer matrix is enhanced with nano-fillers. Different types of polymer nanocomposites can be put into other groups based on their shape, the size of the nanomaterials, how they react to heat, and the type of polymer used. The three most common methods for creating polymer nanocomposites are melt extrusion, solution dispersion, and in situ polymerization, among many others [93]. Ali et al. (2014) have articulated and demonstrated that polymers possess many applications due to their remarkable amalgamation of characteristics, including low weight, long-lasting nature, and ease of processing [94]. Once more, I. Khan et al. [2019] demonstrated that polymers', mechanical, electrical and thermal properties are comparatively feeble compared to those of metals and ceramics. These weaknesses persist despite implementing various polymer modifications, including photopolymers, composite polymers, and copolymers. Supplementary methods for achieving the intended and necessary characteristics include whiskers, platelets, fiber, and nanoparticles [95]. As

stated by S.S. Siwal et al. [2020], polymers can be either natural or synthetic and consist of numerous repeating monomer units joined to form an extensive polymeric chain. In the past, synthetic polymers have played a crucial role. Polyvinyl chloride, polyester, and polyethylene are synthetic polymers [96]. Ali, N. et al. (2015). Polymers, including plastics, rubbers, and fibers, were used as matrices to produce polymer nanocomposites. Polymer nanocomposites can be made using thermoplastic or thermosetting polymers as their matrix. In the same way, elastomers and resins with low molecular weights were used as polymer bases to make different kinds of thermosetting polymer nanocomposites [97]. According to Isiaka Oluwale Oladele [2020], the remarkable properties of polymers have rendered them appealing as intelligent materials, which has led to their growing interest in various applications and disciplines [98]. N. Ali et al. [2015] state that photopolymers, copolymers, block copolymers, and polymer blends [99] are the polymeric matrices utilized in polymer nanocomposites. Wei et al. H. [2020] Despite significant advancements in developing novel polymer matrices, certain limitations persist in pure polymers, such as thermoplastic's relatively low mechanical strength [100]. N. Ali [2015] states that polymers have low modulus and strength and are utilized at low temperatures; consequently, these materials must be upgraded and improved to achieve the required properties [101].

Masoud et al. [2020] say that polymeric nanocomposites are a versatile of composite material where inorganic nanoparticles are mixed in with different types of organic polymer matrices to improve the properties of the matrix. Nanocomposites, classified as multi-phase materials, must incorporate one infill component at the nanoscale [102]. Saeed et al. (2018) propose that polymer nanocomposites offer a novel alternative to substituting traditionally filled polymers. Nanocomposites have unique properties and traits compared to the pure polymer matrix [103]. It is because they contain additives that work on the nanoscale. The prospective applications of polymer nanocomposites are virtually ubiquitous, as M. Sen [2020] noted. Food packaging materials incorporating polymer nanocomposites include processed meat, cheese, and dairy products. Additionally, it serves as a carrying case for drinkable water bottles, infant pacifiers, and blood collection tubes [104].

Compared to conventional composites and pure polymers, polymer nanocomposites offer the following benefits: Possible improved mechanical and thermal characteristics, lighter weight, better barrier characteristics, lower flammability, and more biodegradability. Due to the ample availability of carbon sources, nanomaterials based on carbon are an excellent option for mass production in a variety of applications. Additionally, core-shell morphologies can decrease the critical elements required for various applications. Nanotechnology can significantly aid in both the recycling of effluent and the decontamination of water. The resolution of forthcoming challenges confronting contemporary society may be facilitated through enhanced comprehension and the swift progression of nanotechnology.

2.2 Significance in various industries

The materials present in the dispersed matrix and dispersed phase of nanocomposites determine their classification [105]. Contemporary advancements in this swiftly growing domain have enabled the development of numerous intriguing new materials exhibiting unique characteristics by implementing novel synthetic methodologies [106]. The interfacial and morphological characteristics of their precursors significantly influenced the properties of the allegedly discovered substances, in addition to determining them. The progenitor constituent materials may not know the newly produced material property [107].

So, the concept of nanocomposites is to develop new materials with enhanced physical characteristics and greater flexibility by using building blocks of sizes in the nanoscale range. Polymer nanocomposites are used in various applications, such as food packaging (e.g., processed meat, cheese, and dairy goods), medical device containers (e.g., blood collection tubes), baby pacifiers, and water bottles. Nanocomposites composed of clay-based polymers are being utilized to improve plastic vessels' barrier, mechanical properties, and product longevity [108].

The following section provides an overview of several prospective applications of polymer nanocomposites in well-known domains. Fig. 2.1 illustrates the diverse applications of polymer nanocomposites in various fields. So the nanocomposites, materials comprised of a matrix reinforced with nanoparticles, hold significant promise

across various industries due to their unique properties and potential applications. Here's a breakdown of their significance in different sectors:

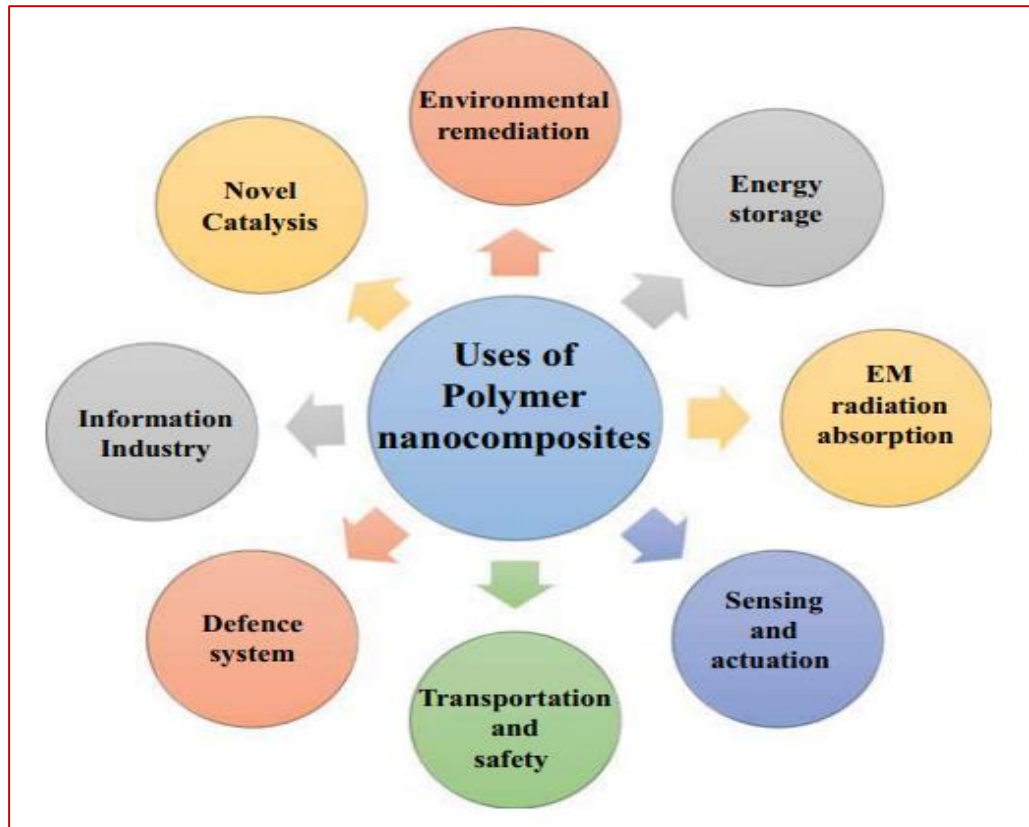


Figure 2.1 Various uses of polymer nanocomposites [108].

(a) Automotive Industries:

- (i) **Light weighting:** Nanocomposites can replace traditional materials like steel and aluminium, reducing vehicle weight and enhancing fuel efficiency without compromising structural integrity.
- (ii) **Improved performance:** They can enhance mechanical properties, such as strength, stiffness, and impact resistance, making vehicles safer and more durable.
- (iii) **Thermal management:** Nanocomposites can help in heat dissipation, improving the performance and longevity of automotive components like engine parts and battery systems.

(b) Aerospace and Aviation:

- (i) Weight reduction: Similar to automotive applications, nanocomposites can reduce weight while maintaining or enhancing mechanical properties, crucial for aircraft fuel efficiency and performance.
- (ii) High-temperature resistance: Nanocomposites can withstand extreme temperatures, making them suitable for aerospace components exposed to harsh environmental conditions.
- (iii) Radar absorption: Certain nanocomposite materials can be engineered to absorb radar waves, potentially useful for stealth applications in military aircraft.

(c) Electronics and Semiconductor Industries:

- (i) Miniaturization: Nanocomposites can enable the development of smaller and more efficient electronic devices due to their exceptional electrical properties.
- (ii) Flexible electronics: Flexible nanocomposite materials can be integrated into wearable devices, bendable displays, and flexible circuits, expanding the possibilities for electronic applications.
- (iii) Thermal management: In electronics, nanocomposites can help dissipate heat efficiently, improving the performance and reliability of electronic components.

(d) Medical and Healthcare:

- (i) Biocompatibility: Drug delivery systems, scaffolds for tissue engineering, and implants are only a few medical uses for nanocomposites, which can be modified to be compatible with biological systems.
- (ii) Diagnostic tools: Nanocomposites are used in advanced diagnostic techniques like biosensors and imaging agents, enabling more sensitive and accurate detection of diseases.
- (iv) Antimicrobial properties: Some nanocomposites exhibit antimicrobial properties, which are valuable for medical devices and surfaces to prevent infections and the spread of pathogens.

(e) Construction and Infrastructure:

- (i) **Durability:** Nanocomposites can improve the durability and longevity of construction materials such as concrete, enhancing resistance to corrosion, weathering, and mechanical stress.
- (ii) **Thermal insulation:** Nanocomposite-based insulating materials offer superior thermal properties, contributing to energy efficiency in buildings and infrastructure.
- (iii) **Self-healing materials:** Certain nanocomposites have the ability to self-repair cracks and damages, potentially reducing maintenance costs in infrastructure.

(f) Energy Sector:

- (i) **Energy storage:** Nanocomposites are explored for use in batteries, supercapacitors, and fuel cells to improve energy storage capacity, cycle life, and charging rates.
- (ii) **Solar energy:** Nanocomposites can enhance the efficiency and stability of solar cells by improving light absorption, charge separation, and electron transport.
- (iii) **Catalysis:** Nanocomposites are used as catalysts for various energy-related processes such as hydrogen production, fuel synthesis, and pollutant degradation.

Overall, nanocomposites offer a wide range of benefits across industries, including improved performance, enhanced functionality, and sustainability, driving innovation and advancements in diverse fields.

2.3 Various types of Additive Manufacturing Processes

2.3.1. Fused deposition modelling (FDM)

The most straight forward additive manufacturing technique for rapid prototype and 3D printing is FDM. For product manufacturing, industries and researchers typically employ fused filament fabrication (FFF) due to its high degree of precision, low cost, and short cycle time. Fused Deposition Modelling (FDM) is an additional user-friendly rapid prototyping machine that operates on the Fused Filament Fabrication (FFP) process. This machine can produce sound additively manufactured printed parts [109]

when an optimal combination of input variables is utilized. As the pseudo-solid thermoplastic filament material is pushed out of the nozzle orifice and onto the build platform, it slowly solidifies. As shown in Figure 2.2, these pseudo-solid thermoplastics mix before solidifying layer-by-layer at room temperature. Solidification occurs sequentially for each layer [110],

Furthermore, distinct printing configurations are necessary to produce the part without defects. The parameters include the following: bed temperature, contour width, raster angle, infill density, printing speed, orientation, support structure, layer thickness, and infill density [111-113].

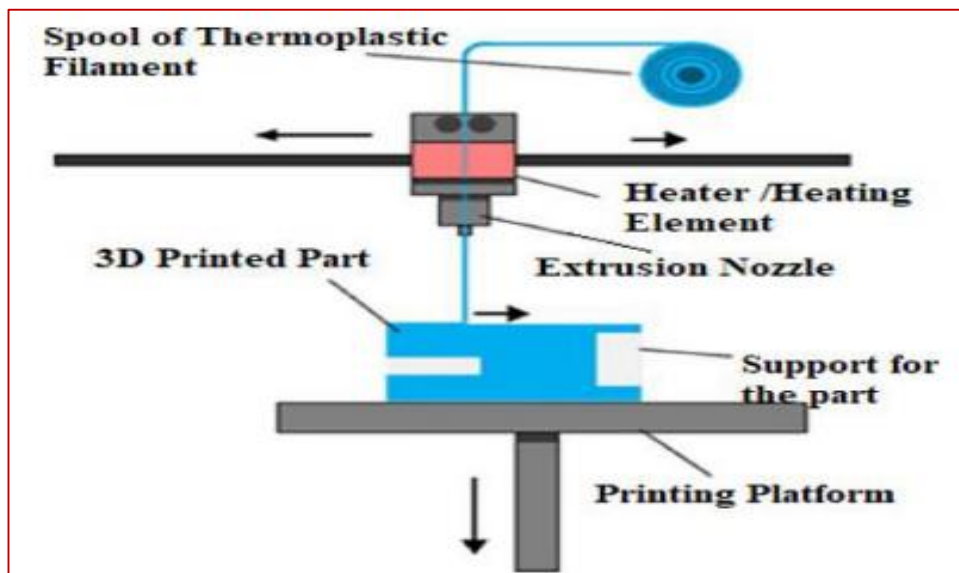


Figure 2.2 Fused deposition modelling [114]

These printing settings must be optimized before the manufacture of any component. Process parameters: Process parameters are important in 3D printing procedures because they enable the fabrication of defect-free items [114]. The process parameter establishes the mechanical characteristics and microstructure of the components. The best way to find the process parameters is to experiment with them and see what works [113]. The FDM technique uses a variety of process parameters for part deposition. The primary process parameters in the FDM method are briefly described here [114, 115].

❖ **Layer thickness**

Layer thickness, or layer height, is a crucial parameter used in layer-by-layer deposition [117]. The layer's height is determined along the vertical direction, specifically the z-axis. The size of the nozzle in FDM printing determines each layer's thickness. In most cases, the nozzle diameter is smaller than the layer thickness [113, 118]. Slicing software allows for the assignment of layer thickness. Thinner layers lead to a smoother surface finish, while thicker layers produce a rougher surface finish. Dealing with the staircase effect is a significant challenge in layer-by-layer deposition [118, 119].

❖ **Build orientation**

It is the inclination of the construction segment along the three-axis platform (X, Y, and Z). Three usual orientations are 0° , 90° , and $\pm 45^\circ$ for tensile sample deposition. Regarding tensile strength, the 0° raster angle is the best, and the $\pm 45^\circ$ raster angle is the worst. The part orientation 90° raster angle comes between them. The part's strength varies according to its orientation. While aligning the pieces, one might work on developing orientation skills [120, 121]. The orientation of the building component, its surface area on the platform, the number of support structures required for overhangs and undercuts, the desired mechanical qualities, and the potential development of surface imperfections, and the dimensional accuracy are all determined by the height of the building part.

❖ **Infill pattern**

The component's outer perimeter is filled to a solid fill level of 100%. A material used for an infill pattern must be sealed within the object [114]. Infill patterns come in a variety of shapes (rasters). Infill patterns include lines, rectilinear, linear, grid, stars, cubic triangles, hexagons, zigzags, honeycombs, Hilbert curves, Octagram cubic and Archimedean chords [122]. During deposition, these designs are used to fill the inside of the component. You can choose from various fill densities in slicing software (like Cura and Slicer) [123]. The infill pattern affects the print time, mechanical attributes, quality, and material consumption of the item [124]. Various fill densities can be adjusted to meet specific needs. The density of infill material at 10%, 20%, and 30% is shown in Figure 2.3 (a). One new feature from the 3D printing company Maker Bot is

an adaptive minimum fill pattern. The program will automatically select the minimum material needed when filling an object. It cuts down on paper consumption and printing time [125]. The infill pattern heavily influences the prototype, final product, and service conditions [116].

❖ **The temperature of the extrusion or nozzle**

When the filament is heated in the nozzle to a point where it melts, this is called the extrusion temperature. Thermocouples linked to the nozzle regulate the temperature. The deposition filament material affects the nozzle's temperature [114]. Faulty melting might result in incomplete melting or incorrect material deposition onto the platform. Each material has a certain melting point and extrusion temperature. It is vital to assess the new material's extrusion temperature through trial and error prior to deposition [113].

❖ **Air gap**

"Inter-raster spacing" refers to the distance between two neighbouring rasters on a deposited layer. The division consists of three categories: Figure 2.3(b-d) shows that (i) zero gap, (ii) positive gap, and (iii) negative gap. There are no gaps when two rasters are joined together with no space or overlap. A space between two adjacent rasters is referred to as a positive gap. When two neighbouring rasters meet, a negative gap is created [122].

❖ **Print speed**

While depositing material, the print head travels horizontally and vertically under the table. The print speed determines the object's printing time and is represented in millimetres per minute or millimetres per second [111, 126]. Improvements in printing speed result in a reduced total construction time. Slicing programs (like Cura) or firmware software allow users to modify the print speed during the FDM process. Typically, prototype printing prioritises faster print speeds over the functionality of the printed pieces. Increased printing speeds lead to decreased dimensional accuracy, higher mistake rates, and reduced product strength [127]. Moreover, the printer's pace depends

on the specific material used to construct the object. For instance, PLA material can be printed faster, but TPU requires a slower printing speed to avoid distorting or warping the object [128].

❖ Extrusion width

The width of the bead is known as the raster or extrusion width, as illustrated in Fig. 2.4. The size of the nozzle and the raster's direction determine its width. When the extrusion width is increased, void structures (negative air gaps) are created since the corners' radii are likewise increased. Overlapping the raster images, as indicated in Figure 2.4, reduces the negative air gap. Reducing the layer height is another way to decrease voids [129].

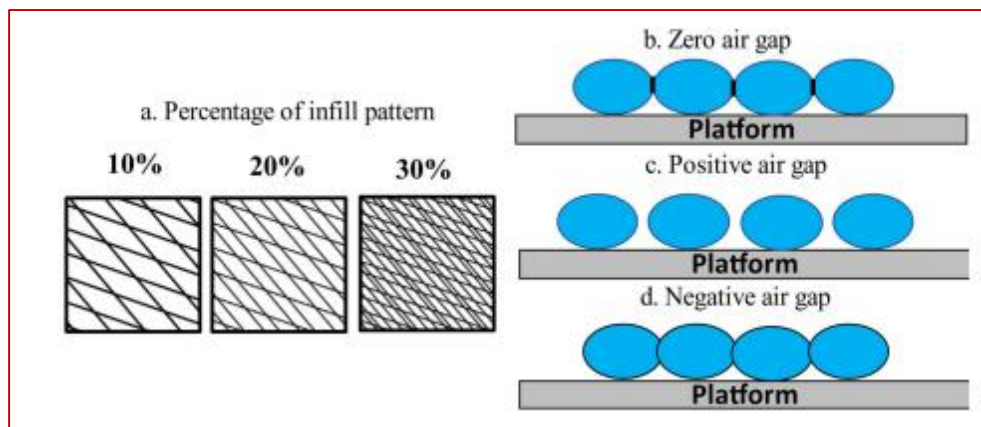


Figure 2.3 (a) Various fill percentages infill pattern (b) Zero air gap, (c) positive air gap, and (d) Negative air gap [122]

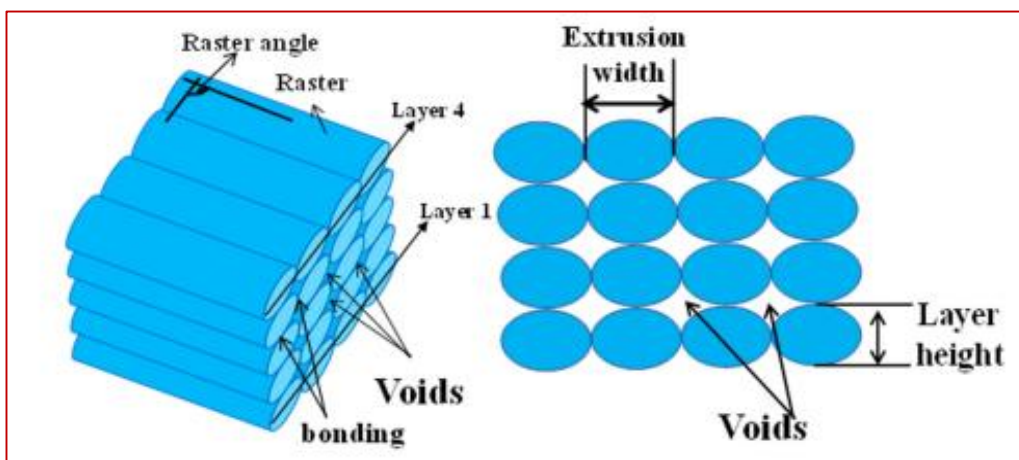


Figure 2.4 The concept of layer height, extrusion width, raster angle and air gap for small layer height [122]

❖ Raster angle

The build platform's and the nozzle raster's X-axis alignment determines the raster angle. Figure 2.4 shows the raster angle of the two adjacent layers, measured at 90°. The selected angle typically lies between 0° - 90° [116,130].

2.3.2 Stereolithography (SLA)

During the 1980s, Chuck Hull had a leading role in developing stereolithography, one of the earliest additive manufacturing processes [131, 132]. Vat photopolymerization is the fundamental principle upon which stereolithography (SLA) and associated technologies are built. Figure 2.5 shows the manner in which a light source, commonly electron beams or ultraviolet light, initiates the chain reaction on a monomer solution or a layer of resin [133]. When activated, the monomers rapidly transform into polymer chains, which is radicalization. Following the polymerization process, the resin pattern layer is hardened to ensure the stability of the subsequent layers. The process parameters are adjusted precisely according to the intended purpose [134–138]. Researchers in selective laser annealing (SLA) technology employ a variety of process parameters. These parameters comprise laser thickness, temperature of the printing bed, laser power, angle of stratification, post-curing time, and fabrication orientation. These parameters are shown in Figure 2.5. The main factors affecting each layer's thickness are the light source's energy and the period of exposure [134,139-140]. The primary factors that establish the thickness of every layer are the energy and exposure of the light source. [141]. SLA method can be incorporated to fabricate intricate nanocomposites [142]. This product offers top-notch resolution, precision, and a wide range of material options. SLA is commonly utilized for functional prototyping, patterns, moulds, and tooling. Despite its higher resolution, SLA has a few drawbacks, such as limited material options and slow printing speeds. The SLA resolution is 10 μm according to reference [143].

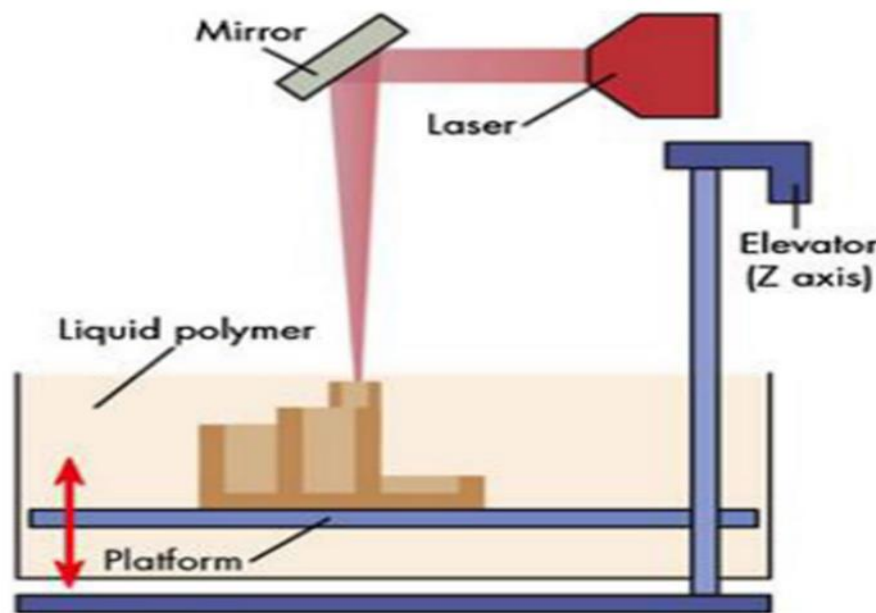


Figure 2.5. Stereolithography (SLA) process [134]

2.3.3 Laminated object manufacturing (LOM)

LOM is now open for commercialisation, one of the earliest forms of additive manufacturing. This method uses lasers or mechanical cutters to precisely recreate the target product's cross-sections by cutting tiny layers of materials including metal, plastic, and paper. The layers are fused progressively until the item is completely produced [144]. LOM is an additive manufacturing process where materials are sliced into sheets or rolls and then stacked one layer at a time. Successive layers are accurately severed and combined using a mechanical cutter or laser, which harnesses energy. LOM has two strategies for combining materials: bond-then-form and form-then-bond. The form-then-bond technique simplifies the construction of interior features by minimising excess material before joining and is helpful for thermal bonding in metals and ceramics. For recycling, surplus materials are repurposed as supports following the machining process [145]. Laser-based additive manufacturing (LOM) can process a wide variety of materials, such as paper, plastics, composites, and ceramics. The LOM system employs a laser beam source to precisely remove desired forms from a continuous sheet roll, forming individual layers of the final product, as shown in Figure 2.6. The layers are fused using a suitable component and a heat-activated plastic coating on one side of the paper. An inherent limitation of this approach is the substantial reduction in size

(12-18%) caused by thermal post-processing, which has the potential to result in dimensional inaccuracies [146]. The resolution of LOM is contingent upon the thickness of the laminate, often averaging approximately 50 μm [147].

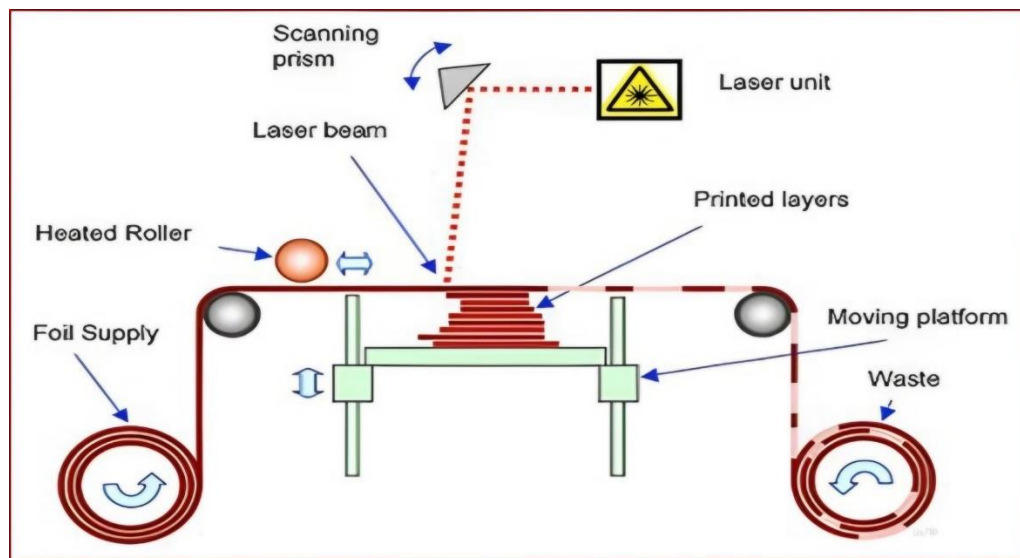


Figure 2.6 LOM setup [134]

2.3.4 Selective laser sintering (SLS)

As shown in Figure 2.7, the SLS technique uses powder material to directly produce different components from CAD models. Many common materials used in part production include thermoplastics (e.g., nylons, polyamides, ABS, and polycarbonate) and metals (e.g., titanium, stainless steel, and tool steel). [148].

The SLS powder-based 3DP approach uses a CO₂ laser beam to selectively fabricate models in the given process. The machine initially receives the 2D slice data. It guides the laser beam's trajectory across a pre-existing powder coating on the tray. During the laser beam process, the powder undergoes heating to fuse and form a rigid layer.

It also uses X and Y-axis translation to build the products from the supplied CAD files. After the initial layer has fused, the build tray is lowered, a new layer of powder is applied, and the layer after that is sintered. The process is iterated until the part is satisfactorily manufactured. Using sandblasting to enhance the surface of the prototype. The prototypes produced using Selective Laser Sintering (SLS) exhibit an opaque visual

appearance and possess a highly porous and uneven surface. This characteristic is widely recognised as the main weakness of this particular process. The SLS model has satisfactory accuracy, from 0.1 to 0.6 mm errors. This enables the production of many components simultaneously. However, the use of costly materials is required [149]. Multiple process variables are used in (SLS).

The layer thickness is the measurement of the material's thickness for each layer deposited onto a powder bed at the start of the operation [150]. The scanner focuses and directs the laser power utilised in the SLS process. Hatch spacing is the term used to describe the distance between successive laser motions. As the hatch spacing grows, the power of the laser beam utilised for sintering diminishes. The prototype's bed in the sinter station must be stored at an exact Hoover level. Consequently, the compartment is controlled above the surrounding temperature, known as the part bed temperature. When comparing an SLA part to an SLS part, the surface smoothness of the SLA part is superior. Moreover, the setup cost for an SLS machine is high because of the need for expensive equipment to handle high-melting temperature materials [151].

Despite the affordable price per part, the high efficiency, and the exceptional mechanical properties similar to injection-molded parts, support and post-processing are not necessary; the resolution depends on the diameter of the laser beam [152–154].

2.3.5 Direct energy deposition (DED)

Figure 2.8 shows the successful production of high-performance superalloys using direct energy deposition (DED). The DED process directs a focused power source, such as a electron beam or laser, onto a small substrate region. As a result, the powder or wire used as feed melts. As the laser beam moves across the melted substrate, the material is dropped and fused into it, hardening it. Dual Electron Beam Deposition (DED) is a technique used for treating materials that involve rapid cooling rates, typically between 103 and 105 K/s [155].

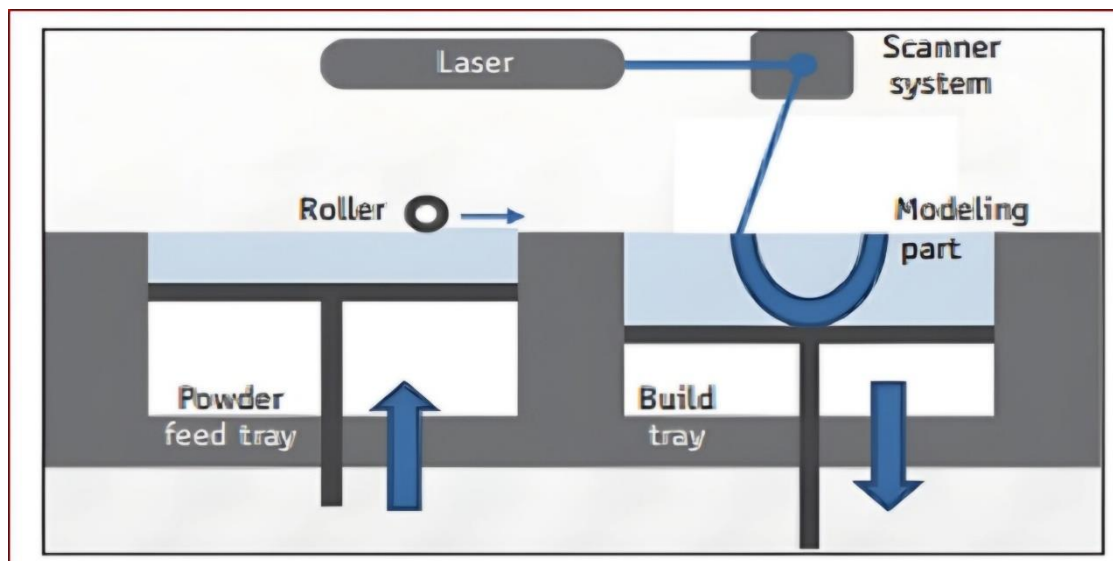


Figure 2.7 SLS apparatus [149]

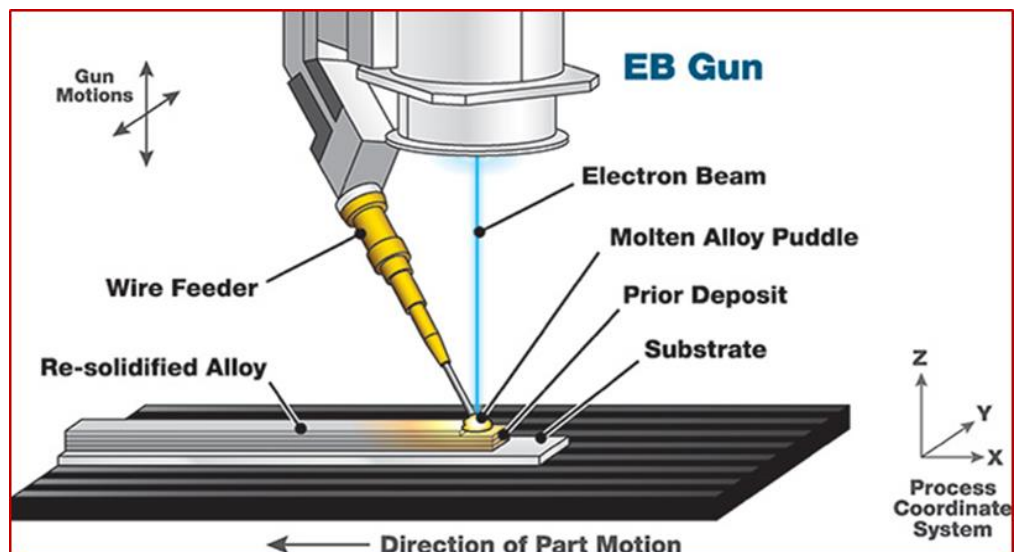


Figure: 2.8 DED Setup[155]

Other types of Directed Energy Deposition (DED) processes exist, but the powder-based DED approach is the most widely used and thoroughly studied in scientific literature. They were using a laser beam as the essential source of heat. Wire-based DED technologies provide a greater rate of material deposition and the capability to manufacture more significant components, even if they may have inferior resolution compared to laser-beam and powder-based DED methods. When performing

experiments in DED, considerations like layer thickness must be made diligently, the power of the laser, the size of the laser beam spot, the pace at which material is fed, the speed at which scanning is done, and the angle at which the clad is applied.

DED's drawbacks compared to SLS and SLM are its 0.25 mm precision, limited surface smoothness, and ability to create less complex components. Due to this, DED is commonly used for large, simple parts. DED boasts outstanding mechanical properties, which aid in cutting down on production time and costs. Here is a comparison of various AM techniques in Table 1.

Table 2.1: Comparison of different AM techniques

S.No.	Additive manufacturing Method	Principle	Significance when to use	Resolution
1.	Fused deposition modeling	Material extrusion	Proof of concept models and simple prototyping	50-200 μm [143]
2.	Stereolithography	Vat Photopolymerization	Versatile materials selection and function prototyping	10 μm [143]
3.	Laminated object manufacturing	Sheet lamination	Versatile materials selection and support materials repurposed	Depends on laminate thickness but typically is 50 μm [141]
4.	Selecting laser sintering	Powder bed fusion	Multiple components manufactured simultaneously	80-250 μm [143]
5.	Direct energy deposition	Laser or electron beam melting	Big low complex components	250 μm [147]

2.4 Modeling and Simulation in Additive Manufacturing

Additive manufacturing (AM) has gained increasing importance, owing to developing processes and tooling that introduced its benefits to different materials' applications.

Many AM uses its intrinsic abilities to utilize existing stock feed materials to create parts with features spanning multiple length scales. It was not possible before via another manufacturing process. These processes' excitement has been tempered by recognizing difficulties introduced by AM, including the inducement of mechanical and chemical Properties, undesirable microstructure, and the challenge of maintaining dimensional stability. Computational modeling is becoming a useful tool in addressing many of the difficulties inherent in the process.

The extensive modeling of the relations between the properties of Additive Manufacturing (AM) materials and process structure includes employing data mining techniques to close the cycle optimization prediction of the design. In relationship with the multiscale, multi-physical process, the process structure begins by modeling a micro scale, setting up a mechanistic thermal source model, using meso-scale models of the individual powder particle evolution, and finally by simulating the process of manufacturing a complicated product. A high efficiency, self-governance clustering analyses the mechanical model it is built to capture different material reactions to connect with structure and features. The model incorporates voids, phase structure, inclusions and structures of grain, which differentiate AM metals' distinctive characteristics [150] in the simulation and modeling of the three-dimensional temperature field, known as a birth and death element in multiple layers of a powder bed. Many researchers have been challenged to simulate the transient temperature field in additive layer manufacturing (ALM) methods. The transient temperature history in the parts processed with ALM that use a motion laser thermal source is crucial for establishing the thermal stress distribution and residual stress states. [157]. The conventional manufacturing process frequently needs a vast amount of machining and cannot meet the constantly increasing requirements of a sustainable, costeffective, and environmentally friendly in modern industry. Additive Manufacturing (AM), also referred to as 3D printing, is a direct digital manufacturing process. 3D digital data can be produced layer by layer with minimum machine and equipment parts or jobs. Wire arc additive manufacturing (WAAM) is a new technique that considerably reduces material usage and production time by providing high deposition rates of near-net-shaped components. Residual strains and distortions of the work piece deposited are one

of the critical problems of this method. Finite element (FE) models are commonly used in understanding and optimization; however, conventional transient models do not simulate a fundamental WAAM process [158]. The computer-based modeling benefits from the experimental techniques of polymer nanocomposites (PNCs) that have advanced characteristics owing to their particular hierarchical microstructures. The advanced nanocomposite materials including a nano-filler such as carbohydrate (CNTs), graphene, methyl tri methoxysthene, or lignin integrated into the bulk matrix of polymers, such as epoxy, polystyrene (PS), polypropylene (PP) cotton and other materials, are advanced polymer nanocomposites (PNCs) [159]. Nanocomposite polymers are a novel class of nanoparticles composed of composites distributed in diverse polymers matrices. In the early years of the composite industry, the development of these materials emerge. The self-assembly in polymer systems of nanoscale particles like nanospheres, nanodes and nanotubes is one of the most prominent and promising possibilities to produce new, high-performance materials. The dispersion across a polymer or block copolymers of these building blocks can substantially increase those nanocomposites' mechanical, optical or electrical characteristics. However, a deep knowledge of the structural formation and kinetic mechanisms, and structure–property connections, is necessary to properly apply them in technological applications and assure efficient scale-up. Tailored computer simulations will provide a unique technique for investigating structural development and formation and for the determination of structural and property correlations between nanocomposites. We first describe in this study multi-scale modelling and simulation approaches that may be applied to nanocomposites of polymers. These approaches are then used to many elements, including nano compound structures, dynamics, and characteristics, consisting of different polymer systems (for example, homogeneous polymers, polymer mixes, and copolymer block mixtures) and nanoparticles with different geometries and purposes. We also focus on the modifications of nanocomposites in multiscale simulation techniques in various approaches, including shear, electrical and magnetic fields, and show how external fields may be utilized to tailors the structures and affect the evolution dynamics of nanocomposites [160]. Modeling of AM processes offers essential insights into competing for physical phenomena that contribute to final material characteristics and product quality. And application the design space towards usable parts and

materials. It is extremely difficult to measure the dimensions needed to describe AM processes and predict the item's properties. The models must cover the length scales resolving the sizes of powder particles and the chamber dimension and the movement to the target of many hundred or thousand heating sources. The modeling task is thus a multi-scale, multiphysics endeavor that entailed the complex interaction of several algorithms. Discussing models that are necessary to cover the breadth of AM processes and forecast the material characteristics as constructed and residual stresses in the final construction. Provided instances of verification and validation. The aim is to provide an overview of existing methods for modeling how they may contribute to additives manufacturing. Since then, computer power has grown significantly, and computer simulation has become an essential tool for academics in several areas in study. The results of computer simulations will be very compatible with experimental work by creating exact force field parameters and the ideal design of simulation methodologies and techniques shown in Fig. 2.9.

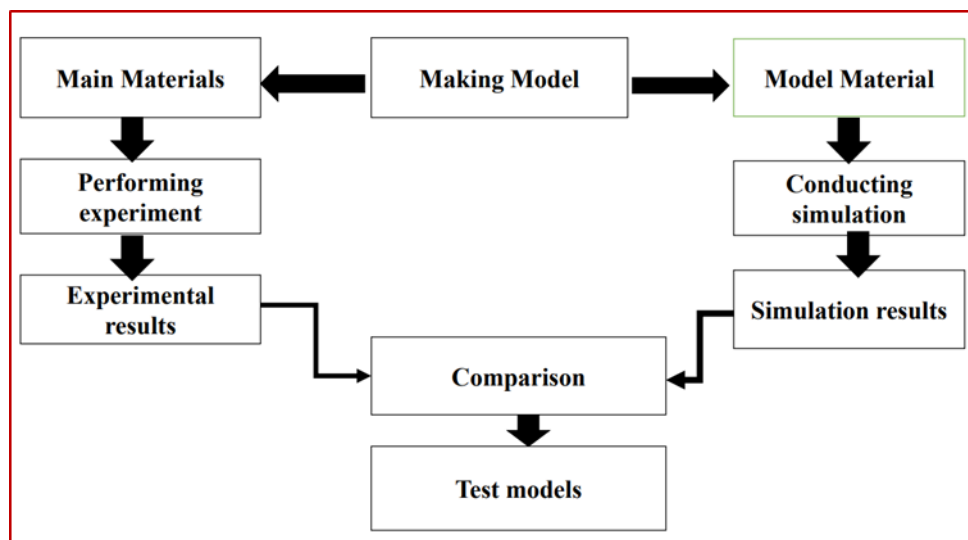


Figure 2.9 The relationship between experiment and computer simulation.

The connection between computer simulations and actual work is shown. A model material may be created to work on the model utilizing primary material as an example as a computer simulation framework. The findings may be compared with experimental results after simulations to determine whether the model is correct. If the simulation results do not match the test data and additional simulations are made, the model should

be updated and corrected. The end goal of AM modelling is to measure the functional or load-bearing capacity of the finished products using the input process parameters (such as characteristics and service life under certain loading situations). Moreover, the properties can be manipulated, and the products' structures and properties can be customized. Using predictive models enables the development of structure and property combinations that maximize the efficiency of raw material utilization. For example, making a custom bio-implant might involve adding different surface roughnesses, microstructures, and voids in certain places to improve the ability of cells to adhere, the stiffness, and the effective densities. This is because the substituted tissues, such as bones, experience varying loads at different positions, necessitating distinct property specifications. This goal is accomplished by developing a data-driven, multi-scale, multi-physics modelling framework (Fig. 2.10) that links process, structure, and property performance. This approach leverages data-mining techniques and blends mechanical and process models

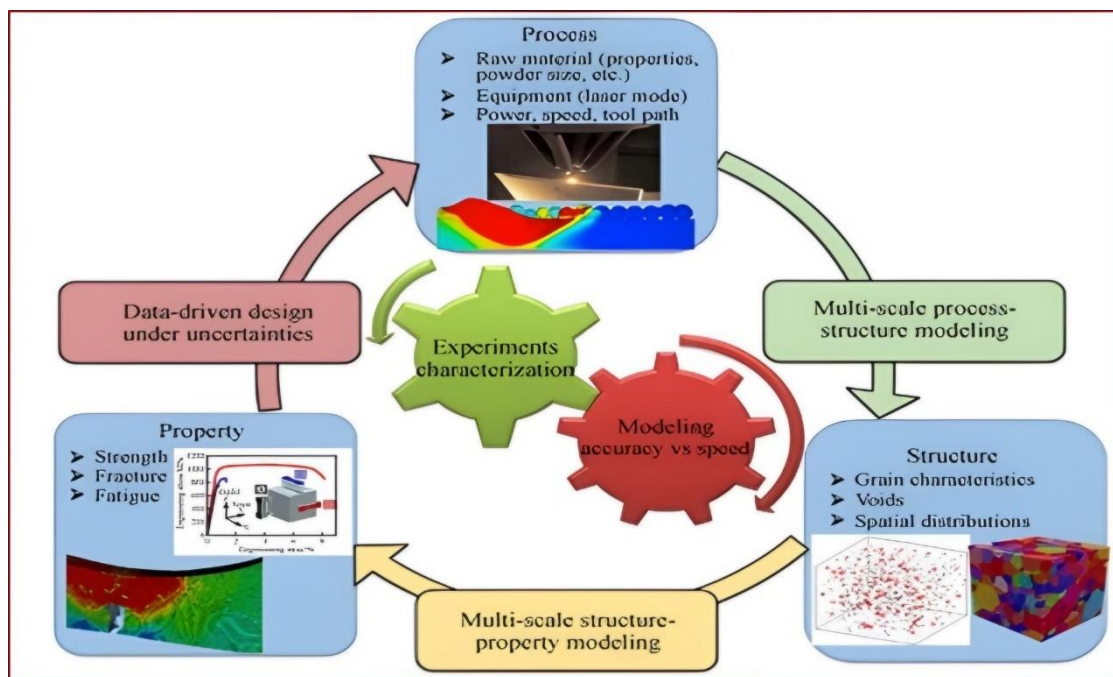


Figure 2.10 Data-driven multi-scale multi-physics modeling framework

2.4.1 Multi-scale multi-physics modeling of AM process

A multi-scale modelling framework was created to enhance our understanding of the production process and facilitate its optimisation. The approach emphasizes a systematic understanding of the AM process and the ability to predict material quality based on processing parameters. After this information is used to create new material structures and choose the best process settings, it must implement and connect multi-physics models of various sizes. The first step in creating this framework involves creating a new model for the heat source. This model is based on simulations of how electrons interact with materials at a microscopic scale. The model simulates the formation of molten pool tracks at a larger scale and a model that predicts how additively manufactured products will evolve.

2.4.1.1 Micro-scale modeling for heat source model

The fundamental principle behind the heating of materials by an electron beam is the collision between high-velocity free electrons and atoms in the material, resulting in the transfer of translational energy to the vibrational energy of the particles. It may employ the Monte Carlo method to model atomic and electron collisions [161]. Monitoring the paths of penetration and energy transfer may construct a heat source model for an electron beam that considers physical parameters [161-163].

2.4.1.2 Meso-scale modeling

A comprehensive modelling framework was devised to represent the (Electron Beam Selective Melting) EBSM process at the meso-scale, encompassing the melting of powder selectively along the prescribed scan path and the spreading of powder layers [164].

Figure 2.11 depicts a powder spreading model using the discrete element methodology (DEM) and a hydrodynamic model using the finite volume method. The hydrodynamic model describes how the powder melts and flows as a molten pool. The powder spreading model, on the other hand, shows how the rake and powder particles collide and spread out. The powder spreading model determines the substrate's initial spatial distribution of powder particles. After finishing a scanning route in one layer, the

solidified geometry is transmitted back to the powder spreading model, which spreads another layer in the FVM. The repetition of these two steps simulates a typical multi-layer manufacturing process. Various variables can be included to examine how experimental setups, connecting machinery, and procedures affect the production process.

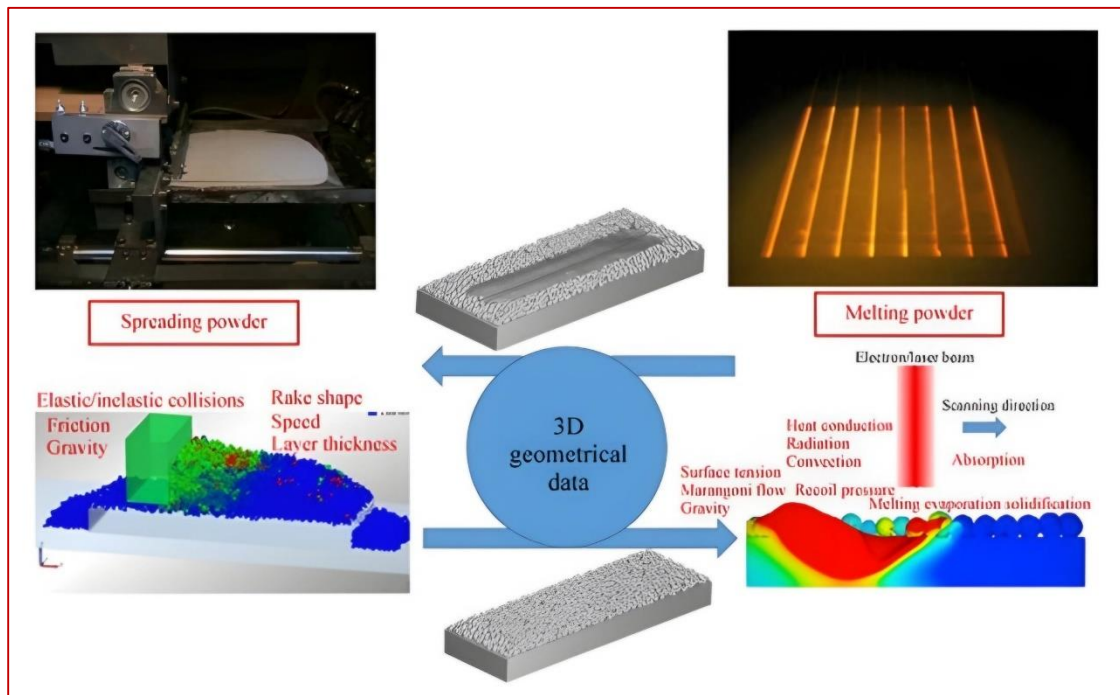


Figure 2.11 Meso-scale modeling of EBSM processes from powder spreading to selective melting [164].

2.4.2 Mechanical modeling for AM products using self-consistent clustering analysis

Direct numerical simulations (DNS) using the finite element method (FEM) are not practical for simultaneous simulations and material design because they require a lot of computing power [165]. Our research group [166, 167] developed selfconsistent clustering analysis (SCA), a reduced-order modelling approach for nonlinear materials with complex microstructural morphologies, to get better results and work more efficiently. This way of modeling with less detail is based on a data-clustering-based approach to computer homogenization. In this approach, the microstructure is connected with macro-micro formulations instead of being explicitly considered at the macroscale.

Data groups with similar mechanical properties are put together to make the database smaller. One example is the local strain concentration tensor. It is done by taking samples from previous DNS and experiment data. The method is adaptable to representative volume element (RVE) analysis. Due to its reliance on DNS and experimental data for clustering, it captures general mechanical properties and applies them to arbitrary microstructural morphologies, such as cavities and other defects. Using SCA, a record can be made in the microstructural material database for each type of microstructure found through imaging or process structure modeling. It includes flaws like pores and inclusions. This entry would contain all the offline clustering data required for optimal structure. One could use a concurrent multi-scale modelling approach to predict the macroscopic level responses for AM materials. To dynamically determine the reactions at each macromaterial point, this framework consults the material database for the corresponding microscale high-fidelity model.

If the agreement between the simulation and experimental data is high, the simulation prediction may explain the molecular properties of the entire material system. The simulation's output could reveal potential directions for developing experimental techniques. Molecular dynamics simulation is the most widely used of the numerous computer simulation methods for forecasting the physical properties of PNCs. Molecular dynamics simulations can be an intermediary between microscopic dynamics and macroscopic experimental interest. For example, they can evaluate the system's micro-aspects (such as atom movement, atom interactions, and molecular geometries) and consider several factors, including glass transition temperature, viscosity and modulus, diffusion coefficients, and equations of state.

For analyzing and optimizing the manufacturing process at various scales, the A.M. Bottom-up approaches are used to understand the AM process and predict the quality of AM-fabricated materials given a set of processing parameters, followed by a top-down strategy to design new material structures and select process parameters. Creating and integrating multi-physics models at various scales. New heat source models derived from micro-scale electron material interaction simulations (for EBSM), meso-scale models simulating individual molten pool tracks at the powder scale, and a

homogeneous macro-scale model simulating the evolution of additively manufactured products are all steps in this framework's creation.

It has been noticed that the dispersion of MWCNTs with thermoplastic materials only occurs uniformly in some cases. The researchers demonstrated a single extrusion procedure to produce PNCs. This literature discovered that relatively few MWCNT-agglomerated materials had been substituted with CB. CB was used instead of nanomaterials. However, it was costly and had poor characteristics. The polymer's dispersion of carbon nanotubes and carbon black increased the features of the composites as published in the literature. The hardness characteristic is quite crucial, yet it is proven in this literature that more work needs to be done. However, more research must be done on dispersed CNTs in metal matrices. MWCNTs must be treated or functionalized, or an extra initiator must be added, resulting in improved MWCNT interaction and dispersion with the polymer base matrix. Additionally, it has been noticed that the current literature needs to be more consistent regarding the quantity of MWCNTs necessary to enhance the mechanical strength of polymer composites. The microhardness properties are significant in improving the hardness properties of the fewer nanocomposites, but based on the literature review, more work needs to be done. Researchers have used various techniques to determine mechanical properties, including tensile testing and dynamic assessment analysis.

2.5 A detailed survey of literature review

This chapter details the literature survey carried out in this study to evaluate polymer nanocomposites, thermoplastics, and functionalized MWCNT. In additive manufacturing, comprehensive details about the research conducted by various investigators have been discussed.

A new family of thermoplastic polymers called nanocomposites, which include trace quantities of carbon nanotube particles, has just emerged. This novel composite class's enhanced physical, mechanical, and thermal properties have made it a hotspot for research. Additional polymers can be reinforced with MWCNTs to meet the high strength requirements. Among the many benefits of MWCNTs are their low density, high specific strength and modulus, availability, kindness to the environment, and

relative lack of abrasiveness. Several surface modification processes have been reported in the literature to improve adhesion between carbon nanotubes and polymers. Before commencing the experimental task, a flexible literature review is conducted.

Valino, Arnaldo D. et al. [2019] conducted a study on utilising thermoplastics and thermoplastic composites as primary materials in additive manufacturing (AM). Their extensive utilisation contributes to the most significant quantity of 3D printed products. The range of available property compositions for current materials is limited. Therefore, there is a strong trend towards expanding additive manufacturing's application to high-performance engineering polymers and nanocomposites despite their lack of commercial adoption. At the moment, high-performance thermoplastic polymers can only be processed with injection moulding, thermoforming, extrusion, and similar technologies. The four main types of thermoplastic composites are particle composites, fibre composites, nanomaterial composites, and polymer blends. In this article introduces the significance of various composite systems in AM. Polymer materials have a crucial role in AM and, in the future, in producing original equipment manufacturer (OEM) parts. Thermoplastics and thermoplastic composites are the two main groups into which most of today's materials fall [168].

Lim, Choon Wee Joel et al. "An overview of 3-D printing in manufacturing, aerospace, and automotive industries." (2016): Recently, there has been a rise in the development of techniques for using large quantities of polymer thermoset and elastomer materials in additive manufacturing. The aim of this study was to present a panoramic analysis of the latest developments in thermoplastic and composite materials used in 3D printing, with a particular focus on enhancing their performance and qualities. The growth of polymer-based additive manufacturing's technological influence and marketability is crucial. AM, also known as 3D printing, involves combining layers of materials to produce 3 D things using a Surface Tessellation Language (STL) [169].

Serdeczny, Marcin P. et al. "Experimental and analytical study of the polymer melt flow through the hot-end in material extrusion additive manufacturing." Additive manufacturing (2020): In this research, material extrusion additive manufacturing utilizes a thermoplastic polymer as a solid filament as a building material to the pressure exerted by the filament feeding force, the polymer melts and flows within the hot-end

channel. Phase transition, shear rate, temperature-dependent viscosity, and viscoelastic effects are only a few of the complex phenomena that remain unresolved in our current understanding of polymer flow through the hot end [170].

Ngo, Tuan D. et al. "Additive manufacturing (3D printing): A review of materials, methods, applications and challenges." *Composites Part B: Engineering* (2018): A number of methods have been developed to create nanocomposites for stereolithography (SLA). The unique properties of the nanofiller and the resin material dictate the processes used. The main objective is to attain a uniform blend with a satisfactory thickness to acquire printed items of superior quality. Homogeneity can be achieved through mechanical mixing, shear mixing, sonication, ultrasonication, or a combination of these approaches [171].

Caminero, M. A. et al. "Impact damage resistance of 3D printed continuous fibre reinforced thermoplastic composites using fused deposition modelling." *Composites Part B: Engineering* (2018): Continuous fiber-reinforced thermoplastic composites (CFRTPCs) are becoming increasingly important in industry because they have many benefits, such as better mechanical performance, the ability to be recycled, and the potential to make lighter structures. One major issue that affects the effective utilization of 3D-printed composites is the potential damage to structural integrity, which is a worry when comparing them to conventional prepreg composites. 3D printing creates polymer composites with enhanced mechanical properties by mixing thermoplastic polymers with reinforcements like particles, fibres, or nanomaterials. This opens the door to the production of polymer matrix composites that are more functional and perform better than before [172].

Torrado, Angel R. et al. "Characterizing the effect of additives to ABS on the mechanical property anisotropy of specimens fabricated by material extrusion 3D printing." *Additive Manufacturing* 6 (2015): Characteristic mechanical Fused deposition modelling (FDM) is a 3D printing material extrusion process that produces components with undesirable anisotropy quality. Along with EBM, SLM, SLS, SLA, and LENS, other AM technologies include electron beam melting, selective laser sintering, stereolithography, and laser-engineered net shaping. One popular way to find mechanical property anisotropy is to compare the impact resistance or ultimate tensile

strength (UTS) of components made in opposite directions. Unless EBM-fabricated, items constructed in the Z-direction usually have lower tensile strength and impact resistance values. Machine factors like raster direction, layer thickness, and air gap affect the mechanical characteristics and level of anisotropy in 3D printed items. However, there is no definitive approach to reducing differences in mechanical properties based on the orientation of the building [173].

Nikzad, Mostafa, S. H. Masood, and Igor Sbarski. "Thermo-mechanical properties of highly filled polymeric composites for fused deposition modelling." *Materials & Design* 32.6 (2011): This study details the creation of novel thermoplastic composites to enhance the FDM process's current thermoplastics [174].

Gray IV, Robert W., Donald G. Baird, and Jan Helge Bøhn. "Effects of processing conditions on short TLCP fiber reinforced FDM parts." *Rapid Prototyping Journal* 4.1 (1998): This work aims to enhance the strength and value of FDM prototypes by incorporating thermotropic liquid crystalline polymers (TLCP) into a polypropylene (PP) matrix. The researchers made the filaments using a dual extrusion process. They next tested how different parameters affected the prototypes' tensile properties and form [175].

Zhong, Weihong, et al. "Short fiber reinforced composites for fused deposition modeling." *Materials Science and Engineering: A* 301.2 (2001): This study examined how incorporating short fiber reinforcements into ABS composites enhances ABS filament strength for FDM processing. [176].

Postiglione, Giovanni et al. "Conductive 3D microstructures by direct 3D printing of polymer carbon nanotube nanocomposites via liquid deposition modeling." *Composites Part A: Applied Science and Manufacturing* 76 (2015): The study shows how to make conductive 3D microstructures of any shape using a modified low-cost benchtop 3D printer and a new LDM 3D printing method that uses solvents to help the additive deposition of a conductive nanocomposite. The study of the materials' electrical properties showed that the MWCNT concentration of the nanocomposite went up significantly compared to the pure material. The printability windows for these systems were determined by estimating the dispersion's shear rate at the extrusion nozzle and analyzing the rheological properties of the nanocomposite dispersions with varying concentrations of PLA [177].

Zhang, Haoqi, Dongmin Yang, and Yong Sheng. "Performance-driven 3D printing of continuous curved carbon fibre reinforced polymer composites: A preliminary numerical study." *Composites Part B: Engineering* 151 (2018): The primary components used in the placement process of carbon fibre-reinforced polymer (CFRP) composites are unidirectional fibres pre-impregnated (prepreg) with the matrix material. On the other hand, 3D printing utilizes filaments or bundles of fibres to create small printing beads, which are then used to make another component. Therefore, it can produce composites with intricate designs while keeping labour and manufacturing expenses low. Due to its exceptional strength and stiffness-to-weight ratio, its primary applications lie within the aerospace, automobile, and infrastructure sectors [178].

Frketic, Jolie, Tarik Dickens, and Subramanian Ramakrishnan. "Automated manufacturing and processing of fiber-reinforced polymer (FRP) composites: An additive review of contemporary and modern techniques for advanced materials manufacturing." *Additive Manufacturing* 14 (2017): Various methods exist for utilizing solid materials as printing materials in additive manufacturing. Thermoplastic polymers are commonly used with the widely recognized material extrusion technique called fused deposition modeling (FDM). For this technique, raw polymer filament is heated in a nozzle until it becomes liquid, then laid in layers on a heated platform. A thermoplastic material is usually used as the main structural component, and a support material is used to hold parts that might go beyond the layers that came before them in this method. The processing step is completed by extracting the support material. Thermoplastic material extrusion enables precise printing with high resolution (0.0254 mm) in the x, y, and z axes. This technology can be employed in office environments due to the user-friendly nature and minimal toxicity of the printed material. However, The extrusion method restricts the 3-D printed material to those substances that can be melted inside the nozzle and cooled and hardened on the print surface [179].

Ning, Fuda, et al. "Additive manufacturing of carbon fiber reinforced thermoplastic composites using fused deposition modeling." *Composites Part B: Engineering* 80 (2015): Fused Deposition Modeling (FDM) is commonly employed to create conceptual prototypes that have reached advanced phases of development. This is because the thermoplastic components produced by FDM do not possess the strength to act as fully operational and load-bearing elements. This limitation hinders the wide range of uses

for FDM technology. Hence, enhancing the durability of pure thermoplastic parts created using FDM is imperative to overcome their existing constraints. Thermoplastic matrix carbon fibre-reinforced plastic (CFRP) composites are a viable option that combines plastic with reinforcing elements like carbon fibres. Composites made of carbon fibres are used to support weight. In addition to joining and protecting the fibres, the thermoplastic matrix can transfer weight to the reinforcing fibres. Airbus A350 fuselages, wind turbine blades, automobile components, and endoscopic surgery are just a few of the many uses for thermoplastic matrix CFRP composites [180].

Kestilä, Antti, et al. "Towards space-grade 3D-printed, ALD-coated small satellite propulsion components for fluidics." *Additive Manufacturing* 22 (2018): The researchers performed experiments on the ABS prints and discovered that the coating used in this study can partially decrease gas emissions at high temperatures. Nevertheless, the overall conclusion remains ambiguous and warrants additional examination. This study carefully looks at how gases are released, like when samples are heated up or when outside factors act on them, and how they can be slowed down by using Atomic Layer Deposition (ALD) coating. Furthermore, it investigates the materials more suitable for ALD and AM procedures. Maximizing the use of additive manufacturing (AM) in space can significantly reduce the time it takes to produce and the costs of producing various space equipment. Furthermore, additive manufacturing (AM) can fabricate space systems that would be impossible to create using traditional manufacturing methods. Other instances include improving the safety of medical applications by efficiently isolating the additive manufacturing component from the human body [181].

Zhu, L., N. Li, and P. R. N. Childs. "Light-weighting in aerospace component and system design." *Propulsion and Power Research* 7.2 (2018): CFRPs, or carbon fiber-reinforced polymers, are widely utilized composite materials in aerospace applications. They possess a stiffness of up to three times more significant and a specific strength of more than five times greater than that of aluminium alloys. Nanocomposites exhibit significantly enhanced characteristics in comparison to traditional materials. Nevertheless, the elevated cost and limited manufacturability of metals hinder the broader utilization of composites [182].

Wu, Chin-San. "Characterization, functionality and application of siliceous sponge spicules additive-based manufacturing biopolymer composites." *Additive Manufacturing* 22 (2018): Composites of Polyhydroxyalkanoate (PHA) and siliceous sponge spicules (SSS) were created using three-dimensional (3D) printing filaments. The compatibility of SSS inside the PHA matrix was enhanced by using Acrylic acid (AA)-grafted polyhydroxyalkanoate (PHA-g-AA) and SSS. Based on mechanical and morphological analyses, it was found that the higher adhesion between the SSS and PHA-g-AA resulted in increased tensile strength at failure and Young's modulus of the composite, as compared to the PHA/SSS. The PHA-g-AA/SSS composites exhibited superior water resistance compared to the PHA/SSS composites. The cytocompatibility of the composites was evaluated by seeding human foreskin fibroblasts (FBs) on two sets of these materials [183].

Hoff, Brad W., et al. "Dielectric strength heterogeneity associated with printing orientation in additively manufactured polymer materials." *Additive Manufacturing* 22 (2018): The results demonstrate that additive manufacturing techniques introduce dielectric anisotropy in produced parts, which is dependent on the printing orientation of the part. The dielectric strength testing data, following the ASTM D149 standard, is provided for samples produced using polymer jetting (Poly-Jet), stereolithography (SLA), fused deposition modeling (FDM), and selective laser sintering (SLS) additive manufacturing methods. Each distinct printing orientation, determined by the printing technique, was systematically analyzed. It was discovered that each printing approach caused the sample coupons to have anisotropic dielectric properties. These properties were influenced by the initial orientation in which the part was printed. Additionally, the direction of structural susceptibility depended on the printing method used. The dielectric strength varied by more than 70% for certain combinations of printing processes and polymer, resulting in differences in the printed coupons' orientations [184].

Blok, Lourens G. et al. "An investigation into 3D printing of fibre reinforced thermoplastic composites." *Additive Manufacturing* 22 (2018): An innovative method of 3D printing called fused filament fabrication (FFF) was introduced. This approach enables the gradual construction of a part by depositing thermoplastic material through a nozzle, layer by layer. The technology allows for the creation of intricate forms with

creative flexibility that cannot be attained with traditional manufacturing techniques. Nevertheless, thermoplastic materials exhibit inferior mechanical qualities compared to conventional engineering materials. An investigation was conducted on the composite 3D printing feedstocks for Fused Filament Fabrication (FFF), in which carbon fibers were incorporated into a thermoplastic matrix to enhance strength and stiffness [185].

Dizon, John Ryan C. et al. "Mechanical characterization of 3D-printed polymers." *Additive Manufacturing* 20 (2018): An investigation has been conducted using FDM on the tensile characteristics of components made from Kevlar fiber-reinforced nanocomposites. The researchers varied the volume fraction of fibres in the composite material, trying it at 4.04%, 8.08%, and 10.1%. A larger volume of reinforcing fibres resulted in mechanical parameters with larger magnitudes, including ultimate tensile strength, ultimate tensile strain, and Young's modulus. Using the Average stiffness method, they also provided a method for determining the polymer/fibre composite's mechanical properties. Post-processing using FDM is occasionally utilized to augment the material strength of printed components. The primary obstacles faced with FDM printed materials are inadequate layer adhesion and layer delamination. Therefore, post-processing is crucial to enhance the resilience of layer adhesion. Zhang's research highlighted the efficacy of microwave treatment for improving the fusion of layers in ABS/CNT nanocomposites produced using FDM printing, resulting in significantly enhanced layer adhesion. The application of microwave irradiation induces a strong reaction in carbon nanotubes (CNT), generating sufficient heat to rapidly melt the ABS molecules surrounding the CNT. This ultimately leads to the fusion of neighbouring ABS layers. Vapor-smoothing has been documented as a successful technique for refining the appearance of layered patterns on surfaces of 3D-printed materials. Acetone vapour polishing was utilized to enhance the surface smoothness of 3D-printed ABS, intended for use as a mould that poses a risk and necessitates a high level of smoothness. Following 12 minutes of polishing, all boundaries become indistinguishable, and a sleek surface becomes visible. However, prolonging the polishing duration would result in the dissolution of the ABS material, creating pores or pits on the surface and ultimately exacerbating the surface roughness. It is crucial to meticulously regulate the temperature, duration, and pressure in the vapour polishing procedure [186].

Nieto, Daniel Moreno, Victor Casal López, and Sergio Ignacio Molina. "Large-format polymeric pellet-based additive manufacturing for the naval industry." *Additive Manufacturing* 23 (2018): New prospects for integrating additive manufacturing (AM) technology into industrial processes, namely for producing large polymeric parts, have been identified. As additive technologies progress and their development process is continuously improved, the use of Polymeric Pellet-Based Additive Manufacturing (PPBAM) systems in 3D printing is on the rise. The PPBAM process uses a Cartesian or robotic arm displacement system to convert a pellet-fed extrusion mechanism. This system is used to construct parts in a multi-layered manner. The fused pellet modelling (FPM) technique integrates the additive process tools used in injection moulding with the traditional 3D printing layer-by-layer building procedures. Because of this, the nozzle size and layer height could be increased [187].

Kalms, Michael et al. "New approach to evaluate 3D laser printed parts in powder bed fusion-based additive manufacturing in-line within closed space." *Additive Manufacturing* 26 (2019): The authors suggested a novel method for evaluating laser-selective melting using high-precision metrology based on structured light. This approach is characterized by its durability and accuracy and may be implemented during manufacturing. They showcased a precisely calibrated fringe projection system that relies on a two-camera setup, and features enhanced general calibration, making it appropriate for dimensional in-process sensing. The system's accuracy is less than ten microns in the z-coordinate. This value is adequate for accurately identifying defects in powder coating or consolidation when the layer thickness is 50 μm or more [188].

Kim, Garam et al. "3D printed thermoplastic polyurethane bladder for manufacturing of fiber reinforced composites." *Additive Manufacturing* 29 (2019): The aerospace industry predominantly relies on autoclave processing as the primary production method for generating composite components. This is mainly because autoclave processing consistently achieves low void content in the manufactured components. Putting together several layers of reinforcing fibers that have already been mixed with a thermoset or thermoplastic resin (also called "prepreg") makes a composite layup. Once the plies have been placed, the composite layup is solidified by applying air pressure through a vacuum bag method. The vacuum applied, and the external gas pressure introduced in the autoclave help eliminate the air trapped between the layers of the

laminate and volatile substances from the composite layups, resulting in the consolidation of the parts. Inadequate part consolidation leads to the formation of empty spaces, which can not only lead to the early failure of the component but also weaken its strength [189].

Golbang, Atefeh et al. "Production and characterization of PEEK/IF-WS2 nanocomposites for additive manufacturing: Simultaneous improvement in processing characteristics and material properties." *Additive Manufacturing* 31 (2020): This study made PEEK nanocomposites that added 0.5%, 1%, and 2% of inorganic fullerene tungsten sulfide (IF-WS2). The aim is to create a high-performance material via additive manufacturing by integrating the beneficial properties of both organic and inorganic materials. When IF-WS2 nanoparticles are mixed with PEEK using a twin-screw extruder, they are spread out very well. Wear and friction are lower in PEEK/IF-WS2 nanocomposites than in pure PEEK. This is because the nanoparticles do not stick together; they interact well with the polymer filler and have a lubricating effect. Thermogravimetric analysis (TGA) showed that adding IF-WS2 to PEEK made the temperatures at which it breaks down much higher. Differential Scanning Calorimetry (DSC) tests showed that adding IF-WS2 nanoparticles made the PEEK crystallize more. The sample with 1% wt% IF-WS2 had the highest crystallinity, at 44%. This is because the nanoparticles were better spread out in this sample. Microscopic images have demonstrated that adding 1 wt% and 2 wt% IF-WS2 reduces the molten material's viscosity and improves the quality of the printed output. The solid's mechanical properties (E') improved because of IF-WS2's strengthening effect and the higher crystallinity in both moulded and printed samples. The superior mechanical properties of injection set samples, compared to FFF printed samples, can be attributed to improved dispersion, increased crystallinity, and enhanced packing of polymer chains in these samples. Therefore, it may be inferred that the addition of IF-WS2 to PEEK can enhance the FFF processing of PEEK by improving its melt rheology and its ultimate mechanical and thermal properties. [190].

Santos, Vicente M. Rivas et al. "Design and characterization of an additive manufacturing benchmarking artefact following a design-for-metrology approach." *Additive Manufacturing* 32 (2020): Several benchmarking artefacts have been developed to assess additive manufacturing systems' various capabilities and study

the made components' geometric characteristics. Nevertheless, the design of the preceding benchmark in artefacts should consider the challenges and intricacies of the measurements needed to accurately characterize them. At this step, we employ a design technique that considers the measuring process during the creation of the object. The final product is designed to work with the AM and high-speed sintering (HSS) systems. It is also designed to work with the contact coordinate measurement machine (CMM), X-ray computed tomography (XCT), and photography (PG). Measurement findings offer insights into the performance of the HSS system and serve as evidence of the effectiveness of the benchmarking artefact design, therefore validating the design methodology [191]

Van de Werken, Nekoda et al. "Additively Manufactured Carbon Fiber-Reinforced Composites: State of the Art and Perspective." *Additive manufacturing* (2019): The utilization of AM carbon fiber composites in the production process and their mechanical characteristics appeal to several industries, such as aerospace, automotive, and energy. 3D-printed composites can surpass machined parts in both performance and cost of tools and fixtures. Carbon fibers can enhance the mechanical and thermal characteristics of 3-D printed products, making them suitable for utilization as moulds and moulding machines in polymer-based production [192].

Bhatt, Prahar et al. "Building free-form thin shell parts using supportless extrusion-based additive manufacturing." *Additive Manufacturing* 32 (2020): This research introduces an innovative method for creating precise thin shell components utilizing supportless extrusion-based additive manufacturing. The layer slicing method, tool-path planning algorithm, and neural network-based compensated trajectory generation scheme are explained for constructing precise thin shell parts utilizing two manipulators, a three-degree-of-freedom build platform, and a three-degree-of-freedom extrusion tool. These thin shell pieces cannot be constructed without assistance from earlier additive manufacturing procedures that do not require support structures. They demonstrated the efficacy of algorithms by constructing many slender shell components [193].

Tian, Xiaoyong et al. "Interface and performance of 3D printed continuous carbon fiber reinforced PLA composites." *Composites Part A: Applied Science and Manufacturing* 88 (2016): Continuous Fiber Reinforced Thermoplastic Composites (CFRTPCs) are becoming alternative materials to replace conventional thermosetting plastics and steel

due to excellent mechanical performance, recycling, and potential lightweight structures. Developing a new fabrication process for CFRTPCs has attracted many research activities for many years. Processes like vacuum-forming filament winding, pultrusion, bladder-assisted moulding, and compression have been used to fabricate CFRTPCs. In all these conventional processes, complicated moulds are required, which is expensive and time-consuming. It is difficult and even impossible to manufacture complex composite components. Also, uncontrollable forming quality and a low degree of automation are the limitations of the vast industrial applications of CFRTPCs. Innovation in the fabrication process is critical and urgent to the future development and application of CFRTPCs [194].

Palaganas, Napolabel B. et al. "3D printing of photocurable cellulose nanocrystal composite for fabrication of complex architectures via stereolithography." *ACS applied materials & interfaces* 9.39 (2017): 3D printing has significant benefits in terms of cost, speed, accuracy, and flexibility, which have led to its adoption in various industries, particularly in medicine, where there is a great demand for customized solutions. This contemporary manufacturing method provides numerous advantages, but it also presents significant obstacles in creating acceptable materials for industrial applications. Although polymers have many beautiful qualities, their weak mechanical properties have greatly hindered their use in biological applications. Prior research on the 3D printing of polymers mainly emphasized the compatibility with living organisms and the ability to sustain biological life. It required careful monitoring to create solid and durable samples. The exceptional mechanical strength and inherent rigidity of cellulose nanocrystal (CNC) derived from the abaca plant impart the required resilience to a 3D printable biopolymer. Therefore, this study showcases the utilization of 3D printing to create a biomaterial filled with computer numerical control (CNC), resulting in notable enhancements in mechanical and surface qualities. This innovative work effectively demonstrates the 3D printing of CNC nanocomposite hydrogels utilizing SLA, achieving high repeatability, fidelity, and mechanical integrity for complicated designs [195].

Kumar, Narendra, et al. "Additive manufacturing of flexible electrically conductive polymer composites via CNC-assisted fused layer modeling process." *Journal of the Brazilian Society of Mechanical Sciences and Engineering* 40.4 (2018): This study is an

initial step towards developing flexible composites, which helps find suitable wt% of graphite to make EVA material conductive with the desired flexibility. Most importantly, the developed composite remains printable through the developed FLM process even after adding up to 50 wt.% of graphite [196].

Dickson, Andrew N., et al. "Fabrication of continuous carbon, glass and Kevlar fibre reinforced polymer composites using additive manufacturing." *Additive Manufacturing* 16 (2017): Using additive manufacturing (AM), nylon composites reinforced with continuous glass, carbon, and Kevlar fibers were produced. The printed composites' tensile and flexural strength showed a maximum increase of 6.3 times and 5 times, respectively, compared to the values obtained for the nylon control samples. It was revealed that the FDM composites had higher tensile capabilities than aluminium. This study determined the following to be the strength of polyamide composites: Carbon fibre >Glass fibre> Kevlar fibre in importance. However, the degree of enhancement in mechanical strength was constrained as the fibre content continued to rise. This can be partly attributed to the inadequate bonding between the layers of fiber and nylon and the higher occurrence of air cavities. Fibre content was observed to enhance the latter. One could say that technology has considerable future development potential and could enable the fabrication of composite materials that are presently unattainable. [197].

Bryll, Katarzyna et al. "Polymer Composite Manufacturing by FDM 3D Printing Technology." *MATEC Web of Conferences*. Vol. 237. EDP Sciences (2018): 3D printing generated individual components of intricate items using a CAD model without costly equipment or moulds. This technology's progress led to the production of prints in various domains. An efficient and effective method utilizing FDM modeling was introduced. Additional benefits encompass the declining costs of printers, enhanced software, and an expanding range of used materials, such as composites, which enhance the mechanical characteristics of 3D prints [198].

Kim, Heechang et al. "Experimental study on mechanical properties of single-and dual-material 3D printed products." *Procedia Manufacturing* 10 (2017): This study demonstrated that the mechanical qualities of objects produced using Fused Deposition Modeling (FDM) were enhanced when various materials were utilized. The optimal parameters were analyzed by examining their effects on the mechanical properties using analysis of variance (ANOVA). Prior studies have mainly focused on investigating the

mechanical characteristics of 3D printed materials by examining their orientation and infill rate. The specimens were fabricated using two different materials, which allowed for the determination of the orientation angles, infill rate, and structural arrangement. The tensile strength of an object is influenced by its structural arrangement, even if it is printed with comparable proportions of two materials. Thus, by appropriately utilizing this structural arrangement, one can achieve optimized efficiency in manufactured parts, including enhanced tensile strength and reduced manufacturing cost. The first experiment involved creating specimens of Acrylonitrile butadiene styrene (ABS) and polylactic acid (PLA) according to the ASTM standards D-638. This experiment aimed to identify the parameters that influence the tensile strength in a single material setting. An ANOVA was used to choose the parameters of orientation angle, infill rate, and kind of material. Multiple findings were derived from the analysis. The mechanical properties of materials in the x-direction were optimal when employing PLA with a fill rate of 100%. The 3D printer utilized in this study could fabricate goods using various materials. ABS and PLA are the filaments that are most often employed. Experiments were undertaken to determine the variation in tensile strength based on the ratio of the two materials. The ANOVA results indicated that the extruding process in FDM 3D printing was unsteady. It was shown that voids and overlaps can arise in the interface between two materials. This issue should be considered when producing a product that involves several materials, as it might generate waste materials or incur inefficient expenses in the manufacturing sector [199].

Balla, Vamsi Krishna et al. "Additive manufacturing of natural fiber reinforced polymer composites: Processing and prospects." *Composites Part B: Engineering* (2019): Additive manufacturing of polymer composites has shown its capability to produce intricate, functional parts with precise dimensions suitable for immediate utilization. Moreover, the distinct advantage of utilizing AM for producing NFRCs is its capability to fabricate functionally graded composites that possess performance and functionality tailored to specific locations. It is feasible to create and manufacture structures with customized fiber alignment by altering the deposition routes in each layer. Nevertheless, additive manufacturing (AM) of these composites presents notable difficulties regarding the preparation of composite filaments for fused filament fabrication (FFF), the tendency of natural fibers to clump together, the presence of excessive moisture and

voids, challenges in 3D printing of natural fiber-reinforced composites (NFRCs) due to nozzle blockage, fiber deterioration or fracture, and uneven curing [200].

Slotwinski John A. "Additive manufacturing: Overview and NDE challenges." AIP Conference Proceedings. No. 1. American Institute of Physics (2014). The additive manufacturing sector, which has long operated without classification schemes for AM technologies, has faced challenges in knowledge sharing and education for both technical and non-technical audiences. However, the use of process categories offers a practical solution, allowing us to focus on specific groups of machines rather than presenting a long list of commercially available process variations, thereby improving the efficiency and effectiveness of our communication.

(i) Binder jetting is a method of additive manufacturing in which a liquid bonding agent is selectively deposited to join particle materials.

(ii) Applied energy deposition, often referred to as directed energy deposition, is a method of additive manufacturing that uses concentrated thermal energy, such as a plasma arc, electron beam, or laser, to melt materials during the deposition process. (iii) Material extrusion is an additive manufacturing procedure wherein a nozzle or orifice is utilised to dispense material selectively.

(iv) Material jetting is an additive manufacturing technology that selectively deposits particles of constructed materials, such as wax and photopolymer.

(v) Powder bed fusion is an additive manufacturing technique wherein specific areas of a powder bed are fused selectively using thermal energy.

(vi) Sheet lamination is an additive manufacturing technique that involves bonding material sheets to create the structure of an object.

(vii) Vat photopolymerisation is an additive manufacturing process wherein light-activated polymerisation selectively cures liquid photopolymer in a vat. [201].

Gnanasekaran, Karthikeyan et al. "3D printing of CNT-and graphene-based conductive polymer nanocomposites by fused deposition modeling." *Applied materials today* 9 (2017): The potential of desktop 3D printing to create intricate structures for cost-effective large-scale manufacturing is immense. This study uses FDM-based 3D printing to create functional 3D model structures using conductive polymer nanocomposites made from CNT and graphene. To achieve highly functional and structurally durable structures, PBT was used as a polymer, as opposed to the regularly

used polymers PLA and ABS. An assessment was conducted on the printability, electrical conductivity, crystallinity, morphology, and viscoelastic properties of the 3D-printed structures. The investigation revealed that PBT/CNT 3D printed materials exhibit superior functional qualities, including enhanced elasticity and conductivity and improved aesthetics, compared to PBT/G 3D printed structures. [202].

Haider, Sajjad et al. "Thermoplastic nanocomposites and their processing techniques." *Thermoplastic: Composite Materials* (2012): Their research has emphasized polymeric nanocomposites' significant technological and economic possibilities, encompassing various nanofillers like clay, carbon nanotubes, SiO₂, SiC, and Si₃N₄, both inorganic and organic. For the production of these nanomaterials on a large scale, it is crucial to address several challenges related to integrating nanoparticles into a polymer matrix, enhancing their properties, and understanding the mechanisms behind these advances. Therefore, it is anticipated that polymeric nanocomposites will permeate several domains of human existence near and distant future, just like plastics did in the previous century. Various industries, including aerospace, automotive, packaging (especially in the food and solar cell sectors), electrical and electronic goods, and household goods, would greatly benefit from introducing novel nanotechnology materials [203].

Jia, Yunchao et al. "High through-plane thermal conductivity of polymer-based product with vertical alignment of graphite flakes achieved via 3D printing." *Composites Science and Technology* 145 (2017): This work demonstrates the achievement of high through-plane thermal conductivities (TPTCs) in polymer/graphite-based products by utilizing Fused Deposition Modeling (FDM) with vertically aligned graphite flakes. The printing technique substantially impacts the alignment of graphite flakes and the arrangement of empty spaces in objects made by FDM fabrication. The TPTC is influenced by the graphite's orientation and the distribution of voids. The product forged using SP has a significantly higher Thermal Performance Test Coefficient (TPTC) than the product created using FP, although having the same graphite content. There are two causes for this phenomenon. Firstly, the graphite flakes are aligned in the through-plane direction in SP manufactured goods.

On the other hand, in FP-made products, similar to conventional moulding processes, the graphite flakes are oriented in the in-plane direction. Another factor is that the voids in products fabricated using FP (Fused Deposition Modeling) obstruct the smooth flow

of heat, which is conducive to efficient heat transfer. On the other hand, the voids in products fabricated using SP (Selective Laser Sintering) are arranged in a manner that allows them to align along the direction perpendicular to the plane of the product. Therefore, the paths for efficient heat conduction can be established without obstructing empty spaces. The significance of this work is that it has successfully produced a thermally conductive product with vertically aligned graphite flakes using FDM technology. This achievement has potential benefits for the practical use of FDM in thermally conductive polymer composites [204].

Tekinalp, Halil L. et al. "Highly oriented carbon fiber–polymer composites via additive manufacturing." *Composites Science and Technology* 105 (2014): ABS resin feedstock with varying amounts of carbon fiber was created, and these feedstock materials were effectively employed to create composite specimens using FDM printing and compression-moulding techniques. The findings indicate a considerable decrease in the average length of the fibers in both procedures, most likely due to the high-shear mixing process during compounding. Although CM (Compression Molding) samples did not exhibit any evident porosity or void, FDM-printed samples displayed noticeable porosity. The presence of more fiber in the FDM-printed beads led to an increase in internal voids, but the spaces between the beads were reduced. The FDM-printed samples exhibit a significant degree of fiber alignment in the printing direction, approaching near-perfect alignment with the beads. The results obtained from the CM specimens clearly demonstrate that porosity significantly impacts tensile characteristics more than fiber orientation. In addition, scanning electron microscope (SEM) images reveal that the fibers have detached from the matrix, suggesting a lack of strong bonding between the fibers and the matrix [205].

Guo, Yichen et al. "Engineering flame retardant biodegradable polymer nanocomposites and their application in 3D printing." *Polymer Degradation and Stability* 137 (2017): This work demonstrates the feasibility of producing a biodegradable nanocomposite with flame retardant properties, rated V0, using PLA combined with MPP (micro-perforated panel) and C-30B. The findings indicate that the compound, including PLA and MPP, exhibits notable creep and causes the cotton to catch fire during the UL-94 test despite its ability to self-extinguish after 2 seconds. Using 1% C-30B eliminates creep by boosting the G0 value by a factor of five while generating an intumescent char

that can self-extinguish. Adding a single extra percentage of C-30B, resulting in a 2%, preserves the G0 improvement but harms the flame retardant characteristics. TEM cross-sectional images show that when the concentration of C-30B is 1%, the clay platelets separate at the interfaces between MPP and PLA, enhancing MPP dispersion within the PLA matrix. This leads to a decrease in the peak heat release rate (PHRR) and average heat release rate (AHRR). However, increasing the C-30B concentration to 2% causes the C-30B to aggregate in the MPP region, blocking contact between MPP and PLA and preventing the formation of the intumescent char [206].

Coiai, Serena et al. "Nanocomposites based on thermoplastic polymers and functional nanofiller for sensor applications." *Materials* 8.6 (2015): This review paper discusses the notable progress made in the development and analysis of thermoplastic nanocomposites that have the potential to be used as sensors. The paper focuses explicitly on successfully distributing zero-dimensional, one-dimensional, and two-dimensional nanostructured organic or inorganic fillers. Expressly, meticulously crafted additives have been incorporated into polymer matrices utilizing various methods such as solution-based techniques, in-situ polymerization approaches, self-assembly techniques, and melt mixing. These methods have been employed to explore the potential of introducing sensing capabilities. The collected results demonstrate the practicality of the methods used and the possibility for these hybrid systems to serve as pH sensors, electrochemical sensors, volatile organic compounds (VOCs) and biological molecules, and sensors for detecting hazardous molecules [207].

Dul, Sithiprumnea, Luca Fambri, and Alessandro Pegoretti. "Fused deposition modelling with ABS–graphene nanocomposites." *Composites Part A: Applied Science and Manufacturing* 85 (2016): Graphene nanoplatelets were effectively incorporated into an ABS matrix through solvent-free melt compounding. Subsequently, these nanoplatelets were extruded into filaments appropriate for fused deposition modelling. As a result of the limitations imposed by the procedure, the filler content was optimised to 4 wt.%. A comparison was made between the thermo-mechanical properties of pure ABS and its nanocomposites on samples produced via various processing techniques, including extrusion, compression moulding, fused deposition modelling, and extrusion. Graphene nanoplatelets enhanced the tensile modulus of ABS in every instance. In FDM samples, this positive effect was also confirmed in various orientations. Also, adding

xGnP lowers the ultimate tensile stress and strain at rupture for specimens built in both horizontal and vertical planes. The effect is more substantial when the specimens are made perpendicular to the aircraft. Additionally, this study demonstrates that xGnP decreases the thermal dilation coefficient of 3D-printed components and enhances their resistance to prolonged loading. [208].

Golbang, Atefeh et al. "Production and characterization of PEEK/IF-WS2 nanocomposites for additive manufacturing: Simultaneous improvement in processing characteristics and material properties." *Additive Manufacturing* 31 (2020): This study involved the production of PEEK nanocomposites with different weight percentages (0.5, 1, and 2 wt%) of IF-WS2. The purpose was to create materials suitable for additive manufacturing by combining the desirable properties of both organic and inorganic materials. The samples were examined for print quality using a microscope. Visible imperfections, such as non-uniformities and voids, were observed in the unfilled PEEK samples and were marked with circles [209].

Lee, Geuntak et al. "Fabrication of ceramic bone scaffolds by solvent jetting 3D printing and sintering: Towards load-bearing applications." *Additive Manufacturing* 33 (2020): An investigation was conducted on the cost and time-effective production of hierarchical porous structures for load-bearing purposes. This text outlines the techniques for preparing nano and micron-sized alumina powders for the solvent jetting powder bed 3D printing method (P-3DP). Under the testing settings, increasing the nozzle temperature and reducing the layer height in this 3D printing procedure resulted in higher green density, sintered density, and compressive strength. The P-3D P technique can generate inherently porous structures by manipulating 3D printing parameters and powder properties. Increased porosity is advantageous for the bone scaffold. Nevertheless, the ceramic parts produced by P-3DP tend to suffer post-sintering issues, such as inadequate final densities (or even a failure to sinter) and associated poor strength. The primary reason for this is the correlation between porous structures and the sinterability of the green components [210].

Loh, Giselle Hsiang et al. "An overview of functionally graded additive manufacturing." *Additive Manufacturing* 23 (2018): This study has provided a comprehensive overview of the functionally graded additive manufacturing process, including all aspects from design to production. FGAM technologies offer significant

opportunities for designers and engineers to create structures with varying properties by precisely manipulating substance density and material mixing. Future efforts will be directed towards adjusting the proportions of aggregates, foaming agents, and bio-printing scaffolds and bio-inks utilizing FGAM as the technology advances and its applications expand. FGAM is expected to undergo another significant metamorphosis by utilising numerous stimulus-responsive materials. This means the manufactured component can change shape from one form to another when triggered by the appropriate stimuli [211].

Gnanasekaran, Karthikeyan et al. "3D printing of CNT-and graphene-based conductive polymer nanocomposites by fused deposition modeling." *Applied Materials today* 9 (2017): This study indicates that desktop 3D printing has significant potential to create intricate structures that can be utilised for cost-effective large-scale manufacturing. Conductive polymer nanocomposites comprising carbon nanotubes and graphene are used to create functional 3D model structures. This is achieved using filament extrusion and FDM-based 3D printing. To further clarify, polybutylene terephthalate (PBT) has been employed as a fundamental polymer. In contrast to PLA and ABS, which are frequently used polymers, PBT is used to construct sturdy and valuable structures. An assessment was conducted on the printed structures' printability, electrical conductivity, crystallinity, morphology, and viscoelastic properties. The investigation revealed that PBT/CNT 3D printed materials exhibit superior functional qualities, including enhanced elasticity and conductivity and improved aesthetics, compared to PBT/G 3D printed structures. The optimisation of new materials for 3D printing grades is necessary to ensure the appropriate flow rate, crystallisation and shrinking qualities, and functional properties. Substantial advancements are required in the design of nozzles for printing abrasive substances to minimise the risk of clogging caused by conductive fillers [212].

Kim, Heechang et al. "Experimental study on mechanical properties of single-and dual-material 3D printed products." *Procedia Manufacturing* 10 (2017): This study indicates that desktop 3D printing has significant potential to create intricate structures that can be utilised for cost-effective large-scale manufacturing. Conductive polymer nanocomposites comprising carbon nanotubes and graphene are used to create functional 3D model structures. This is achieved using filament extrusion and FDM-based 3D printing. To be more specific, polybutylene terephthalate (PBT) has been used

as a basic polymer, and compared to PLA and ABS, which are commonly used polymers, it is used to make valuable and strong structures. An assessment was conducted on the printed structures' printability, electrical conductivity, crystallinity, morphology, and viscoelastic properties. The investigation revealed that PBT/CNT 3D printed materials exhibit superior functional qualities, including enhanced elasticity and conductivity and improved aesthetics, compared to PBT/G 3D printed structures. The optimisation of new materials for 3D printing grades is necessary to ensure the appropriate flow rate, crystallisation and shrinking qualities, and functional properties. Substantial advancements are required in the design of nozzles for printing abrasive substances to minimise the risk of clogging caused by conductive fillers [213].

Prakash, K. Satish, T. Nancharaih, and VV Subba Rao. "Additive manufacturing techniques in manufacturing-an overview." *Materials Today: Proceedings* 5.2 (2018): AM methods, categorised into four groups based on the condition of the initial material, have the potential to revolutionise manufacturing. The process of producing a layer involves various techniques such as UV light-induced polymerization, ink-jet printing, extrusion, laser melting, and more. While polymers were initially the focus of AM technology, the focus has now broadened to include metals, ceramics, and composite materials. Despite the significant advantages of AM technology over subtractive manufacturing methods, it is still often perceived as a specialised technology. To increase industry acceptance, there is an urgent need for research and development in numerous fields, including materials, energy and sustainability applications, design, innovative processes and machines, process modelling and control, and biomedical applications. This will not only expand the range of applications for additive manufacturing technology but also establish it as a widely used technology [214].

Reddy, Kanuparti Vishnu Prashant, Ishrat Meera Mirzana, and A. Koti Reddy. "Application of Additive Manufacturing technology to an Aerospace component for better trade-off." *Materials Today: Proceedings* 5.2 (2018): Utilising additive manufacturing technology to enhance the trade-off of an aerospace component. This paper demonstrates the successful optimisation of the Aerospace Flap lever component used by the design objective. The optimised component has decreased its weight by approximately two-thirds of the original volume and exhibits an improved safety margin. The use of additive manufacturing (AM) is anticipated to reduce the time

required to manufacture the part. The component's size reduction in energy deposition methods can be attributed to the material properties, process parameters, and the final part's geometry. Producing the flap lever component using additive manufacturing will enable individuals to investigate the superior characteristics of this manufacturing method [215].

Bryll, Katarzyna et al. "Polymer Composite Manufacturing by FDM 3D Printing Technology." MATEC Web of Conferences. Vol. 237. EDP Sciences, 2018. The evolution of 3D printing technology as it relates to various aspects of daily life is examined in this article. One of the few 3D printing systems that is especially prevalent is the one that utilises FDM modelling due to its capabilities and straightforwardness. Additional benefits encompass reduced printer costs, enhanced software capabilities, and an expanded range of materials used, such as composites, which contribute to the improved mechanical properties of 3D printing. Despite the growing attention towards printing composite materials, many concerns still necessitate additional examination. Fibre alterations or intermittent printing give rise to critical technical challenges that require resolution. Additionally, it is essential to explore novel material pairings and modify them to suit the printing process, so long as such modifications are both economically viable and environmentally sustainable [216].

Thompson, Mary Kathryn et al. "Design for Additive Manufacturing: Trends, opportunities, considerations, and constraints." CIRP annals 65.2 (2016): The progress in additive manufacturing leads to novel design opportunities, products, and production models. Although further design development for additive manufacturing is required, small and large enterprises are rapidly studying and embracing AM to produce final parts. Both individuals and industry are actively contributing to advancements in research and practice, exerting influence from both the highest levels and the grassroots level. The outcomes will revolutionise the principles of product development and unveil novel items. This study has outlined the notable design possibilities, limitations, and expenses related to DFAM (Design for Additive Manufacturing) and has showcased the current feasible and cost-effective options.

Nevertheless, the design for additive manufacturing (AM) is currently in its early stages. Greater comprehension is needed regarding the appropriate timing and methodology for AM design, and several of the necessary technologies to facilitate it still need further

development. This section examines the forthcoming difficulties and emerging trends that will influence DfAM (Design for Additive Manufacturing) and the technologies it will facilitate [217].

Van de Werken, Nekoda et al. "Additively Manufactured Carbon Fiber-Reinforced Composites: State of the Art and Perspective." *Additive manufacturing* (2019): This paper does not provide an in-depth analysis but offers an overview of AM carbon fibre composite technologies and highlights some of the remaining issues in this field. However, most investigations have primarily concentrated on characterising the tensile properties of additive manufacturing (AM) composites. Studying the non-tensile characteristics and failure/fracture mechanics is crucial to developing AM parts effectively. Some thermosetting polymers can be printed in 3D. We require new chemical compositions and nanocomposites to enhance additive manufacturing components' performance. Multiple flaws are introduced during additive manufacturing. Gaining insight into the formation of these faults can pave the way for techniques to minimise or eradicate them. This will facilitate improved characteristics and expedite the validation procedure for these innovative materials [218].

Wang, Shuheng, et al. "Implementation of an elastoplastic constitutive model for 3D-printed materials fabricated by stereolithography." *Additive Manufacturing* 33 (2020): This study developed an elastoplastic constitutive model to describe the mechanical behaviour of SLA-printed materials quantitatively. The influences of the printing angle and layer thickness are considered. We got the parameters for the Hill anisotropic yield model and the transversely isotropic elastic model by testing the material in a single direction. The experimental and theoretical results obtained are in good agreement. The following conclusions can be drawn from the results: The equations of the elastic modulus and ultimate tensile strength as functions of the printing angle are derived, and the theoretical results agree well with the experimental results. Both layer thickness and printing angle can affect the mechanical properties of SLA-printed materials; the more significant the layer thickness, the smaller the elastic modulus and the ultimate tensile strength. [219].

Singh, Sunpreet, Seeram Ramakrishna, and Rupinder Singh. "Material issues in additive manufacturing: A review." *Journal of Manufacturing Processes* 25 (2017): This paper shows that AM and its capabilities of producing customised implants have successfully

overtaken most of the traditional manufacturing processes and occupied a key position. In the present review, with the emergence of AM technologies, medical services have matured enough to tackle critical health issues rapidly and precisely. Moreover, mechanical, physical and metallurgical properties are yet to be established for these alternative materials-based components. To tackle such pressing issues, the following roadmaps should be taken care of to explore the actual field of the problem.

- ❖ Build a problem-relevant knowledge.
- ❖ By establishing research facilities.
- ❖ Training of personnel.
- ❖ Involvement of individuals from industries.
- ❖ Adoption of industrial standards.
- ❖ Material research and development.
- ❖ Establishment of materials and products.
- ❖ Sharing project outcomes. [220]

Salmi, Mika, et al. "Patient-specific reconstruction with 3D modeling and DMLS additive manufacturing." *Rapid Prototyping Journal* (2012). This paper aims to develop a workflow for 3D modelling and additive manufacturing (AM) of patient-specific medical implants. The comprehensive workflow consists of four steps: medical imaging, 3D modelling, additive manufacturing, and clinical application. Implants reconstruct bone damage or defects caused by trauma or disease. Traditionally, implants have been manually bent and shaped, either preoperatively or intraoperatively, with the help of anatomic solid models. The proposed workflow obviates the manual procedure and may result in more accurate and cost-effective implants. This method enables the exact fitting of implants to surrounding tissues. Creating implants before surgery improves accuracy, may reduce operation time and decrease patient morbidity, hence improving the quality of surgery. [221].

Kumar, Narendra, et al. "Experimental investigations on suitability of polypropylene (PP) and ethylene vinyl acetate (EVA) in additive manufacturing." *Materials Today: Proceedings* 5.2 (2018): 4118-4127. This experimental study shows the suitability of EVA and PP materials for additive manufacturing. The parts could be fabricated with desirable properties, which offer the fabrication of flexible and lightweight parts with EVA and PP, respectively, directly on the developed MDT system. Further

improvement is required in the MDT system in terms of optimization of process parameters, better accuracy and the quality of the produced parts. [222].

Kumar, Narendra, et al. "Extrusion-based additive manufacturing process for producing flexible parts." *Journal of the Brazilian Society of Mechanical Sciences and Engineering* 40.3 (2018): 143. It has developed a pellet-based extrusion AM process for fabricating flexible parts using EVA material. This paper explains the developed hardware, tool path-planning software, sub-systems, and process parameter tuning. And that the EVA printed specimen could elongate up to 575.5%, which is very high compared to ABS and PLA materials. And indicate that the developed system can produce highly flexible parts using EVA material. In the extrusion AM process, when extruded material deposits in a semi-molten state on the heated bed, then the circular cross-sectional profile of the filament slightly deforms and changes into an elliptical one due to self-weight improvement. [223].

Taufik, Mohammad, and Prashant K. Jain. "Characterization, modeling and simulation of fused deposition modeling fabricated part surfaces." *Surface Topography: Metrology and Properties* 5.4 (2017): 045003. In the preprocessing phase of the FDM process, optimal process strategy can be achieved by characterization, modelling and simulation of roughness parameters in advance. The effect of the study provides vital findings to characterize, model and simulate the part surfaces fabricated by the FDM process. Three roughness parameters were considered important factors to be studied, and findings of an experimental study that describes the effect of layer thickness and build orientation on the kurtosis (R_{ku}), skewness (R_{sk}) and average surface roughness (R_a) of the FDM part surface. From this study, it is found that various surface defect uncertainties are associated with horizontal surfaces. Therefore, the kurtosis value of flat surfaces is relatively different from a typical aspect of surface fabricated and built orientation. In this research work, the average roughness does not characterize a surface with sharp peaks and deep valleys. Kurtosis and skewness appear to be significant factors in determining distinct surface profile features of the FDM part profile. [224].

2.6 Summary of literature review

There are several reasons for implementing Additive Manufacturing in product development like a rapid response to market demand and market changes, reduced

manufacturing lead time, reduced cost of operation, customer satisfaction, improved business performance, minimize sustaining changes, increased product lifetime. It has studied the most polymeric nanocomposite materials have mechanical, thermal, and electrical properties that are significantly enhanced through additive manufacturing.

2.7 Motivation

Innovative Synthesis: Additive manufacturing offers a novel approach to synthesizing polymeric nanocomposites with precise control over their structure and properties. By exploring this technique, you're at the forefront of innovation in materials science.

Tailored Properties: Polymeric nanocomposites possess unique mechanical, thermal, and electrical properties compared to traditional materials. Through additive manufacturing, these properties can be customized to suit specific applications, opening doors to new technologies and advancements.

Sustainability: Additive manufacturing promotes sustainability by minimizing material waste and energy consumption. By studying polymeric nanocomposites through this process, you're contributing to the development of eco-friendly materials and manufacturing practices.

Versatile Applications: Polymeric nanocomposites have a wide range of applications, from aerospace to biomedical engineering. By understanding how additive manufacturing influences their structure and performance, you're paving the way for breakthroughs in various industries.

Interdisciplinary Collaboration: Studying polymeric nanocomposites through additive manufacturing requires collaboration across disciplines such as materials science, chemistry, physics, and engineering. By working at the intersection of these fields, you have the opportunity to foster interdisciplinary research and drive innovation.

Market Demand: As industries seek lightweight, durable, and multifunctional materials, the demand for polymeric nanocomposites continues to grow. By advancing our understanding of these materials through additive manufacturing, you're positioning yourself at the forefront of a rapidly expanding market.

Academic Contribution: Your research contributes to the academic knowledge base in materials science and additive manufacturing. By publishing your findings, you're advancing the collective understanding of polymeric nanocomposites and inspiring future generations of researchers.

Overall, studying polymeric nanocomposites through additive manufacturing is not just about exploring new materials—it's about pushing the boundaries of what's possible, driving innovation, and shaping the future of materials science and engineering.

2.8 Research Gaps

The following research gaps identified:

- (i) For the design of additive manufacturing (AM) parts that have yet to be examined, it is vital to conduct investigations of non-tensile characteristics and failure/fracture mechanics.
- (ii) These novel chemistries and nanocomposites, which are not reported in the literature review, have the potential to provide high-performance additive manufacturing parts.
- (iii) Methods for reducing or eliminating defects during AM have not been focused in detailed.
- (iv) 3D Printed structure have not been tried different nanocomposites. Then, new materials need to be optimized for 3D printing grades to have the proper flow rate, crystallization, and shrinking properties, in addition to their functional properties.
- (v) The researchers have identified about in Graphene nanoplatelets were not compounded in another material except of ABS matrix.
- (vi) The literature review provides further evidence that polymeric nanocomposites are anticipated to permeate all facets of life in the medium to long term, much like plastics did in the previous century. Aerospace, automotive, packaging (particularly for solar cells but also for food), electrical and electronic products, and home goods are just a few of the industries that will surely gain a great deal from introducing a novel material palette made possible by nanotechnology.

CHAPTER 3

MATERIALS AND METHODS

This chapter deals with the raw ingredients, experimental setups and processing processes used to prepare the polymeric nanocomposite. It also covers the procedures for developing the material. The prepared materials used for the fabrications of specimens through micro injection moulding machine and 3 D printings. The study begins with a discussion of the specific polymer and polymeric nanocomposite materials, followed by examining the processing processes and characterization methods utilized for identification and analysis.

3.1 Selection of base polymer and nanocomposites

MWCNTs/ABS composites have several benefits, although they can be more expensive than standard materials. However, decreased material consumption, increased performance, and design flexibility can offset this higher initial cost, making the composite more cost-effective in some applications. The application, production volume, and composite's increased properties will also affect cost-effectiveness. The 1, 2, and 3 wt.% of MWCNTs were used as reinforcing agents in the pure ABS thermoplastic resin. The ABS was procured from Bhansali Group of India at the cost of 1.5\$ per kg. ABS ($C_8H_8:C_4H_6:C_3H_3N$) has a density of 1.068 g/cm³ and a melting temperature of 260 °C. The MWCNTs were procured from NANOCYL, Belgium as NC7000™ series at the cost of 60\$/ kg. The average diameter and length of procured MWCNTs were 9.5 nm and 1.5 μm respectively. The weight of MWCNT mixed in 1.0 kg of ABS was 10, 20, and 30 g for different types of samples. Hence 1, 2, and 3 wt.% of MWCNTs were mixed into the ABS for single- and double-extrusion process.

3.2 Fabrication of MWCNTs/ABS nanocomposites specimen.

The experimental setup used a co-rotating twin-screw extruder. MWCNTs and ABS were mixed and melted to make a composite using Thermo Scientific Prism Euro lab 16, as shown in Figure 3.1. The composite was extruded using a twin-screw extruder at 100 r/min and 260 °C to ensure a homogeneous distribution of MWCNTs throughout the polymer. The extruded wire composite was cut into granules [225].

The preparation of multi-walled carbon nanotubes (MWCNTs)/acrylonitrile-butadiene-styrene (ABS) nanocomposites through a twin-screw extruder process involves the incorporation of MWCNTs into the ABS matrix to enhance its mechanical, thermal, and electrical properties. Here's a general guide on how you can prepare MWCNTs/ABS nanocomposites using a twin-screw extruder. It was prepared by adding 1,2, and 3 wt.% of MWCNTs in Acrylonitrile Butadiene Styrene (ABS) in two types of material: (i) single time extruding and (ii) second time extruding process. The nanocomposites have been found in the form of granular. specimens were prepared containing 1, 2, and 3 wt.% of MWCNTs. The flow process of specimen preparation is shown in Figure 3.2. The specimens were prepared as per ASTM standard 638 D, the drawing and dimensions are shown in figure 3.4.

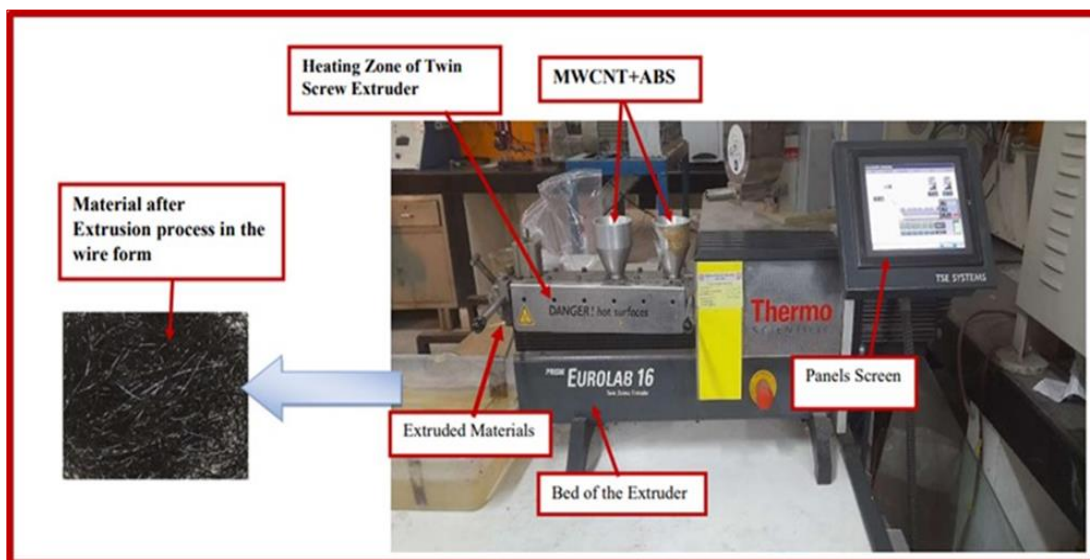


Figure 3.1: Experimental Setup for preparation of MWCNTs/ABS Nanocomposites, Twin screw extruder (THERMO SCIENTIFIC PRISM EUROLAB 16).

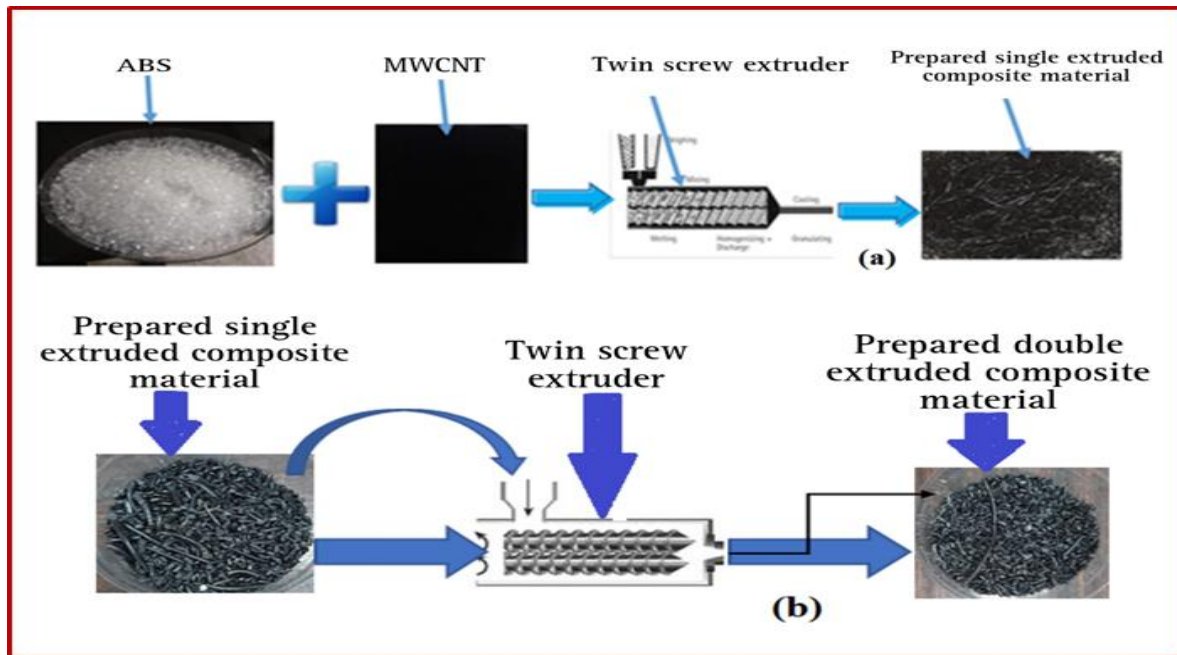


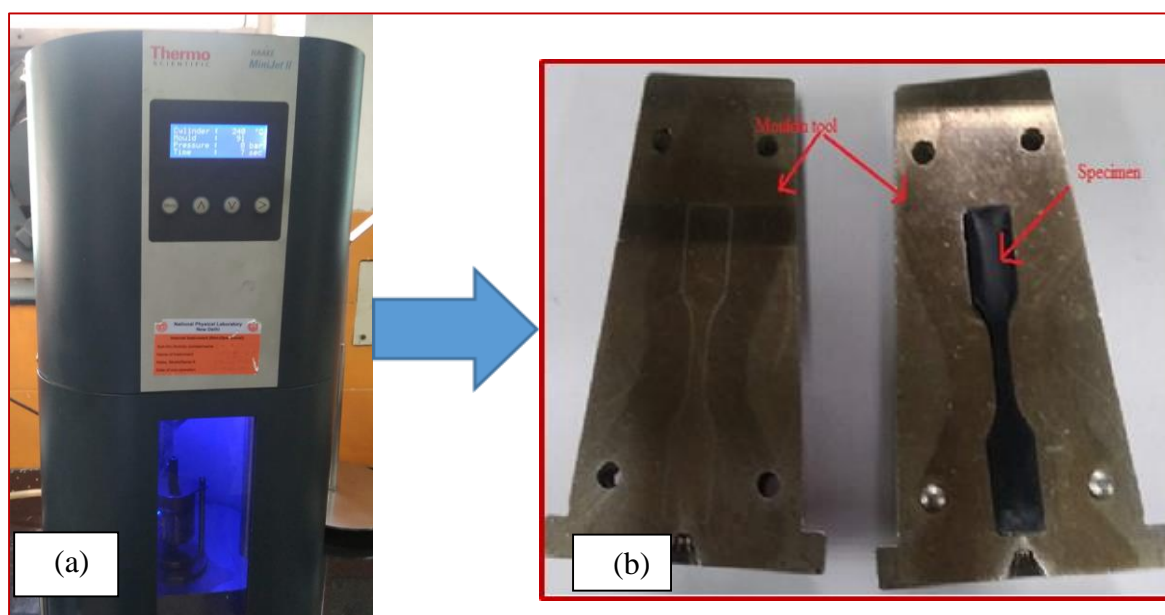
Figure 3.2. Flow process diagram for preparing the specimen samples of single time extruding and second time extruding by twin screw extruder.

3.3 Preparation of specimens by microinjection moulding:

The Thermo Scientific HAAKE MiniJet II piston injection moulding machine shown in Fig. 3.3 (a) prepares samples efficiently for mechanical and rheological testing. Mechanical testing often requires many sample specimens. These specimens can be injection moulded, cut from pressed sample plates, or made manually using a sample test instrument. Creating numerous sample shapes with limited material quantities complicates product development. The HAAKE MiniJet II technology optimises development and reduces costs. They were making test specimens from 5g. The samples obtained from moulding tools it shows in Fig. 3.3. (b). Test specimens can be powders, pellets, or melts, simple control and design strategy with reproducible results. Sample geometries range from standard to bespoke. With a unique slit backflow channel, the HAAKE MiniLab II processes small amounts of material and measures viscosity. Mechanical and rheological testing can then be done on specimens [226].

Table 3.1 Technical specifications of Thermo Scientific Haake MiniJet II

Injection pressure	max. 1,200 bar
Dimensions	300 mm x 460 mm x 710 mm
Power	230 V \pm 10 %, 3.15 A, 50...60 Hz 110 V \pm 10 %, 3.15 A, 60 Hz
Air pressure	max. 10 bar
Mold temperature	max. 250°C
Cylinder temperature	max. 400°C

**Figure 3.3 (a) Micro Injection moulding (b) Moulding tool with moulded specimens**

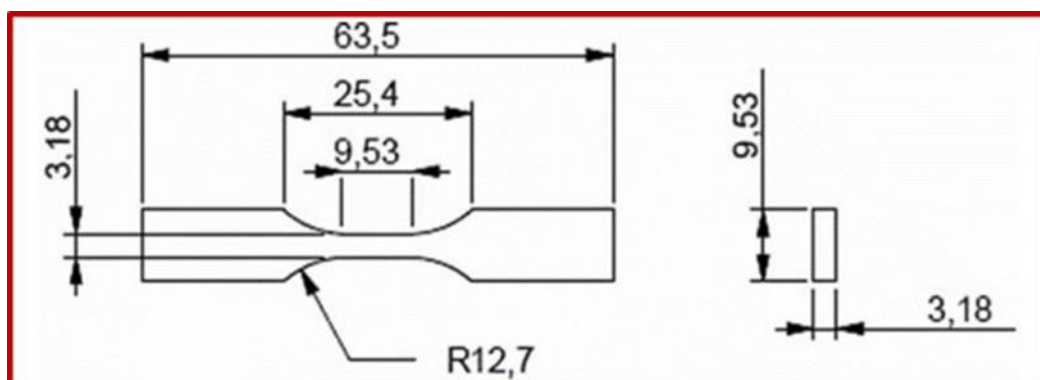


Figure 3.4 Drawing of prepared sample with proper dimensions as per ASTM 638 D by micro injection molding and 3 D printing.

3.4. Fused filament fabrication of MWCNTs/ABS composites

The flow process diagram for MWCNTs/ABS composite filament extrusion from granular composite material is shown in figure 3.5. The filament extrusion process was performed through single screw extruder at Solidspace Technology, Nashik, India [227]. Table 3.2 shows the specifications of single screw filament extruder used for filament fabrication from granular composite material.

The filament production parameters are given in Table 3.3. Filaments of 1.75 mm diameter were fabricated from the prepared MWCNTs/ABS granular composite

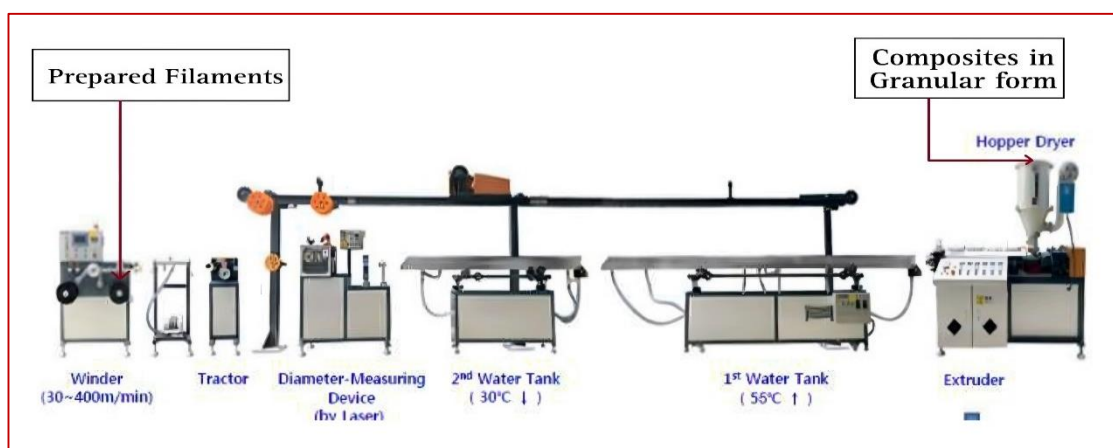


Figure 3.5 Schematic diagram of filament extrusion process for preparing the filament for various wt.% of MWCNTs/ABS

Table 3.2 Specification of filament Extruder Scientific machine.

Extruder Type	Single Screw
Diameter of Screw	45mm
Length /Diameter Ratio	30:1
Power of Motor	6Kw/ 8 HP
Motor RPM	1440
Production Trial Screw Speed	30 RPM
Maximum Screw Speed	90 RPM
Extruder Die Diameter	4mm

Table 3.3 Production parameters for filaments extruders:

Feed Zone Temperature	160 °C
Compression Zone Temperature	170 °C
Mixing zone Temperature	185 °C
Die Temperature	180 °C
Hot Water Cooling Temperature	55 °C

The figure 3.6 shows prepared filament as per required specification which were used to make specimens through 3 D printing process.



Figure 3.6 Prepared filaments ready to 3 D print (a) Pure ABS, (b) 1wt. % of MWCNT/ABS, (c) 2wt. % of MWCNT/ABS and (d) 3 wt. % of MWCNT/ABS.



Figure 3.7 Flashforge Dreamer 3D printer used to prepare specimens

3.5 Preparation of specimens by FDM 3D printing

Fused deposition modelling (FDM) is a 3D printing technique developed in 1989 by Stratasys co-founder Scott Crump for thermoplastic polymers and composites [228]. The Table No. 4 shows the specification of Flashforge Dreamer 3D printer setup shown in Fig. 3.7, used to prepare the specimen for tensile strength testing. Using various monofilament blends, several models and samples were printed using an FDM printer (Zhejiang Flashforge 3D Technology Co., Ltd.). Here's how a regular FDM print job goes down: The software was first used to create digital models, then exported as standard triangle language (STL) files. Second, the printer software was used to alter the STL files, exported as g-code slides files. The FDM printer received the g-code slides files. Finally, the FDM printer fed two pinch rollers of a 1.75 mm monofilament. The FDM printer used a 0.40 mm nozzle with a nozzle temperature of 210 °C [229]. The Standardised tensile test specimens were printed with the composite filaments

utilising pure ABS and 1, 2, and 3 wt. % of MWCNTs reinforced and fabricated specimens according ASTM D-638 shown in figure 3.4. Pure ABS and each loading percentage specimens were tested.

Table 3.4 The FDM process used for experimental setup of *DREAMER FLASH FORGE* Specifications

No of Extruder	2
Diameter of Nozzle	0.4mm
Maximum Extruder Temperature	240°C
Printing Speed in mm/s	30-100
Maximum Temperature of platform	110°C (230°F)
Compatibility of Filament	PLA, TPU95A, ABS, PETG
Diameter of Filament	1.75 mm
Maximum Print Volume	230*150*140 mm
Thickness of Layer	0.1-0.4 mm
Accuracy of Print	±0.2 mm

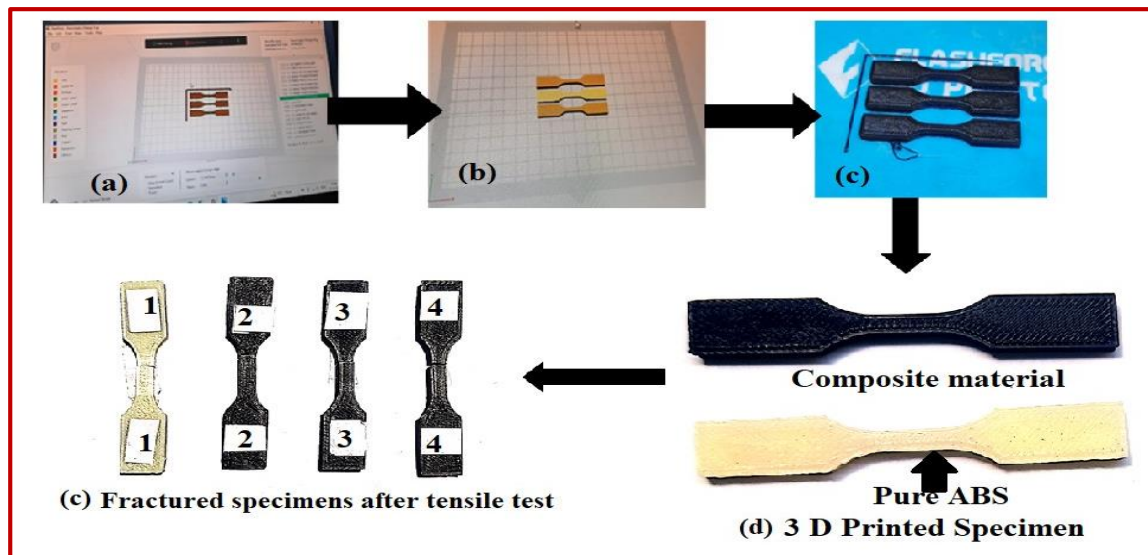


Figure 3.8 Process flow diagram of experimental work (a) Model prepared (b) Process for slicing (c) Printing process (d) Specimen for tensile test (e) Sample after tensile test

CHAPTER 4

CHARACTERIZATION:

This chapter details the investigation, which involved numerous characterization techniques to analyse the functional group. It discusses equipment characterisation for mechanical characteristics, structural properties, thermal behaviour, crystallographic nature, and morphological properties of the obtained specimens.

4.1 Tensile Properties

The prepared samples from developed material were tested for tensile strength on UTM (Model H50KL): Tinius Olsen, loading capacity of 50 KN, speed range 0.001 mm/min to 500 mm/min) as shown in figure 4.1. The specifications are given below:

Construction: Precision ball screws, ball screw cover/protection bellows, pre-loaded lead screw thrust races, a precision DC servo motor, programmable crosshead limit switches, an emergency stop switch, and a vertical bench mounting style are all features of this setup.

Travel and stiffness: The maximum crosshead travel, excluding grips, is 1075 mm, the distance between columns is 405 mm, and the frame stiffness is 100 KN/mm at full load.

Control Panel: One auxiliary option slot for external equipment, Crosshead Up, Down, Stop, Test Keys, LED Direction and Alarm Indicators, High-Speed RS232 Interface Port 16 Bit Microcontroller, Audible Alarms, and System Watch Dog Timer.

Force Measurement: They are building a load cell Z beam under EN10002, ASTM E4, DIN 51221, and ISO 75001 standards. Extended Range of 1% with a Guaranteed Accuracy of 1%, Range of 2% to 100% with a Guaranteed Accuracy of 0.5% of applied force Rapid Alteration Carry Cells In stock: -50kN. Automatic load cell recognition via digital encoding; automated load cell protection system activated at a 9 % increase in load cell capacity. The typical force sampling rate is 200 times per second, the load cell resolution is 1 part 64,000 (compression or tension), and the digital load tear is $\pm 20\%$, all while preserving the total capacity of the load cell.

Extension Measurement

An accurate optical encoder-based extension measurement of 0 to 1000mm is the range of a single measurement. Resolution 0.0001mm, Accuracy 0.01mm/300mm.

Speed Control

Dual Speed Function has two default test speeds (5 mm/min and 100 mm/min) and one default jog speed (1 mm/min) during testing. Programmable speed velocity in 0.001 mm/min increments Speed precision of 0.05 % of maximum speed, 32-bit precision motor controller.

Drive system: - Automatic Over/Under Speed Alarms, DC Four Quadrant Motor Drive, Under/Over Voltage, Current, and Temperature Motor Drive Alarms.

Velocity Speed Range

H50KL 0.001 mm/min to 250 mm/min (up to 25kN)

Hardware Options

The range of Clip Extensometers and Displacement Transducers manufactured by Tinius Olsen. A variety of grips and attachments by Tinius Olsen, Clear dust cover and protective screen

Dimensions

Height 1620 mm width 720 mm, depth 500 mm, weight 180 Kgs.

Temperature

Operating 0°C to 38°C

Storage -10°C to 45°C

Humidity

10% to 90% Non-Condensing Wet Bulb Method

Power

H50KL Type TX****-H50KL, Input Supply Voltage 230V +/- 10% 50/60Hz, Output Voltage 48v 50/60Hz @ 530VA, Internally Fused (5x20mm HRC 6.30A Type (T) for 230V Supply).

Machine Supply Requirements

H50KL 48v +/-10% 50/60Hz @ 530VA

Specimens shaped like dumbbells through microinjection moulding were subjected to tensile tests by the internationally acknowledged test method ASTM D 638:2014. Conducting a tensile test enables the evaluation of the resistance of various materials, including thermoplastics, composites, and metals, against shear forces. Additionally, it determines the material's elongation limit before failure. Toughness is quantified in terms of the area under the stress-strain curve for polymeric nanocomposites. The average values of percentage elongation at the point of failure and tensile strength were determined using five specimens.



Figure 4.1 Universal Testing Machine (UTM) makes Tinus Olsen

4.2 Microhardnes

The microhardness of developed nanocomposite was investigated through Struers

Duramin-40 M1 Vickers microhardness tester (Hardness scale: 0.2 Hv and dwell time: 10 seconds) shown in Fig.4.2

Versatile hardness testing that ensures repeatability over a wide load range Duramin-40 is the primary range of Struers micro/macro hardness testers. It is available on a manual

and motorised XY stage with an overview camera. Duramin-40 comes with three load ranges: 10 gf - 10 kgf, 10 gf - 31.25 kgf, and 1 gf - 62.5 kgf. The tester includes an integrated PC with a separate monitor for touch screen or mouse operation. Dual monitors are also an option. The test cycle is fully automatic, and a motorised 6-position turret is standard. Add-on modules include Kc fracture measurements, mapping and weld measurements.

Table 4.1: Microhardness tester Data used in the study

Parameter	Specification
Model	Duramin-40 M1
Manufacturer	Struers
Method	VICKERS
Load Range	10gf-10Kgf
Indentation Size	0.1650-0.1750
Accuracy	$\pm 5\%$
Dwell Time	10 Sec.
Hardness scale	HV 0.2

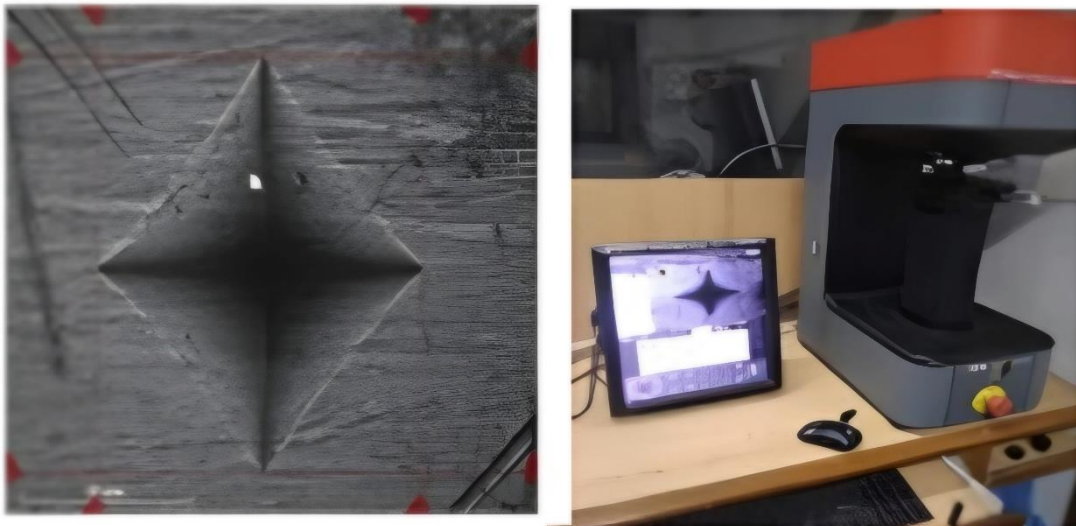


Figure 4.2 Microhardness tester

4.3 FT-IR

The Fourier transforms infrared (FT-IR) spectra of developed nanocomposites were recorded on the PerkinElmer spectrum 2. The FT-IR spectrum was acquired using the ATR mode of pure ABS. The setup of FTIR is shown in Fig. 4.3. Its specification of given below:

- ❖ **Features:** Feature-rich apparatus: data collection optical system with KBr windows; Dynascan interferometer; Optics Guard technology; Atmospheric Vapour Compensation (AVC); Sigma-Delta Conversion; and Optics Guard technology; all of which contribute to precise and replicable outcomes by enhancing ordinate linearity, minimizing spectral artefacts, and expanding the dynamic range.
- ❖ Includes: Spectrum Touch software.
- ❖ Detector: LiTaO₃ (lithium tantalate) MIR detector with an SNR of 9,300:1.
- ❖ Operating Range: 5 - 45 °C.
- ❖ Wavelength: 8.
- ❖ Signal-to-noise ratio: 9,300:1 (LiTaO₃ detector), 14,500:1 (Peltier stabilized detector).
- ❖ Wavelength Length Range: 8,300 - 350 cm⁻¹.
 Modes: ratio, single-beam and interferogram. Accessories and Options:
 Portability Pack, Universal ATR Sampling, HATR Sampling, Portability

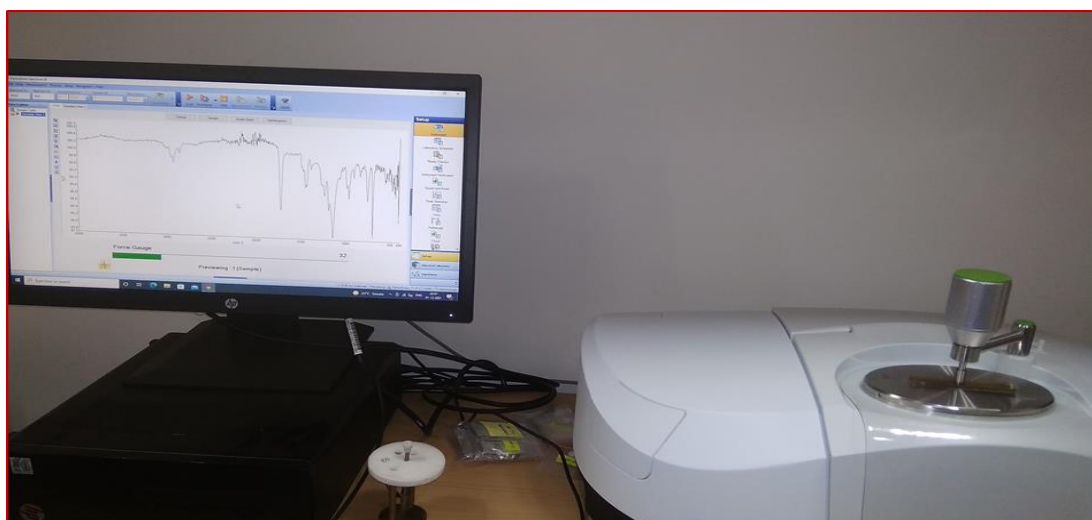


Fig.4.3 FT-IR Setup

Options, Training Software, Documentation, Services and Warranties, Spectrum 10 ES software

4.4 Scanning Electron Microscopy

SEM analysis of developed nanocomposite was performed using TESCAN MAGNA GMH microscope (Electron Gun: High brightness Schottky emitter, Electron Optics: Triglav™ column equipped with the three-lens compound Tri Lens™ objective, Resolution: (i) Standard mode: In-Beam SE 0.6 nm at 15 keV 1.2 nm at 1 keV, (ii) Beam Deceleration Mode (option): SE (BDM) 0.9 nm at 1 keV, STEM mode (option): 0.6 nm at 30 keV Probe and Current: up to 400 nA).



Figure 4.4 Scanning Electron Microscopy (SEM) makes TESCAN MAGNA GMH

After removing moisture from the samples by drying them in an oven, the fractured ends were mounted and sputter-coated with a thin layer of gold to prevent electrical charging during the examination procedure. As it provides indirect information regarding particle size, SEM is a widely used technique for identifying microstructural characteristics of composites. SEM generates high-resolution images of fillings and fibers by employing an electron beam focused across the specimen's surface. Additionally, it offers details regarding the specimen's phase morphology, distribution, and fracture characteristics.

4.5 X-Ray Diffraction

The crystalline structure of the polymeric nanocomposite was determined by employing the transmission technique and XRD on an M/s Bruker D8-Advance Diffractometer with Cu-K α radiation at a wavelength of 0.15406 nm. at a scanning rate of 2 per minute, scattered radiations have been detected in the angular region 2θ spanning from 2° to 60° by utilising nickel foil as a filter for K β radiation. XRD is a



Figure 4.5 X-ray Diffractometer makes Bruker D8-Advance

swift and nondestructive analytical methods that can determine the composites' crystallographic structure. This method assures the degree of silica intercalation in the hybrid composite.

The XRD is used to characterize the structure of composites; by this method, we determine the spaces between the structural layers by using Bragg's Law;

$$\sin \theta = n\lambda/2d$$

where θ is the measured diffraction angle λ is the wavelength of X-ray radiation. XRD also shows the type of material and dispersion quality of various constituents of the composite. Sharp diffraction peaks in XRD measurements are evidence of good exfoliation.

4.6 Thermal-gravimetric Analyser:

TGA is a technique in which, upon heating a material, its weight increases or decreases shown in Figure 4.6. A Simple TGA Concept to remember: TGA measures a sample's weight as it is heated or cooled in a furnace. A TGA consists of a sample pan that is supported by a precision balance. That pan resides in a furnace and is heated or cooled during the experiment. The mass of the sample is monitored during the experiment.



Figure 4.6 TGA 4000 Thermogravimetric Analyzer

A sample purge gas controls the sample environment. This gas may be inert or a reactive gas that flows over the sample and exits through an exhaust. Thermal-gravimetric analysis of the developed nanocomposite was performed using TGA 4000 analyser (maximum temperature range of 1000 °C).

Table 4.2 Technical Description and Specifications of the TGA setup:

<i>TGA balance type</i>	Top-loading balance and	Easier to use and more robust than other design types
<i>Temperature range:</i>	Ambient to 1000 °C	
<i>Temperature calibration :</i>	Curie point	
<i>Scanning rates :</i>	0.1 to 200 °C/min	Fast scan means provide faster experiment cycle times
<i>Scanning temperature accuracy</i>	±1 °C	10 runs using curie point reference material
<i>Scanning temperature precision</i>	±0.8 °C	
<i>Sample temperature precision</i>	±0.3 °C @ 300 °C ±0.5 °C @ 900 °C	
<i>Sample to program temperature correlation</i>	±0.5 °C @ 300 °C ±1 °C @ 900 °C	Difference between the set temperature and the actual sample temperature
<i>Scanning baseline dynamic drift</i>	<50 µg	50 to 1000 °C at 20 °C/min with empty sample pan
<i>Balance digital resolution</i>	0.2 µg	

<i>Balance sensitivity</i>	1 µg	
<i>Balance accuracy</i>	±0.02%	10 runs using 100 mg certified reference material
<i>Balance precision</i>	±0.01%	
<i>Balance capacity</i>	1500	mg Larger capacity than other design types.
<i>Sample pans</i>	180 µl Ceramic 180 µl Platinum	Sample pan liners available in aluminum, tin and silver
<i>Cooling time</i>	1000 °C to 100 °C in under 8 minutes. 1000 °C to 50 °C in under 11 minutes	with chiller set to 15 °C and forced air
<i>Atmosphere</i>	Static or dynamic, including nitrogen, argon, helium, carbon dioxide, air, oxygen or other inert or active gases over full temp range	Inert furnace design allows a wide choice of gas type
<i>User control</i>	Pyris™ Software 116e Benchmark software in thermal analysis	

CHAPTER 5

RESULTS AND DISCUSSION

This chapter discusses the details for finding the optimum process parameter and the effect of process parameters for obtaining the maximum tensile properties and microhardness of the fabricated polymeric nanocomposite through microinjection moulding and 3-D printing. The microhardness was tested only in injection moulded samples due to the very good finished surfaces. The 3D printed samples were not fusible to take this analysis. And other properties are also covered in this chapter like XRD, FTIR, TGA and SEM.

5.1 Tensile Properties

5.1.1 Tensile properties of MWCNTs/ABS composites through micro injection moulding

The samples were prepared by single and double extrusion process. The samples of each material were tested to obtain mean values of the tensile properties. The stress-strain curves of single and double extruded composite materials for pure ABS and 1, 2, and 3 wt.% of MWCNTs/ABS composites are shown in Fig. 5.1 (a) and (b), respectively. The tensile strength of single extruded MWCNTs/ABS composite increased by 17.6%, 21.6%, and 30.8% for 1, 2, and 3 wt.% of MWCNT reinforcement, respectively, shown in Fig. 5.2 (a). The tensile strength of double extruded MWCNTs/ABS composite increased by 19.45%, 34.75%, and 36.67% for 1, 2, and 3 wt.% of MWCNT reinforcement, respectively, shown in Fig. 5.2 (b). Table 4 shows the enhanced value of tensile strength for single and double-extruded nanocomposites in %age with pure ABS thermoplastic polymer. The five samples of ABS and MWCNTs/ABS nanocomposite were tested and compared by taking the mean value of all the results. It was concluded that the value, that the value of strain and stress increases after mixing the MWCNTs [230]. The stress and strain of MWCNT-reinforced polymer composites increased due to the following reasons: i) The extrusion process improves MWCNT dispersion in the polymer matrix. The

efficient dispersion uniformly distributes MWCNTs throughout the composite. ii) Mechanical extrusion and compounding improve the bonding between the MWCNTs and the polymer matrix. iii) Extrusion aligns and orients MWCNTs in the polymer matrix along the extrusion direction. iv) Extrusion breaks down MWCNT agglomerates, resulting in more uniform nanotube dispersion in the polymer matrix.

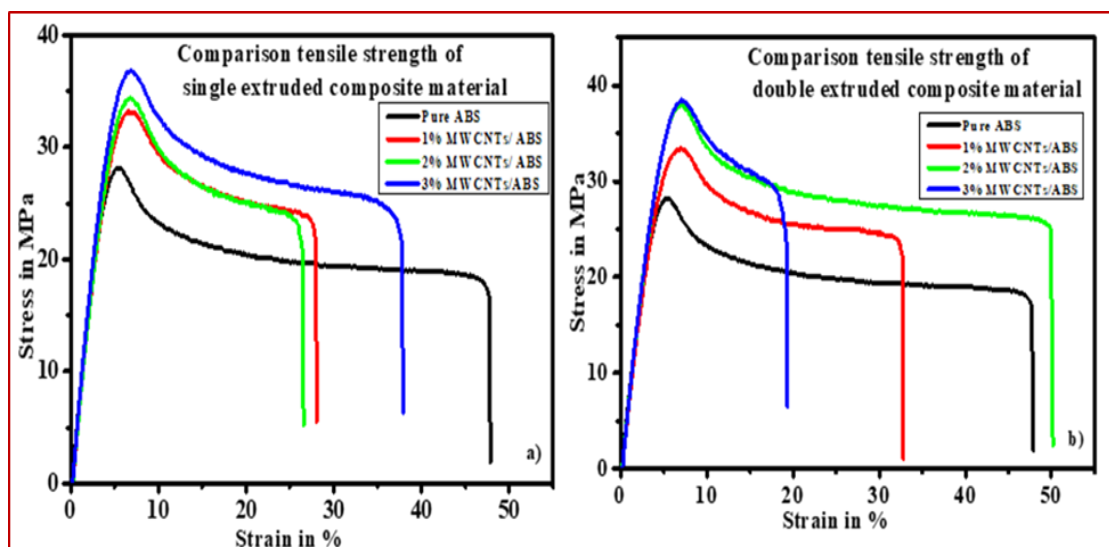


Figure 5.1 Comparison stress and strain curve for 1, 2, and 3 wt.% of MWCNT reinforced in ABS a) single-time extruded materials b) second-time extruded materials prepared by micro injection molding

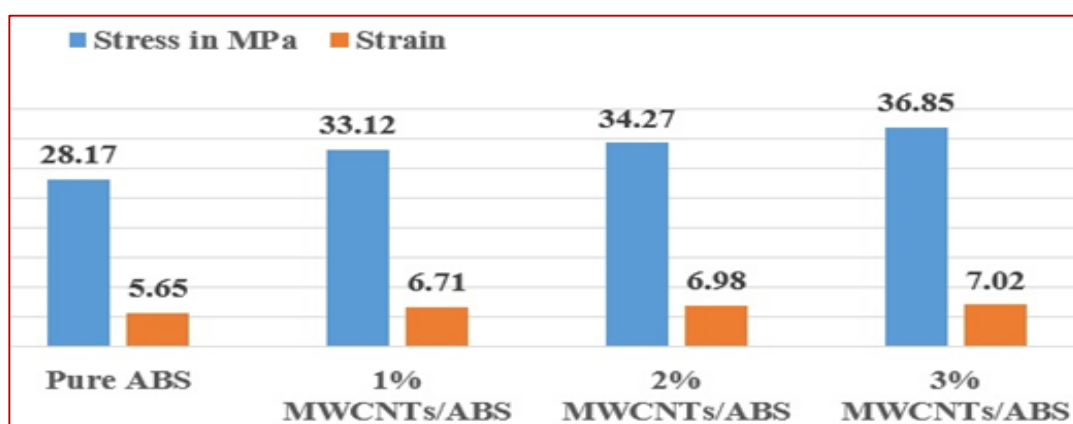


Figure 5.2 (a) Comparative strain and stress graph of single extruded composite materials

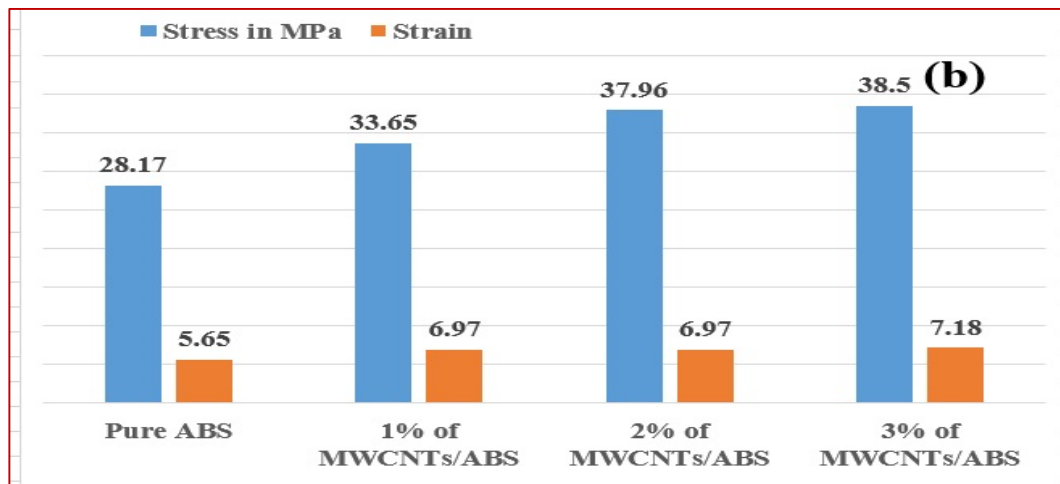


Figure 5.2 (b) Comparative strain and strain graph of double extruded composite materials

Table 5.1 Enhanced tensile strength of single extruded and double extruded composites materials with respect of pure ABS.

Material	Single Extruded composites Strength in MPa	Double Extruded composites Strength in MPa	Improved Strength In single extruded Composites	Improved Strength In double extruded Composites
Pure ABS	28.17	---	---	-----
1 wt.% MWCNTs/ABS	31.25	33.65	17.6%	19.45%
2 wt.% MWCNTs/ABS	34.27	37.96	21.6%	34.75%
3 wt.% MWCNTs/ABS	36.85	38.50	30.0%	36.67%

5.1.2 Tensile properties of MWCNTs/ABS composites of 3 D printed samples.

The materials were prepared by double extrusion process for fused filament fabrication. Then prepared samples of 3 D printed by 0, 1, 2, and 3 wt.% of

MWCNTs/ABS. Five samples were tested for tensile properties by UTM. Figure 5.3 shows the obtained mean values of the stress-strain curves. The tensile strength of 3-D printed composites increased as per Table 4. This table shows the enhancement in %age of the tensile strength. The ultimate tensile stress of pure ABS was 25 MPa and for the 1, 2, and 3 wt.% MWCNT reinforced composite were 31.25, 34.1, and 40.2 MPa respectively [231-233].

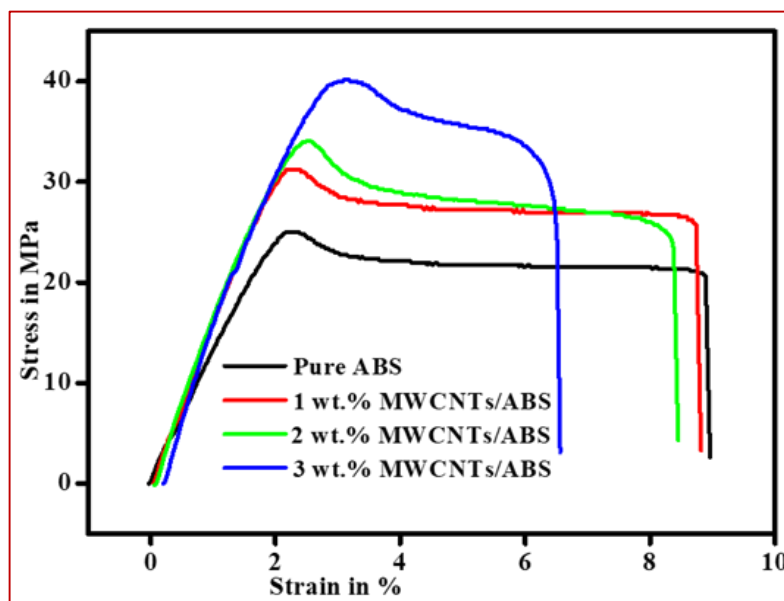


Figure 5.3 3 D printed comparative graph of stress and strain for pure ABS and 1, 2, and 3%wt. of MWCNTs reinforced Composites.

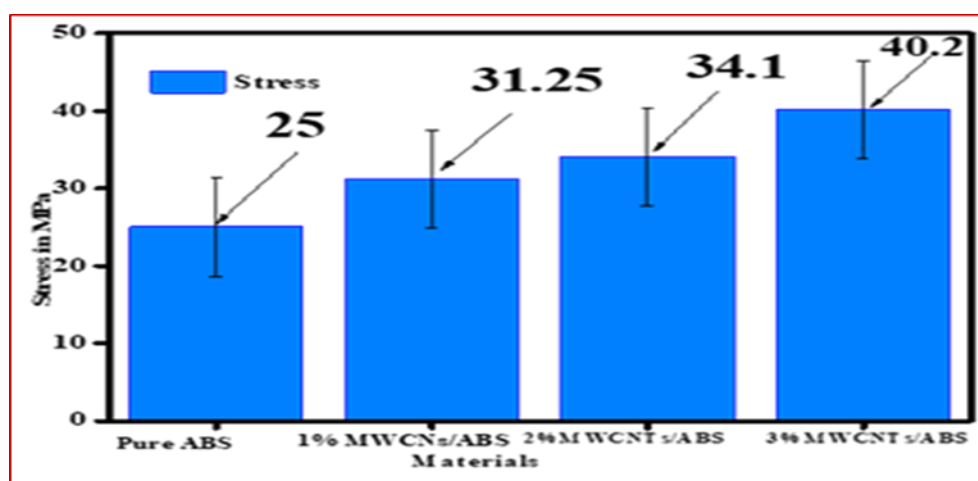


Figure 5.4 Comparative ultimate tensile stress in various nanocomposite materials with pure ABS.

Table 5.2 Comparative enhanced tensile strength of 3 D printed pure and composites materials

Material	Stress in MPa	Strain	Enhanced stress in %
Pure ABS	25.00	2.16	-----
1 wt.% MWCNTs/ABS	31.25	2.11.	25%
2 wt.% MWCNTs/ABS	34.10	2.51	36%
3 wt.% MWCNTs/ABS	40.20	3.10	60%

5.2 Micro hardness of MWCNTs/ABS composite's specimens

The micro-hardness of single extruded MWCNTs/ABS nanocomposite for 1, 2 and 3 wt.% of MWCNT reinforcement increased by 5%, 5.5%, and 7.61% in comparison to pure ABS as shown in Fig. 5.5 (a). Similarly, Fig.5.5 (b). The micro-hardness of .double extruded MWCNT/ABS nanocomposite for 1, 2 and 3 wt.% of MWCNT

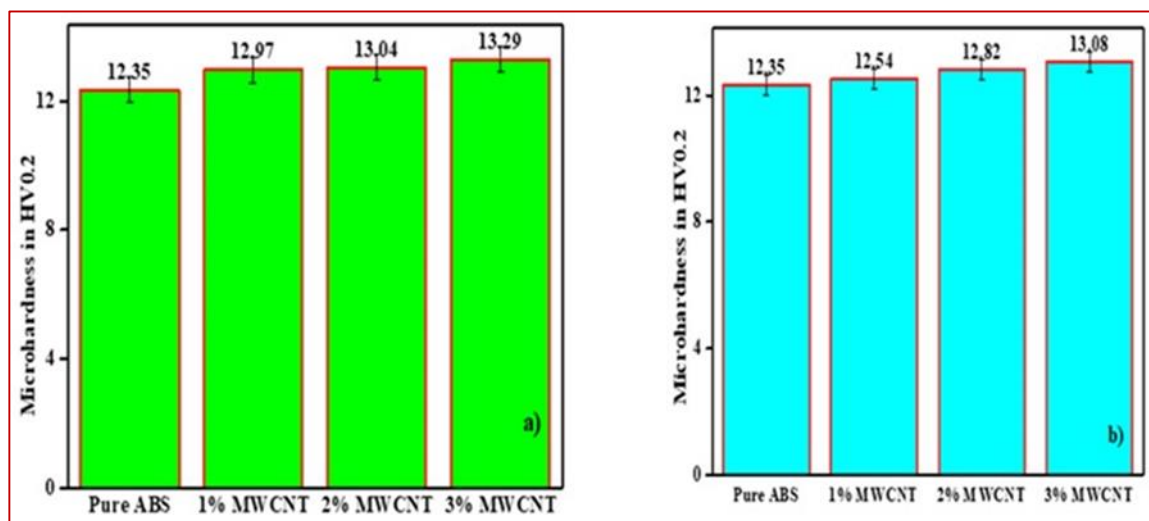


Figure 5.5 Comparison of pure ABS and 1, 2, and 3 wt.% MWCNT/ABS (a) single extruded composites (b) double extruded composites for microhardness

reinforcement increased by 2.26%, 3.8%, and 5.59% in comparison to pure ABS as shown in Fig. 5.4 (b). The results showed that the micro-hardness of double extruded composites was less than that of single extruded composites. These results are in

accordance with the published literature [234-235]. In 3 D printed components could not to be possible due to the smoothness of surface texture.

5.3 FTIR Analysis

5.3.1 FTIR of MWCNTs/ABS composites by microinjection molded specimen

The FTIR spectrum was acquired using the ATR mode for all the samples. The significant peaks for ABS polymer were 700, 761, 965, 1141, 1189, 1243, 1452, 1726, and 2922 cm^{-1} . The presence of C-H causes C-H out-of-plane bending, C-H in-plane bending, and asymmetry. C-H bending, C-N stretching, and symmetric C-H stretching bonds are all caused by the presence of C-H. The percentage of transmittance ranges from 50 to 100, as provided in the FTIR graphs in figure 5.6.

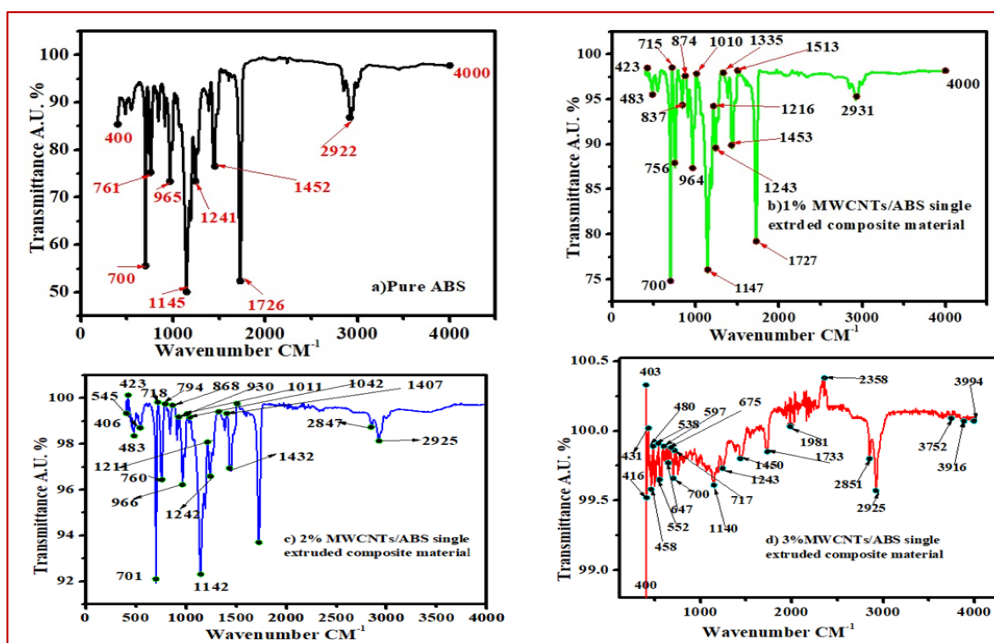


Figure 5.6: FTIR curves of single extruded composites (a) Pure ABS, (b) 1 wt.% of MWCNTs/ABS, (c) 2 wt.% of MWCNTs/ABS, and (d) 3 wt.% of MWCNTs/ABS

The comparative study of 1 wt.% and 2 wt.%, MWCNTs reinforced nanocomposite shows nearly the same wavenumber peaks. The only difference was found in the transmittance range for 1 wt.% (75 to 100 and 2 wt.% 92 to 100). The 3 wt.%

reinforced MWCNTs composites the transmittance range changed in the minor points of peaks from beginning to end. These values are read on the graph from 400 lower and similarly top 403 its ranges from 98.2% to 100.4% transmittance. It shows the effects of the higher percentage of MWCNTs. The absorption peak begins at 400 and peaks at 2925 cm^{-1} for C–H and N–H bonds. The FTIR spectrum for double extruded MWCNTs/ABS nanocomposite is shown in Fig. 5.7 (a), (b), (c), and (d) for 1 wt.%, 2 wt.%, and 3 wt.% of MWCNT at cm^{-1} . An absorption peak arises due to the ABS. The absorption peaks at 1,453, and $1,728\text{ cm}^{-1}$ are ascribed to the ABS's styrene block stretching vibration. The vibrations of aliphatic and aromatic C–H bonds are represented by the peaks at $2,931\text{ cm}^{-1}$ respectively [236]. The infrared spectrum is characteristic of carbonaceous materials, displaying a large absorption envelope in the wavelength range $700\text{--}3000\text{ cm}^{-1}$, with three maxima at around 1581, 1360, and 1200 cm^{-1}

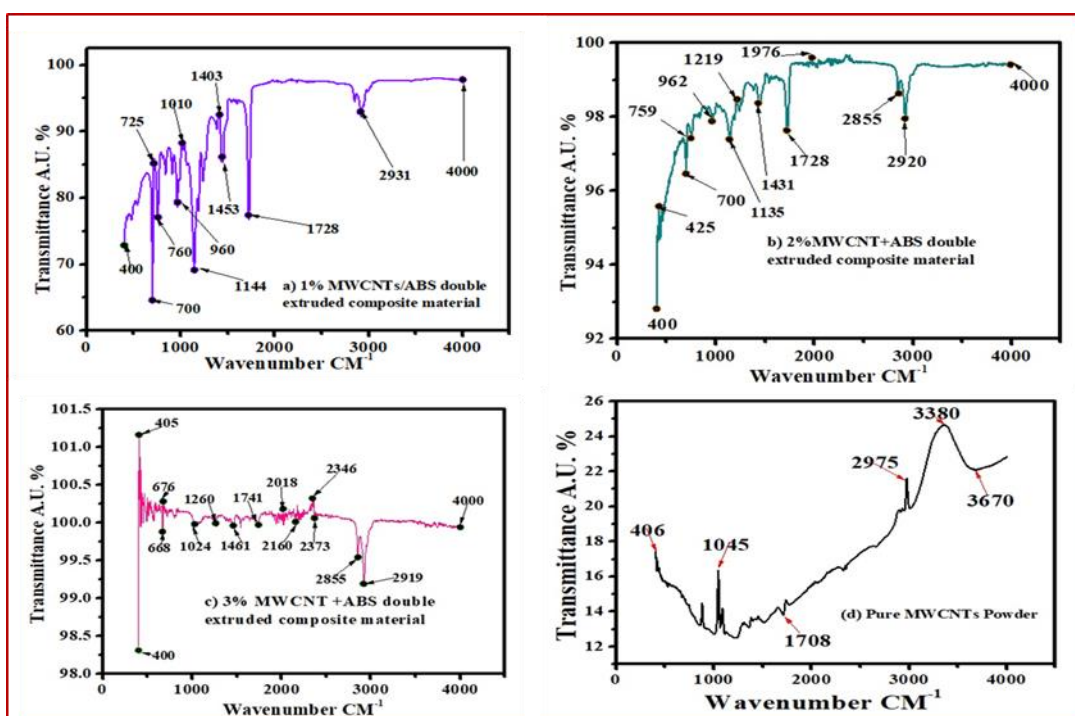


Figure 5.7 FTIR curves of double extruded MWCNT/ABS composites for (a)1 wt.% of MWCNTs reinforcement (b) 2 wt.% of MWCNTs reinforcement (c) 3 wt.% of MWCNTs reinforcement (d) Pure MWCNTs

The presence of carbon nanotube groups on CNW is shown by the peaks. The third band at 1200 cm^{-1} is due to C-O group stretching vibrations. On the other hand, the spectra of a separate wt.% of the MWCNTS sample indicate oxidation on the carbon surface [237-238]. On comparing the graphs, a minimal difference between single and double extruded MWCNTs/ABS nanocomposite was found. Fig. 5.7 (d) shows the peak of pure MWCNTs shows the peak $406, 1045, 2975$ and 3380 cm^{-1} in its top level.

5.3.2 FTIR of MWCNTs/ABS composites from 3 D printed specimens

The 3 D printed material of MWCNTs ABS nanocomposites were analyzed by FT-IR spectroscopy to determine structural differences. Fig. 5.8 shows the FT-IR absorption spectra of ABS-MWCNTs nanocomposite of varying Wt. % of MWCNTs/ABS has IR bands at $2974, 1731, 1454, 1241$, and 1067 cm^{-1} .

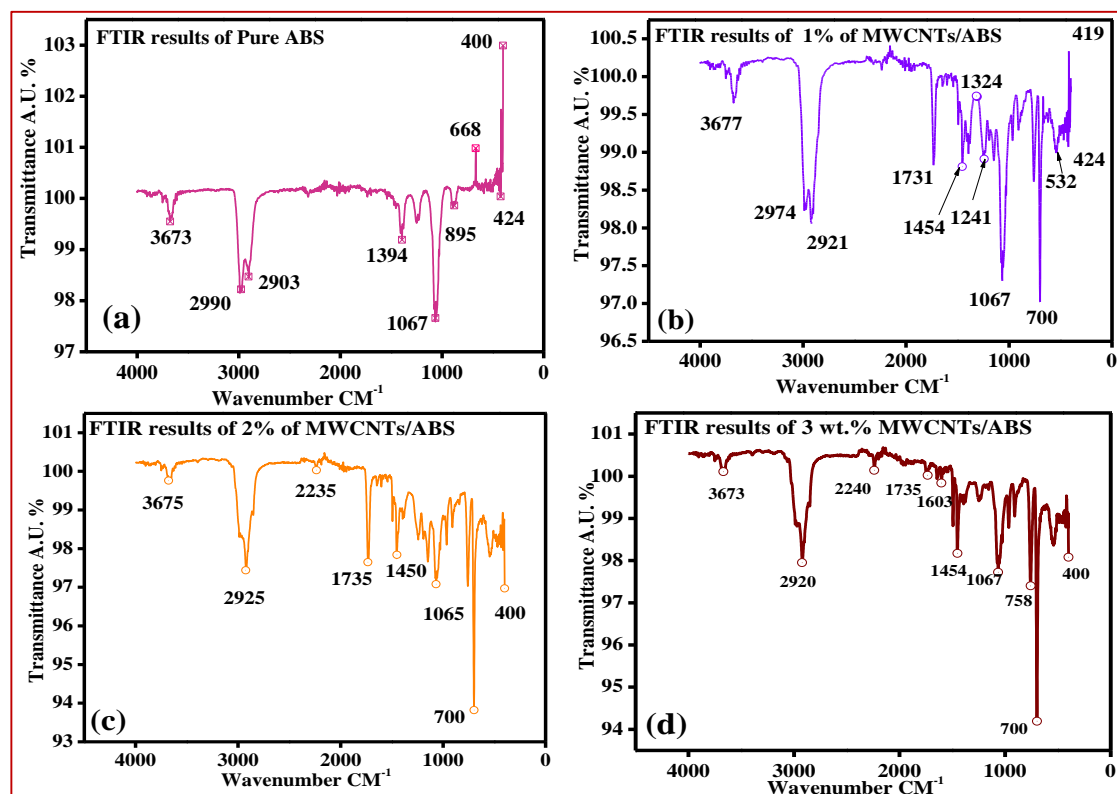


Figure 5.8 FTIR Results of 3D printed pure ABS and 1, 2, and 3 wt. % MWCNTs reinforced composites

Similarly, another composites shown in fig. 5.8 (c- d), FT-IR absorption bands are 2920-25, 1726, 1471, and 1388 cm^{-1} . Due to MWCNTs/ABS interaction, certain bars disappear, and others change intensity [239].

5.4 TGA Investigations

5.4.1 TGA of MWCNTs/ABS composites

The TGA graphs of pure ABS and MWCNT/ABS nanocomposite prepared with single extrusion and double extrusion process are shown in Figs. 5.9 (a) and 5.9 (b) respectively. Thermo- gravimetric analysis was performed at 600 °C for single and double extruded MWCNTs/ABS composites (3 mg). It was observed that the percentage TGA residue of MWCNTs/ABS composite increased with the increase in MWCNTs reinforcement. The TGA analysis confirmed that MWCNTs/ABS composite is more thermal resistant as compared to pure ABS. The thermal decomposition temperature of the produced nanocomposite shifted to higher temperature range due to the inclusion of MWCNTs in the ABS. During the thermal decomposition of the polymer composite, MWCNTs acts as barrier for decreasing product volatilization and heat transport [230, 239-242].

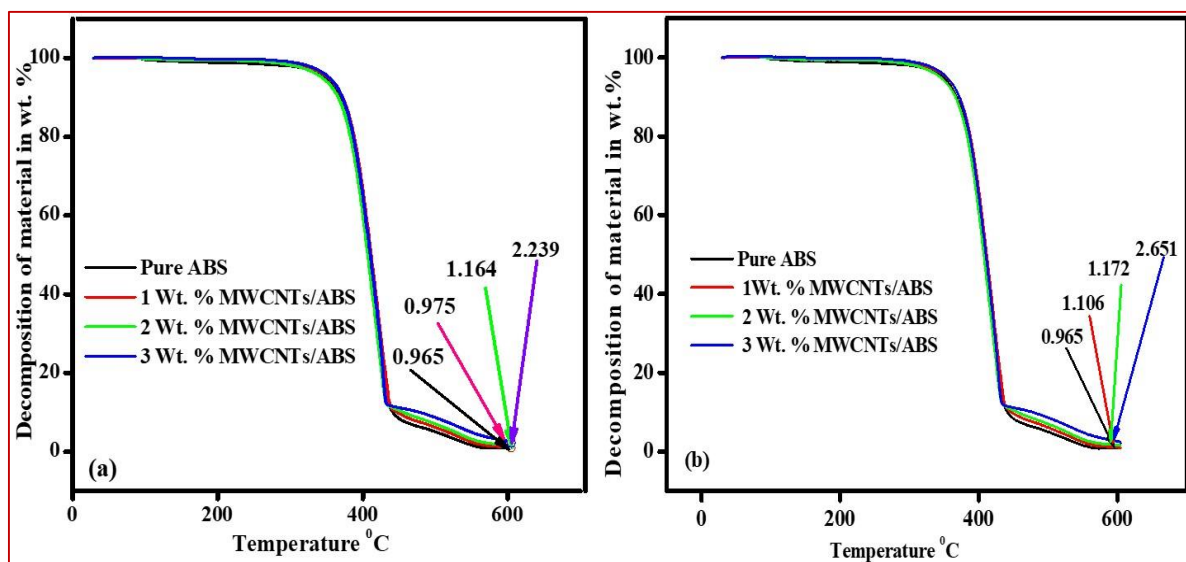


Figure 5.9 (a) TGA of single extruded MWCNTs/ABS nanocomposites of 1, 2, and 3 wt.% of MWCNTs reinforcement and pure ABS(b)) TGA of double extruded MWCNTs/ABS nanocomposites of 1, 2, and 3 wt.% of MWCNTs reinforcement and pure ABS.

5.4.2 TGA of 3 D printed materials.

Thermogravimetric analysis in an inert atmosphere at 10 °C/minute was used to study the thermal degradation stability of pure ABS and MWCNT/ABS nanocomposite materials. Fig. 8 shows Pure-ABS and MWCNT/ABS nanocomposite TGA curves. Evaporation of all taking materials causes pure ABS weight loss between 50–600 °C. At 400–500 °C, polymer chain breakdown, oxidation of organic groups, and dopant evaporation cause weight losses in pure ABS and ABS/MWCNTs nanocomposites. MWCNTs in ABS limit mass transfer, stopping weight loss [244]. All MWCNTs/ABS nanocomposite samples exhibit a slight weight loss at a predicted temperature and better thermal stability than pure ABS. Figure 5.10 shows ABS and MWCNT-ABS nanocomposites weight loss curves. The research shows that adding 1–3% MWCNTs to nanocomposites increases thermal degradation temperature over pure ABS. Pure ABS was 3.013, and 1 wt. %, 2 wt. %, and 3 wt. % in MWCNTs were 3.161, 3.308, and 4.229. After 600°C degradation, these values were 4.91%, 9.79%, and 40.36% higher than pure ABS. At 40.36% weight, the 3wt% MWCNT-ABS nanocomposite performs better. The 1 wt. % and 2 wt. % MWCNT/ABS nanocomposite had slightly less heat deterioration than pure ABS.

The dispersion of MWCNTs in the polymer matrix, their interfacial interactions, and the nanocomposite's thermal conductivity affect thermal degradation. Physical barriers, heat dissipation, and interfacial interactions stabilize MWCNTs/ABS nanocomposite. The physical presence of MWCNTs can block polymer chain mobility and volatile degradation product distribution. This physical barrier can improve nanocomposite thermal stability. Due to their excellent thermal conductivity, MWCNTs can dissipate degrading heat. This can reduce localized overheating and improve nanocomposite thermal stability. Strong MWCNT-polymer matrix interactions can stabilize the nanocomposite.

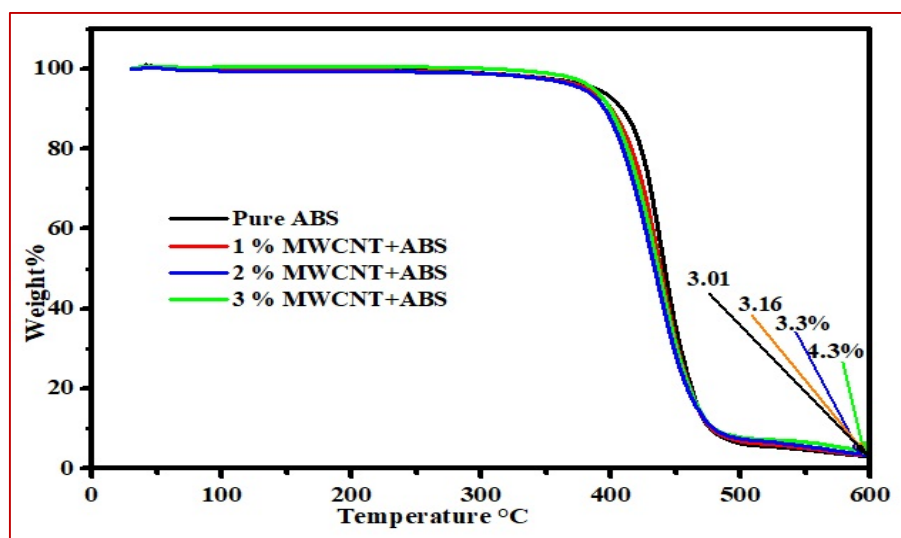


Figure 5.10: Thermogravimetric analysis curves for materials made of ABS and MWCNT/ABS 3 D printed nanocomposites.

MWCNTs/ABS nanocomposite destabilizes via catalytic and aggregation processes. MWCNT may accelerate polymer thermal breakdown. It can hasten decomposition and diminish thermal stability. Poor MWCNT dispersion and aggregation in the polymer matrix might cause dense patches. These locations may affect catalytic effects or physical barrier qualities, reducing heat stability.

5.5 XRD Analysis

5.5.1 XRD characterization of MWCNTs/ABS composites through Micro Injection moulded specimen.

The X-ray diffraction (XRD) patterns of pure MWCNTs and pure ABS are shown in Fig. 5.11 (a) and (b) in the terms of angle (2θ) and intensity. The upper peak (2θ) for pure MWCNTs were 5° and 23.11° . The upper peak (2θ) for pure ABS was 14.8° . The X-ray diffraction (XRD) patterns of single extruded MWCNTs/ABS composite for 1, 2, and 3wt.% of MWCNTs reinforcement are shown in Fig. 5.10 (c-e). The maximum angle of diffraction (2θ) for 1, 2, and 3 wt.% of MWCNTs reinforcement was 13.96° , 14.12° , and 14° respectively for single extruded composites. The X-ray diffraction (XRD) patterns of double extruded MWCNTs/ABS composite for 1, 2, and 3 wt.% of

MWCNTs reinforcement are shown in Fig. 5.10 (f-h). The maximum angle of diffraction (2θ) for 1, 2, and 3 wt.% of MWCNTs reinforcement was 14.96° , 13.72° , and 14.64° respectively for double extruded composites. Due to the addition of MWCNTs and ABS, the immobilisation of CRL (Crown-Rump Length) and the diffraction patterns showed that pure MWCNTs, ABS, and MWCNTs/ABS composites were amorphous in nature [50]. Despite the functionalization process, the ABS structure remained amorphous in the nanocomposites containing MWCNTs. It is plausible to deduce that the percentage of MWCNTs can be well spread only using a simple melt mixing approach [242-243].

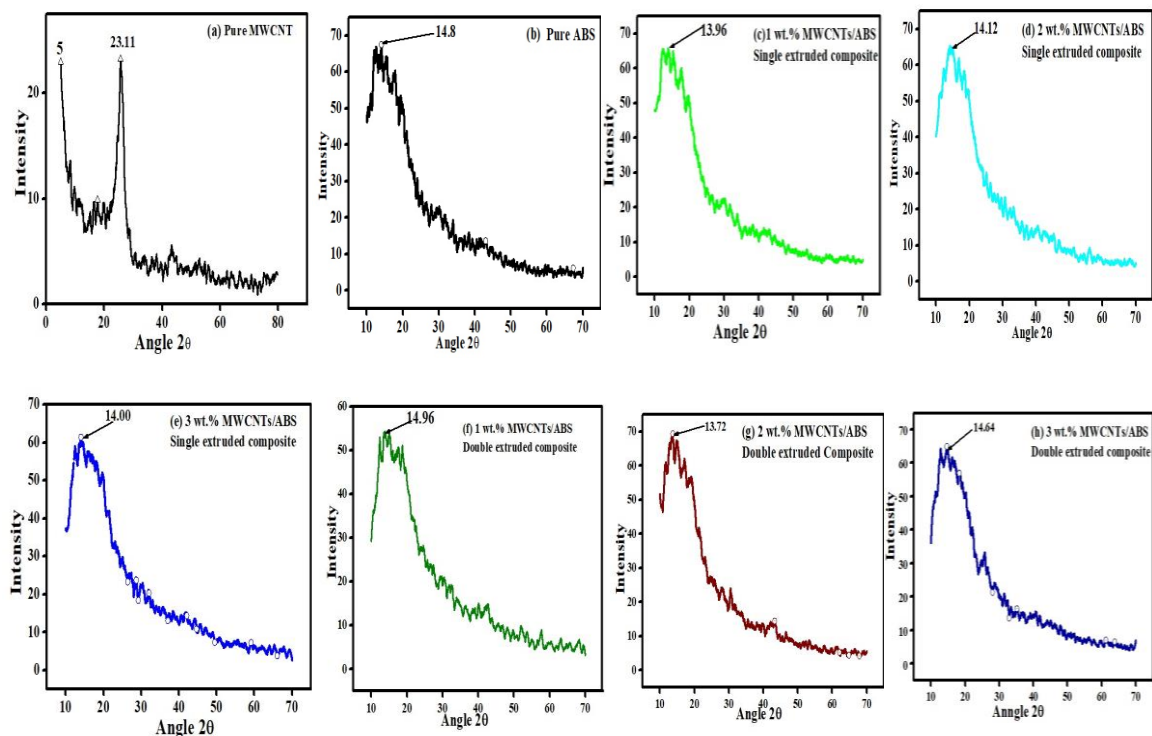
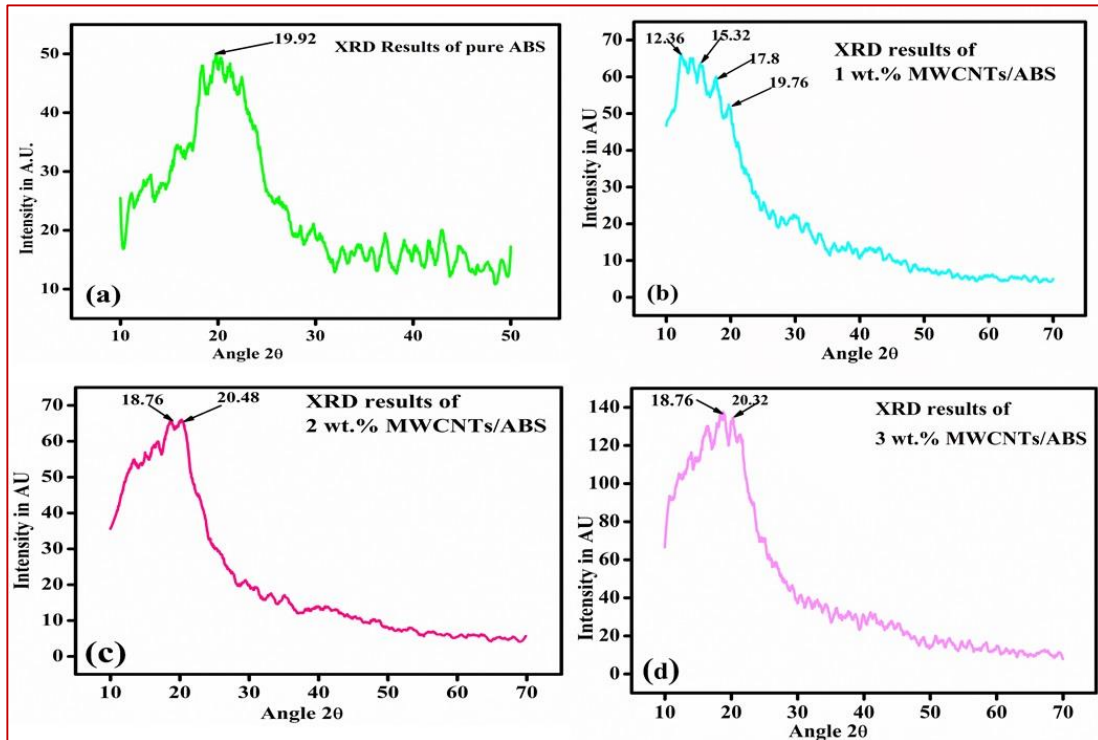


Figure 5.11 XRD pattern for single and double extruded MWCNTs/ABS nanocomposites

5.5.2 XRD characterization of MWCNTs/ABS composites through 3 D printed specimen

3D printed samples of pure ABS and MWCNT/ABS containing XRD properties are shown in Fig. 5.12. Pure ABS exhibited prominent diffraction peaks at $2\theta = 19.92^\circ$ as seen in Fig. 5.12 (a), which were attributed to the diffraction of the 50 lattice plane in semi-crystalline ABS. However, an amorphous hump was spotted at $2\theta = 19.92^\circ$, and concluded that ABS has single peak. The graph indicates that incorporating MWCNTs

did not significantly alter the crystallisation or crystal structure of ABS, as the XRD patterns of the ABS-MWCNT nanocomposites maintained the typical ABS peaks [245]. The impact of 1wt. % MWCNTs on separating three diffraction peaks in an XRD spectrum is seen in Fig 5.12(b). As seen in Fig 5.12(c) and 6(d), the strength of



the peaks shifts somewhat to lower space up to 3 wt. % (18.76) as the concentration of MWCNTs increases. This indicates that when the concentration of MWCNTs in ABS crystals increased, so did their size [246].

Figure 5.12 XRD Analysis of 3D printed (a) Pure ABS, (b) 1 wt. % MWCNTs/ ABS, (c) 2 wt. % MWCNTs/ABS (d) 3 wt. % MWCNTs/ABS composite.

5.6 Morphology Analysis

5.6.1 Morphology analysis of micro injection moulding processed specimens

The surface morphology of fractured tensile specimens of single and double extruded MWCNTs/ABS composites with pure ABS were performed through scanning electron microscopy (SEM). The SEM micrographs of single extruded pure ABS, 1 wt.% MWCNTs/ABS composite, 2 wt.% MWCNTs/ABS composite, and 3 wt.% MWCNTs/ABS composite are shown in Fig. 5.13 (a), (b), (c), and (d) respectively.

The SEM micrographs of double extruded pure ABS, 1 wt.% MWCNTs/ABS composite, 2 wt.% MWCNTs/ABS composite, and 3 wt.% MWCNTs/ABS composite are shown in Fig. 5.14 (a), (b), (c), and (d) respectively. The obtained micrographs show a more homogeneous dispersion of MWCNTs in the single extruded composites as compared with the double extruded matrix

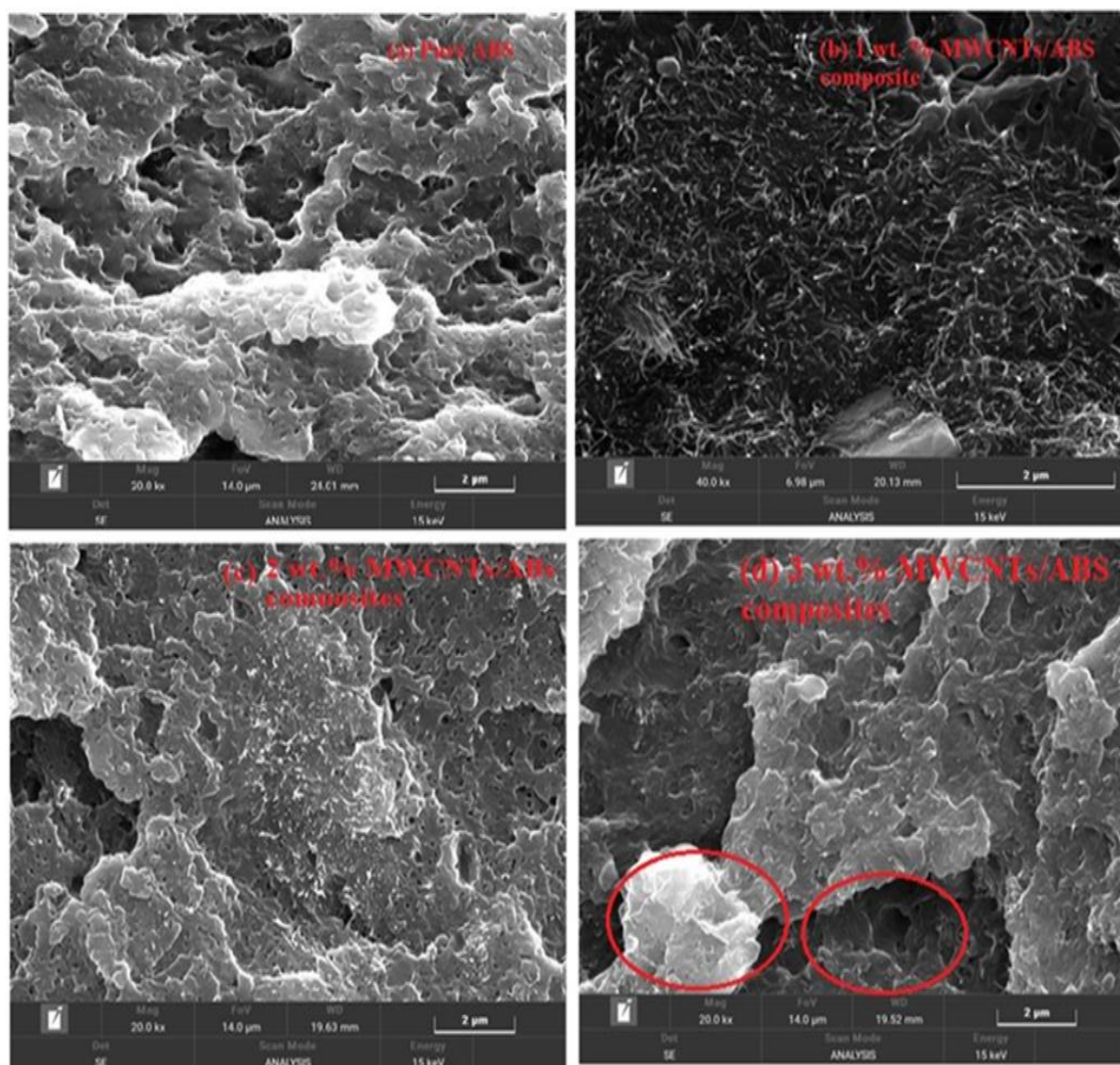


Figure 5.13: SEM images of single extruded nanocomposite (a) Pure ABS (b) 1wt.% of MWCNTs/ABS (c) 2 wt.% MWCNTs/ABS (d) 3 wt.% of MWCNTs/ABS composite.

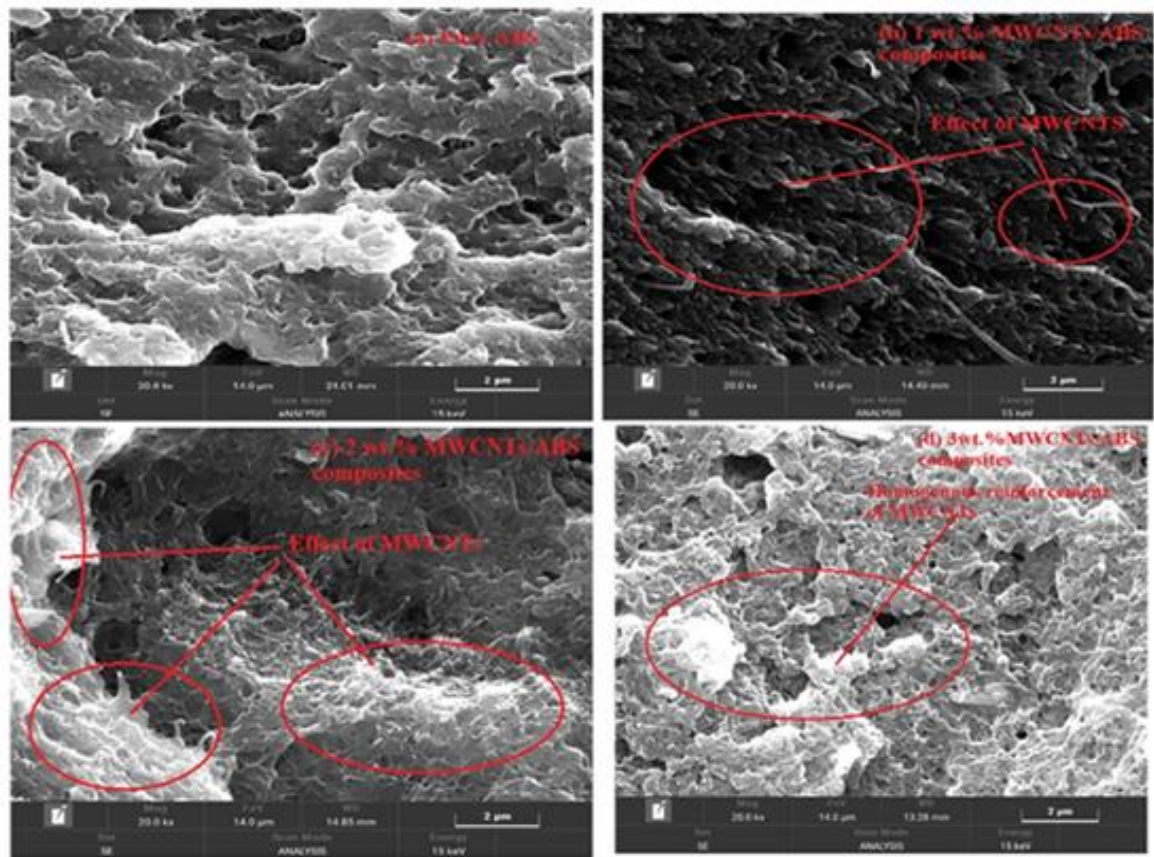


Figure 5.14: SEM images of double extruded nanocomposite (a) Pure ABS (b) 1wt.% of MWCNTs/ABS (c) 2 wt.% MWCNTs/ABS (d) 3 wt.% of MWCNTs/ABS composite.

5.6.2 Morphology analysis of 3D printed specimens

Similarly, for the surface morphology of 3D printed composites to significantly improve their properties, the MWCNTs must be dispersed uniformly throughout the polymer matrix. SEM was used to examine the morphology of the tensile fractured surface and the dispersion of MWCNTs in the ABS matrix. Fig. 5.15 (a-d) are scanning electron micrographs of 1, 2, and 3wt. % of MWCNTs reinforced in ABS respectively. The MWCNTs are scattered evenly across the matrix, as seen in Fig. 5.15 (a)-(d). Fig. 5.15 (d) is a scanning electron micrograph of a sample with 3wt. %age MWCNTs, revealing agglomerations of the MWCNTs that are the primary cause of the

composites increased UTS. The white spots inside the red marked circles shows the presence of MWCNTs in the MWCNTs/ABS composites.

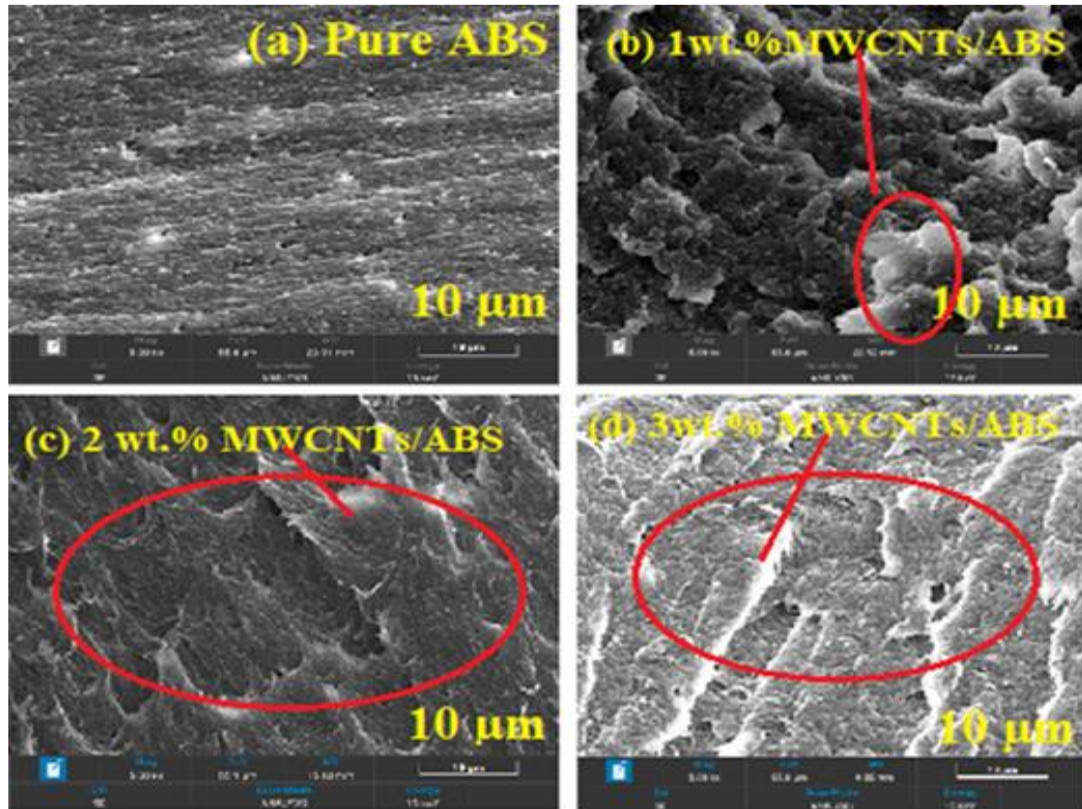


Figure 5.15: Scanning Electron Microscopy images of the 3D printed MWCNTs / ABS tensile test specimen fracture surfaces (a) Pure ABS (b) 1% wt. (c) 2% wt. MWCNT loading percentages. d) 3% wt. MWCNT loading shows its agglomeration.

CHAPTER 6

CONCLUSION AND FUTURE SCOPE

This chapter presents the concluding results for various properties, such as mechanical and thermal properties, and discusses the future scope. In summary, it can be inferred that incorporation of MWCNT in a reorganized polymer matrix would lead to better dispersion of MWCNT. This chapter shows the improvement of mechanical and thermal properties.

6.1 CONCLUSION

This work presents an approach for the development of materials for additive manufacturing processes and other specific purposes that can be used to develop high-performance polymeric nanocomposite materials. The developed nanocomposites will be mechanically strong and light in weight. The developed materials allow the smooth operation of the additive manufacturing process. MWCNTs/ABS composites materials were prepared by using twin-screw extruder followed by micro injection molding. The microhardness and tensile strength for single and double-extruded materials are compared with pure ABS. The following conclusions are drawn from the mechanical properties investigation:

The tensile strengths of single extruded composites increased to 17.9%, 20.7%, and 30 %, respectively, for 1,2, and 3 wt.% of MWCNT reinforced in ABS compared with pure ABS.

- i) Similarly, the tensile strength of double extruded composites increased by 19.45%, 34.75% and 36.67%, respectively, for 1,2,3 wt.% of MWCNT reinforced ABS as compared with pure ABS.
- ii) Micro hardness of the fabricated composites increased by 5%, 5.5%, and 7.61% for single extruded samples and 2.26%, 3.8%, and 5.59% for double extruded samples respectively for 1,2 ,3 wt.% of MWCNT reinforced ABS as compared with pure ABS.
- iii) The XRD, TGA and FTIR properties have also been investigated.

- iv) SEM results confirmed the homogeneous distribution of MWCNTs in the ABS.

It has also analysed and concluded 3D printed specimens prepared by developed materials as following manner: Specimens with higher MWCNT ratios (1, 2, and 3 wt. %) were more durable than pure ABS. The ultimate tensile strength of 1, 2, and 3 wt. % specimens was higher than pure ABS. Compared to pure ABS, MWCNT-reinforced composites increased by 25%, 36%, and 60%, respectively. The TGA results also show that the percentage degradation of ABS is higher than 1, 2, and 3 wt. % of MWCNTs/ABS composite. The nanoparticle agglomerations of 1, 2, and 3 wt. % of MWCNTs reinforced samples are shown in SEM images. MWCNTs/ABS 3D-printed composites demonstrated overall superior mechanical properties.

6.2 Future scope

1. Exploring the possibility of incorporating other nanostructures or functional additives with MWCNTs to create multifunctional nanocomposites with unique properties.
2. Collaborative efforts between material scientists, engineers, chemists, and other researchers are essential to unlock the full potential of MWCNTs/ABS nanocomposites and pave the way for practical applications in various industries.

REFERENCES

- [1] Allel, Amina, et al. "Poly (styrene-co-butadiene)/Maghnia-Organo-Montmorillonite Clay Nanocomposite. Preparation, Properties and Application as Membrane in the Separation of Methanol/Toluene Azeotropic Mixture by Pervaporation." *Membranes* 11.12 (2021): 921.
- [2] Jubsilp, Chanchira, Tsutomu Takeichi, and Sarawut Rimdusit. "Polymerization kinetics." *Handbook of Benzoxazine Resins*. Elsevier, 2011. 157-174.
- [3] Sheng, James J. *Modern chemical enhanced oil recovery: theory and practice*. Gulf Professional Publishing, 2010.
- [4] Arslan, Mehmet, Gokhan Acik, and Mehmet Atilla Tasdelen. "The emerging applications of click chemistry reactions in the modification of industrial polymers." *Polymer Chemistry* 10.28 (2019): 3806-3821.
- [5] Ramakrishnan, S. "Condensation polymerization." *Resonance* 22 (2017): 355-368.
- [6] Yamazaki, Yuka, et al. "Synthesis of well-defined miktoarm star copolymers of aromatic polyether and polystyrene by chain-growth condensation polymerization and atom transfer radical polymerization." *Macromolecules* 42.3 (2009): 606-611.
- [7] Stefanescu, Eduard A., Codrin Daranga, and Cristina Stefanescu. "Insight into the broad field of polymer nanocomposites: from carbon nanotubes to clay nanoplatelets, via metal nanoparticles." *Materials* 2.4 (2009): 2095-2153.
- [8] Sadowski, Jens, and Johann Gasteiger. "From atoms and bonds to three-dimensional atomic coordinates: automatic model builders." *Chemical Reviews* 93.7 (1993): 2567-2581.
- [9] Zhihua Xu, Hsinhan Tsai, Hsing-Lin Wang, and Mircea Cotlet, Solvent Polarity Effect on Chain Conformation, Film Morphology, and Optical Properties of a Water-Soluble Conjugated Polymer, *J. Phys. Chem. B* 2010, 114, 11746–11752.

- [10] J. M. Huang, P. P. Chu and F. C. Chang. Conformational changes and molecular motion of poly (ethylene terephthalate) annealed above glass transition temperature, *Polymer*, 41: 1741-1748, 2000.
- [11] J. L. Koenig and S. B. Lin Spectroscopic characterizing of solvent-induced crystallization. *Journal of Polymer Science: Polymer Physics Edition*, 21: 1539-1558, 1983.
- [12] MATSE, Redwing R. "Materials in Today's World." Pennstate, John A. Dutton e-education institute, Dr Ronald Redwing, Senior Lecturer, Department of Material Sciences and Engineering, College of Earth and Mineral Sciences, The Pennsylvania State University (81).
- [13] Guo, Qipeng. *Polymer morphology: principles, characterization, and processing*. John Wiley & Sons, 2016.
- [14] Antwi, Elijah Kwabena, Kui Liu, and Hao Wang. "A review on ductile mode cutting of brittle materials." *Frontiers of Mechanical Engineering* 13 (2018): 251-263.
- [15] Y. H Roos, 1995, *Phase Transitions in Foods* Academic Press, San Diego, USA, 360 p.
- [16] Defonseka, Chris. *Water-Blown Cellular Polymers: A Practical Guide*. Walter de Gruyter GmbH & Co KG, 2019.
- [17] Dudowicz, Jacek, Karl F. Freed, and Jack F. Douglas. "The glass transition temperature of polymer melts." *The Journal of Physical Chemistry B* 109.45 (2005): 21285-21292.
- [18] Kalpakjian, Schmid *Manufacturing Processes for Engineering Materials*, 5th ed. © 2008, Pearson Education.
- [19] <https://www.geeksforgeeks.org/difference-between-tg-and-tm-polymers/>

- [20] Y. H Roos, 2010, Glass Transition Temperature and its Relevance in Food Processing. Annual Review of Food Science and Technology, 1469496.
- [21] Kelly A. Ross, Susan D. Arntfield and Stefan Cenkowski, A Polymer Science Approach to Physico-Chemical Characterization and Processing of Pulse Seeds, "Polymer Science" book edited by FarisYilmaz, ISBN 978-953-51-0941-9, 2013.
- [22] L. H Sperling, 2006, Introduction to Physical Polymer Science. 3rd ed. Wiley, New York, 845 pp.
- [23] C Norton, 1998, Texture and Hydration of Expanded Rice. [Thesis] Nottingham University.
- [24] Y Roos, M Karel, 1991Plasticizing Effect of Water on Thermal Behavior and Crystallization of Amorphous Food Models Journal of Food Science and Technology, 563843
- [25] Pinal R., Effect of molecular symmetry on melting temperature and solubility, Org Biomol Chem, 2004 Sep 21;2(18):2692-9. Epub 2004.
- [26] T. A. Bullions, M. Wei, F. E. Porbeni, M. J. Gerber, J. Peet, M. Balik, J. L. White, Allan Tonelli, Reorganization of the Structures, Morphologies, and Conformations of Bulk Polymers via Coalescence from Polymer Cyclodextrin Inclusion Compounds, Journal of Polymer Science: Part B: Polymer Physics, Vol.40,992–1012, 2002.
- [27] Jyotsna Vedula and Alan e. Tonelli, Reorganization of Poly (ethylene terephthalate) Structures and Conformations to Alter Properties, Journal of Polymer Science: Part B, Vol. 45, 735–746, 2007.
- [28] Vineeta. D. Deshpande, Sandeep Jape, Nonisothermal Crystallization Kinetics of Nucleated Poly (ethylene terephthalate), Journal of Applied Polymer Science, Vol. 111, 1318–1327 2009.

- [29] Sabu Thomas, Kuruvilla Joseph, Sant Kumar Malhotra, Koichi Goda, and Meyyarappalliln Sadasivan Sreekala, *Advances in Polymer Composites: Macro- and Microcomposites – State of the Art, Polymer Composites: Volume 1*, 2012.
- [30] Garg, R. K., et al. "Review of research work in sinking EDM and WEDM on metal matrix composite materials." *The International Journal of Advanced Manufacturing Technology* 50 (2010): 611-624.
- [31] Samal, Subhranshu Sekhar, and Smrutisikha Bal. "Carbon nanotube reinforced ceramic matrix composites-a review." (2008).
- [32] Rajendra A. Kalgaonkar, *Amorphous copolyester and organo inorganic nanofillers: a structure and property study*, Thesis, University of Pune, 2007.
- [33] Kawasumi, M., Hasegawa, N., Kato, M., Usuki, A. & Okada, A. *Macromolecules*. 30, 20, 6333, (1997).
- [34] A. Polyakova, R. Y. F. Liu, D. A. Schiraldi, A. Hiltner and E. Baer. Oxygen-barrier properties of copolymers based on ethylene terephthalate. *Journal of Polymer Science: Polymer Physics Edition*, 39: 1889-1899, 2001.
- [35] M. Wei, T. A. Bullions, C. C. Rusa, X. Wang and A. E. Tonelli. Unique morphological and thermal behaviors of reorganized poly (ethylene terephthalates), *Journal of Polymer Science: Polymer Physics Edition*, 42: 386-394, 2004.
- [36] D. J. Sekelik, E. V. Stepanov, S. Nazarenko, D. Schiraldi, A. Hiltner and E. Baer, Oxygen barrier properties of crystallized and talc-filled poly (ethylene terephthalate), *Journal of Polymer Science: Polymer Physics Edition*, 37: 847-857, 1999.
- [37] L. E. Nielsen in: *Mechanical Properties of Polymers and Composites*; Marcel Dekker, New York (1974).
- [38] A. Okada, A. Usuki, *Mater. Sci. Eng.:* C3 109 (1995).

- [39] Hari, J.; Pukanzsky, B. Nanocomposites: Preparation, structure, properties. In *Applied Plastics Engine Handbook: Processing Materials*; Kutz, M., Ed.; Elsevier Inc.: Waltham, MA, USA, 2011; pp. 109–142.
- [40] Solvent Blend) Demetzos, Costas, and Natassa Pippa. "Advanced drug delivery nanosystems (aDDnSs): a mini-review." *Drug Delivery* 21.4 (2014): 250-257.
- [41] Melt Blending 54) Franco-Urquiza, E.A. Clay-Based Polymer Nanocomposites: Essential Work of Fracture. *Polymers* 2021, 13, 2399. [CrossRef] [PubMed]
- [42] Porel, S.; Venkatram, N.; Rao, D.N.; Radhakrishnan, T.P. In situ synthesis of metal nanoparticles in polymer matrix and their optical limiting applications. *J. Nanosci. Nanotechnol.* 2007, 7, 1887–1892. [CrossRef]
- [43] Kashiwara, K.; Uto, Y.; Nakajima, T. Rapid in situ synthesis of polymer-metal nanocomposite films in several seconds using a CO₂ laser. *Sci. Rep.* 2018, 8, 14719. [CrossRef] [PubMed]
- [44] Adnan, M.M.; Dalod, A.R.M.; Balci, M.H.; Glaum, J.; Einarsrud, M.-A. In Situ Synthesis of Hybrid Inorganic–Polymer Nanocomposites. *Polymers* 2018, 10, 1129. [CrossRef]
- [45] De Oliveira, A.D.; Beatrice, C.A.G. Polymer nanocomposites with different types of nanofiller. In *Nanocomposites-Recent Evolutions*; IntechOpen Limited: Rijeka, Croatia, 2018; pp. 103–104. Available online: <https://www.intechopen.com/chapters/64843> (accessed on 21 October 2021). [CrossRef]
- [46] (Solution mixing) [64] Cheng, S.; Grest, G.S. Dispersing Nanoparticles in a Polymer Film via Solvent Evaporation. *ACS Macro Lett.* 2016, 5, 694–698. [CrossRef].
- [47] Díez-Pascual, A.M.; Díez-Vicente, A.L. ZnO-reinforced poly(3-hydroxybutyrate-co-3-hydroxyvalerate) bionanocomposites with antimicrobial function for food packaging. *ACS Appl. Mater. Interfaces* 2014, 6, 9822–9834. [CrossRef] [PubMed]

- [48] Mehr, R.K.; Peighambardoust, S.J. Preparation and Characterization of Corn Starch/Clay Nanocomposite Films: Effect of Clay Content and Surface Modification. *Starch-Stärke* 2018, 70, 1700251. [CrossRef]
- [49] Hussein, L.I.; Abdaleem, A.H.; Darwish, M.S.A.; ElSawy, M.A.; Mostafa, M.H.; Hassan, A. Chitosan/TiO₂ nanocomposites: Effect of microwave heating and solution mixing techniques on physical properties. *Egypt J. Chem.* 2020, 63, 449–460. [CrossRef]
- [50] Niu, H.; Wang, X.; Lin, T. Needleless Electrospinning: Developments and Performances. In *Nanofibers—Production, Properties and Functional Applications*; IntechOpen Limited: Rijeka, Croatia, 2011; pp. 17–36. Available online: <https://www.intechopen.com/chapters/23290> (accessed on 1 October 2021). [CrossRef]
- [51] Huang, Z.-M.; Zhang, Y.-Z.; Kotaki, M.; Ramakrishna, S. A review on polymer nanofibers by electrospinning and their applications in nanocomposites. *Compos. Sci. Technol.* 2003, 63, 2223–2253. [CrossRef]
- [52] Yu, W.; Lan, C.-H.; Wang, S.-J.; Fang, P.-F.; Sun, Y.-M. Influence of zinc oxide nanoparticles on the crystallization behavior of electrospun poly(3-hydroxybutyrate-co-3-hydroxyvalerate) nanofibers. *Polymers* 2010, 51, 2403–2409. [CrossRef]
- [53] Cai, J.; Lei, M.; Zhang, Q.; He, J.-R.; Chen, T.; Liu, S.; Fu, S.-H.; Li, T.-T.; Liu, G.; Fei, P. Electrospun composite nanofiber mats of Cellulose@Organically modified montmorillonite for heavy metal ion removal: Design, characterization, evaluation of absorption performance. *Compos. Part A Appl. Sci. Manuf.* 2017, 92, 10–16. [CrossRef]
- [54] Mahdieh, Z.M.; Mottaghitalab, V.; Piri, N.; Haghi, A.K. Conductive chitosan/multi walled carbon nanotubes electrospun nanofiber feasibility. *Korean J. Chem. Eng.* 2011, 29, 111–119. [CrossRef]

- [55] Chan KH, K.; Wong, S.Y.; Tiju, W.C.; Li, X.; Kotaki, M.; He, C.B. Morphologies and electrical properties of electrospun poly [(R)-3-hydroxybutyrate-co-(R)-3-hydroxyvalerate]/multiwalled carbon nanotubes fibers. *J. Appl. Polym. Sci.* 2020, 116, 1030–1035. [CrossRef]
- [56] Lu, P.; Hsieh, Y.-L. Multiwalled Carbon Nanotube (MWCNT) Reinforced Cellulose Fibers by Electrospinning. *ACS Appl. Mater. Interfaces* 2010, 2, 2413–2420. [CrossRef] [PubMed]
- [57] Talal, J.H.; Mohammed, D.B.; Jawad, K.H. Fabrication of Hydrophobic Nanocomposites Coating Using Electrospinning Technique for Various Substrate. *J. Phys. Conf. Ser.* 2018, 1032, 012033. [CrossRef]
- [58] P. Ciselli, Z. Wang, and T. Peijs, “Reinforcing potential of carbon nanotubes in oriented polymer fibres,” *Materials Technology*, vol. 22, no. 1, pp. 10–21, 2007.
- [59] Yu, M.-F., Files, B. S., Arepalli, S., & Ruoff, R. S. (2000). Tensile loading of ropes of single wall carbon nanotubes and their mechanical properties. *Phys. Rev. Lett.*, Vol. 84, pp. 5552-5555, ISSN 0031-9007
- [60] Yu, M.-F., Lourie, O., Dyer, M. J., Moloni, K., Kelly, T. F., & Ruoff, R. S. (2000). Strength and breaking mechanism of multiwalled carbon nanotubes under tensile load. *Science*, Vol. 287, pp. 637-640, ISSN 0036-8075.
- [61] Jose, Josmin P., and Kuruvilla Joseph. "Advances in polymer composites: macro-and microcomposites—state of the art, new challenges, and opportunities." *Polymer composites* (2012): 1-16.
- [62] Huang, Silu, et al. "Characterization of interfacial properties between fibre and polymer matrix in composite materials—A critical review." *Journal of Materials Research and Technology* 13 (2021): 1441-1484.
- [63] <https://www.dsiac.org/resources/journals/dsiac/fall-2014-volume-1-number-2/carbon-nanotubes>.

- [64] Dresselhaus, M.S., Dresselhaus, G., Saito, R., 1995. Carbon 33, 883.
- [65] Dresselhaus, M.S., Dresselhaus, G., Eklund, P.C., 1996. Science of Fullerenes and Carbon Nanotubes. Academic Press, New York, USA
- [66] Ahmad Aqel et. al., Carbon nanotubes, science and technology part (I) structure, synthesis and characterization, Arabian Journal of Chemistry, 5, 1–23, 2012.
- [67] Daenen, M., de Fouw, R.D., Hamers, B., Janssen, P.G.A., Schouteden, K., Veld, M.A.J., 2003. The
- [68] Wondrous World of Carbon Nanotubes, a review of current carbon nanotube technologies, Eindhoven University of Technology, February 2003.
- [69] Ajayan, P.M.; Schadler, L.S.; Braun, P.V. Nanocomposite Science and Technology; Wiley-VCH Verlag GmbH & Co.: Weinheim, Germany; p. 239, 2003.
- [70] Ziegler KJ, Gu Z, Peng H, Flor EL, Hauge RH, Smalley RE. Controlled oxidative cutting of single-walled carbon nanotubes. J Am ChemSoc 2005; 127:1541–7.
- [71] Bednarczyk, B.A. (2003) Composites Part B, 34, 175–197.
- [72] Huang, H. and Talreja, R. (2006) Composites Science and Technology, 66, 2743–2757.
- [73] Tabiei, A. and Aminji karai, S.B. (2009), Composite Structures, 88, 65–82.
- [74] Haibo Yu, YanliQu, Zaili Dong, Wen J. Li, Yuechao Wang, WencaiRen, and Zeshi Cui, Separation of Mixed SWNTs and MWNTs by Centrifugal Force -- an Experimental Study,
- [75] Datsyuk V, Kalyva M, Papagelis K, Parthenios J, Tasis D, Siokou A, et al. Chemical oxidation of multiwalled carbon mnanotubes. Carbon 2008; 46:833–40.

- [76] Wang, X. S., Wang, H.C., Huang, Y.J., Zhao, Z.X., Qin, X., Wang, Y.Y., Miao, Z.Y., Chen,Q., &Qiao, M.Q. (2010). Noncovalently functionalized multi-wall carbon nanotubes in aqueous solution using the hydrophobic HFBI and their electroanalytical application. *Biosensors and Bioelectronics*, Vol.26, No.3, (November 2010), pp.1104-1108
- [77] Dilberoglu UM, Gharehpapagh B, Yaman U, Dolen M. The role of additive manufacturing in the era of industry 4.0. *Proc Manufact.*2017;11:545-554
- [78] Nazir, Aamer, and Jeng-Ywan Jeng. "A high-speed additive manufacturing approach for achieving high printing speed and accuracy." *Proceedings of the Institution of Mechanical Engineers, Part C: Journal of Mechanical Engineering Science* 234.14 (2020): 2741-2749.
- [79] <https://wohlersassociates.com/product/wr2024//>
- [80] Ngo, Tuan D., et al. "Additive manufacturing (3D printing): A review of materials, methods, applications and challenges." *Composites Part B: Engineering* 143 (2018): 172-196.
- [81] Sezer, H. Kürşad, and Oğulcan Eren. "FDM 3D printing of MWCNT re-inforced ABS nano-composite parts with enhanced mechanical and electrical properties." *Journal of manufacturing processes* 37 (2019): 339-347.
- [82] Liu, Kun, Fajun Ding, and Jianing Teng. "Research on Application of 3D Printing Technology in Maintenance of Civil Aviation Machinery." *Mech. Eng. Technol* 5 (2018): 356-361.
- [83] Shahrubudin, Nurhalida, Te Chuan Lee, and R. J. P. M. Ramlan. "An overview on 3D printing technology: Technological, materials, and applications." *Procedia Manufacturing* 35 (2019): 1286-1296.

- [84] Chen, Xiangfan, et al. "High-speed 3D printing of millimeter-size customized aspheric imaging lenses with sub 7 nm surface roughness." *Advanced Materials* 30.18 (2018): 1705683.
- [85] Nayak, Radharani, et al. "An approach towards economized 3D printing." *Applied Mechanics and Materials* 852 (2016): 185-191.
- [86] Javadi, Mohammad Sadegh, Mohammad Vahid Ehteshamfar, and Hamed Adibi. "A comprehensive analysis and prediction of the effect of groove shape and volume fraction of multi-walled carbon nanotubes on the polymer 3D-printed parts in the friction stir welding process." *Polymer Testing* 117 (2023): 107844.
- [87] Birosz, Márton Tamás, Daniel Ledenyak, and Matyas Ando. "Effect of FDM infill patterns on mechanical properties." *Polymer Testing* 113 (2022): 107654.
- [88] Chohan, Jasgurpreet Singh, and Rupinder Singh. "Pre and post processing techniques to improve surface characteristics of FDM parts: a state of art review and future applications." *Rapid Prototyping Journal* 23.3 (2017): 495-513.
- [89] Yadav, Aniket, et al. "Fused filament fabrication: a state-of-the-art review of the technology, materials, properties and defects." *International Journal on Interactive Design and Manufacturing (IJIDeM)* (2022): 1-23.
- [90] Long, Haibo, et al. "Mechanical and thermal properties of bamboo fiber reinforced polypropylene/polylactic acid composites for 3D printing." *Polymer Engineering & Science* 59. s2 (2019): E247-E260.
- [91] Nathaphan, Supphachai, and Worrasid Trutassanawin. "Effects of process parameters on compressive property of FDM with ABS." *Rapid Prototyping Journal* 27.5 (2021): 905-917.
- [92] Rashid, Adib Bin, et al. "Nanotechnology-enhanced fiber-reinforced polymer composites: Recent advancements on processing techniques and applications." *Heliyon* (2024).

- [93] Khan, Idrees, et al. "Polymer Nanocomposites: An Overview." *Smart Polymer Nanocomposites*, 2022, pp. 167-184, <https://doi.org/10.1016/B978-0-323-91611-0.00017-7>.
- [94] N. Ali, B. Zhang, H. Zhang, W. Zaman, W. Li, Q. Zhang, Key synthesis of magnetic Janus nanoparticles using a modified facile method, *Particuology* 17 (2014) 5965.
- [95] K. Saeed, I. Khan, Preparation and characterization of functionalized multiwalled carbon nanotubes filled polyethylene oxide nanocomposites, *J. Rubber Res.* 23 (2020) 187192. Available from: <https://doi.org/10.1007/s42464-020-00048-6>
- [96] S.S. Siwal, Q. Zhang, N. Devi, V.K. Thakur, Carbon-based polymer nanocomposite for high-performance energy storage applications, *Polymers (Basel)* 12 (2020). Available from: <https://doi.org/10.3390/polym12030505>.
- [97] N. Ali, B. Zhang, H. Zhang, W. Zaman, X. Li, W. Li, et al., Inter-facially active and magnetically responsive composite nanoparticles with raspberry like structure; synthesis and its applications for heavy crude oil/water separation, *Colloids Surf. A: Physicochem. Eng. Asp.* 472 (2015) 3849.
- [98] I.O. Oladele, T.F. Omotosho, A.A. Adediran, Polymer-based composites: an indispensable material for present and future applications, *Int. J. Polym. Sci.* 2020 (2020). Available from: <https://doi.org/10.1155/2020/8834518>.
- [99] N. Ali, B. Zhang, H. Zhang, W. Zaman, W. Li, L. Tian, et al., Novel Janus magnetic micro particle synthesis and its applications as a demulsifier for breaking heavy crude oil and water emulsion, *Fuel* 141 (2015) 258267.
- [100] H. Wei, H. Wang, A. Li, D. Cui, Z. Zhao, L. Chu, et al., Multifunctions of polymer nanocomposites: environmental remediation, electromagnetic interference shielding, and sensing applications, *ChemNanoMat* 6 (2020) 174184. Available from: <https://doi.org/10.1002/CNMA.201900588>.

- [101] N. Ali, B. Zhang, H. Zhang, W. Zaman, S. Ali, Z. Ali, et al., Monodispers and multifunctional magnetic composite core shell microspheres for demulsification applications, *J. Chin. Chem. Soc.* 62 (8) (2015) 695702.
- [102] E.M. Masoud, L. Liu, B. Peng, Synthesis, characterization, and applications of polymer nanocomposites, *J. Nanomater.* 2020 (2020). Available from: <https://doi.org/10.1155/2020/5439136>
- [103] K. Saeed, I. Khan, Z. Ahmad, B. Khan, Preparation, analyses and application of cobaltmanganese oxides/nylon 6,6 nanocomposites, *Polym. Bull.* 75 (2018). Available from: <https://doi.org/10.1007/s00289-018-2292-3>
- [104] M. Sen, Nanocomposite materials, Nanotechnology and the Environment, Intech Open, 2020. Available from: <https://doi.org/10.5772/intechopen.93047>.
- [105] Wang, Jiacheng, and Stefan Kaskel. "KOH activation of carbon-based materials for energy storage." *Journal of materials chemistry* 22.45 (2012): 23710-23725.
- [106] Wang S, Xiao C, Xing Y, Xu H, Zhang S. Carbon nanofibers/nanosheets hybrid derived from cornstalks as a sustainable anode for Li-ion batteries. *Journal of Materials Chemistry A*. 2015; 3:6742-6746
- [107] Abdel Salam M, Mokhtar M, Basahel SN, Al Thabaiti SA, Obaid AY. Removal of chlorophenol from aqueous solution by multi-walled carbon nanotubes: Kinetic and thermodynamic studies. *Journal of Alloys and Compounds*. 2010; 500:87-92
- [108] Kokuoz, Basak Yazgan, et al. "Er-Doped Y2O3 Nanoparticles: A Comparison of Different Synthesis Methods." *Journal of the American Ceramic Society* 92.10 (2009): 2247-2253.
- [109] Mohamed O.A., Masood S.H., Bhowmik J.L. Optimization of fused deposition modeling process parameters: a review of current research and future prospects. *Journal of Advanced Manufacturing* 2015; 3: 42–53.

- [110] Ngo T., Kashani A., Imbalzano G., Nguyen K., Hui D. Additive manufacturing (3D printing): A review of materials, methods, applications, and challenge. *Journal of Composites Part B* 2018; 143: 172–196
- [111] FDM Process 2. Z., Wang, Y., Wu, B., Cui, C., Guo, Y., Yan, C.: A critical review of fused deposition modeling 3D printing technology in manufacturing polylactic acid parts. *Int. J. Adv. Manuf. Technol.* 102, 2877–2889 (2019). <https://doi.org/10.1007/s00170-019-03332-x>
- [112] Jayanth, N., Jaswanthraj, K., Sandeep, S., Mallaya, N.H., Siddharth, S.R.: Effect of heat treatment on mechanical properties of 3D printed PLA. *J. Mech. Behav. Biomed. Mater.* 123, 104764 (2021). <https://doi.org/10.1016/j.jmbbm.2021.104764>
- [113] Dey, A., Nita, Y.: A systematic survey of FDM process parameter optimization and their influence on part characteristics. *J. Manuf. Mater. Process.* 3, 64 (2019). <https://doi.org/10.3390/jmmp3030064>
- [114] Sood, A.K., Chaturvedi, V., Datta, S., Mahapatra, S.S.: Optimization of process parameters in fused deposition modeling using weighted principal component analysis. *J. Adv. Manuf. Syst.* 10, 241–259 (2011). <https://doi.org/10.1142/S0219686711002181>
- [115] Wang, S., Ma, Y., Deng, Z., Zhang, S., Cai, J.: Effects of fused deposition modeling process parameters on tensile, dynamic mechanical properties of 3D printed polylactic acid materials. *Polym. Test J.* 86, 106483 (2020). <https://doi.org/10.1016/j.polymertesting.2020.106483>
- [116] Li, H., Wang, T., Sun, J., Yu, Z.: The effect of process parameters in fused deposition modelling on bonding degree and mechanical properties. *Rapid Prototyp. J.* 1, 80–92 (2018). <https://doi.org/10.1108/RPJ-06-2016-0090>
- [117] Milling, D., Ali, M.Y., Abd, M.: Studies on effect of fused deposition modelling process parameters on ultimate tensile strength and dimensional accuracy of Nylon.

- IOP Conf. Ser. Mater. Sci. Eng. (2016). <https://doi.org/10.1088/1757-899X/149/1/012035>
- [118] Krajangsawasdi, N., Blok, L.G., Hamerton, I., Longana, M.L.: Fused deposition modelling of fibre reinforced polymer composites: a parametric review. *J. Compos. Sci.* 5, 29 (2021). <https://doi.org/10.3390/jcs5010029>
- [119] Ayrimis, N.: Effect of layer thickness on surface properties of 3D printed materials produced from wood flour/PLA filament. *Polym. Test.* 71, 163–166 (2018). <https://doi.org/10.1016/j.polymertesting.2018.09.009>
- [120] Jiang, S., Liao, G., Xu, D.: Mechanical properties analysis of polyetherimide parts fabricated by fused deposition modeling. *High Perform. Polym.* 31, 97–106 (2019). <https://doi.org/10.1177/0954008317752822>
- [121] Venuvinod, P.K., Ma, W.: Rapid prototyping laser based and other technologies. vol. na. 1st ed. City University: Springer Science+Business Media, LLC (2004). <https://doi.org/10.1007/978-1-4757-6361-4> Copyright
- [122] Akhoundi, B., Behraves, A.H.: Effect of filling pattern on the tensile and flexural mechanical properties of FDM 3D printed products. *Exp. Mech.* 59, 883–897 (2019). <https://doi.org/10.1007/s11340-018-00467-y>
- [123] Chiniwar, D.S., Alva, H., Varada, V.R., Balichakra, M., Hiremath, S.: Investigation of automatic bed levelling system for fused deposition modelling 3D printer machine. *Int. J. Mod. Manuf. Technol.* XIV, 23–32 (2022)
- [124] Derise, M.R., Zulkarnain, A.: Effect of infill pattern and density on tensile properties of 3D printed polylactic acid parts via fused deposition modeling (FDM). *Int. J. Mech. Mechatron. Eng. IJMME-IJENS* 20, 54–63 (2020). <https://doi.org/10.1177/0954406219856383>
- [125] Tyson, E.: How to use 3D print infill settings-increase strength, save filament. *RigidInk* 2021:2–11. <https://rigid.ink/blogs/news/optimum-infill>

- [126] Kopets, E.E., Karimov, A.I.: Mechanical vibration analysis of a gantry 3D printer. 2021 IEEE Conf. Russ. Young Res. Electr. Electron. Eng., pp. 956–60 (2021)
- [127] Wickramasinghe, S., Do, T., Tran, P.: FDM-based 3D printing of polymer and associated composite: a review on mechanical properties, defects and treatments. *Polymers* 12, 1529 (2020). <https://doi.org/10.3390/polym12071529>
- [128] Miazio, L.: Impact of print speed on strength of samples printed in fdm technology. *Agric. Eng.* 23, 33–38 (2019). <https://doi.org/10.1515/agriceng-2019-0014>
- [129] Pal, K., Banerjee, I.: Polymeric gels characterization, properties and biomedical applications. vol. na. Duxford, CB22 4QH, United Kingdom 50: Woodhead Publishing, (2018). <https://doi.org/10.1016/C2016-0-04092-5>
- [130] Wenzheng, Wu., Ye, W., Zichao, Wu., Peng Geng, Y.W., JZ, Influence of layer thickness, raster angle, deformation temperature and recovery temperature on the shape-memory effect of 3D-printed polylactic acid samples. *Materials* (2017). <https://doi.org/10.3390/ma10080970>
- [131] Hull C.W. Apparatus for production of three-dimensional objects by stereolithography. US Patent 4: 575; 330.
- [132] Prinz F.B., Atwood C.L., Aubin R.F. JTEC/WTEC panel report on rapid prototyping in Europe and Japan. Rapid Prototyping Association of the society of Manufacturing Engineers (Loyala College in Maryland). 1997; 1.
- [133] Dizon J., Espera Jr.A., Chen Q., Advincula R. Mechanical characterization of 3D-printed polymers. *Journal of Additive Manufacturing* 2018; 20: 44–67.
- [134] Yang Y., Li L., Zhao J. Mechanical property modeling of photosensitive liquid resin in stereolithography additive manufacturing: bridging degree of cure with tensile strength and hardness. *Journal of Materials and Design* 2019; 162: 418–428.

- [135] Yuki Suzuki Y., Tahara H., Michihata M., Takamasu K., Takahashi S. Evanescent Light Exposing System under Nitrogen Purge for Nano-Stereolithography. *Procedia CIRP* 2016; 42: 77–80. <https://doi.org/10.1016/j.procir.2016.02.192>
- [136] Heller C., Schwentenwein M., Russmueller G., Varga F., Stampfl J., Liska R. Vinyl esters: low cytotoxicity monomers for the fabrication of biocompatible 3d scaffolds by lithography based additive manufacturing. *Journal of Polymer Science (Part A: Polymer Chemistry)* 2009; 47 (4): 6941–6945.
- [137] Lim K.S., Castilho M.D., Malda J., Levato R., Alcala-Orozco C.R., Melchels F.P.W., Gawlitta D., Hooper G.J., Woodfield T.B.F., Dorenmalen K., Costa P.F. Bio-resin for high-resolution lithography-based biofabrication of complex cell-laden constructs. *Journal of Biofabrication* 2018; 10(3): 034101. <https://doi.org/10.1088/1758-5090/aac00c>.
- [138] Gowda R., Udayagiri C., and Narendra D. Studies on the Process Parameters of Rapid Prototyping Technique (Stereolithography) for the Betterment of Part Quality. *International Journal of Manufacturing Engineering* 2014. <https://doi.org/10.1155/2014/804705>
- [139] Akilesh M., Elango P., Devanand A., Soundararajan R., Varthanan P. Optimization of selective laser sintering process parameters on surface quality. *3D Printing and Additive Manufacturing Technologies Journal* 2018: 141–157.
- [140] Kazemi M., Rahimi A. Stereolithography process optimization for tensile strength improvement of products. *Rapid Prototyping Journal* 2018; 24(4): 00-00. <https://doi.org/10.1108/RPJ-05-2015-0049>
- [141] Melchels F.P.W., Feijen J., Grijpma D.W. A review on stereolithography and its applications in biomedical engineering. *Journal of Biomaterials* 2010; 31(24): 6121–3.

- [142] Manapat J.Z., Chen Q., Ye P., Advincula R.C. 3D printing of polymer nanocomposites via stereolithography. *Journal of Macromolecular Materials and Engineering* 2017; 302(9): 1600553
- [143] Wang X., Jiang M., Zhou Z., Gou J., Hui D. 3D printing of polymer matrix composites: A review and prospective. *Composites Part B: Engineering*. 2017; 110: 442–58.
- [144] Tao Y., Yin Q., and Li P. An Additive Manufacturing Method Using Large-Scale Wood Inspired by Laminated Object Manufacturing and Plywood Technology. *Polymers* 2021; 13: 144. <https://doi.org/10.3390/polym13010144>
- [145] Gibson I., Rosen D., Stucker B. Sheet lamination processes. *Additive manufacturing technologies: 3D printing, rapid prototyping, and direct digital manufacturing*. New York, NY: Springer New York 2015: 219–44.
- [146] Vaezi M., Seitz H., Yang S. A review on 3D micro-additive manufacturing technologies. *International Journal of Advance Manufacturing Technology* 2013; 67: 1721–1754. <https://doi.org/10.1007/s00170-012-4605-2>
- [147] Gibson I., Rosen D.W., Stucker B. *Additive Manufacturing Methodologies: Rapid Prototyping to Direct Digital Manufacturing*, Springer 2010, New York
- [148] Singh S., Sachdeva A., Sharma V. Optimization of selective laser sintering process parameters to achieve the maximum density and hardness in polyamide parts. *Journal of Progress in Additive Manufacturing* 2017; 2:19–30. <https://doi.org/10.1007/s40964-017-0020-4>
- [149] Kim G., Lee S., Kim H., Yang D., Kim Y., Kyung Y., Kim C., Choi S., Kim B., Ha H., Kwon S., Kim N. Three-Dimensional Printing: Basic Principles and Applications in Medicine and Radiology. *Korean Journal of Radiology* 2016; 17(2): 182-197.
- [150] Ruban W., Vijayakumar V., Dhanabal P., and Pridhar T. Effective process parameters in selective laser sintering. *International Journal of Rapid Manufacturing* 2014; 4 (2/3/4). <https://doi.org/10.1504/IJRAPIDM.2014.066036>

- [151] Kim G., Oh Y. A benchmark study on rapid prototyping processes and machines: quantitative comparisons of mechanical properties, accuracy, roughness, speed, and material cost. *Proceedings of the Institution of Mechanical Engineers Part B: Journal of Engineering Manufacture* 2008; 22: 201–215.
- [152] Williams J., Adewunmi A., Schek R., Flanagan C., Krebsbach P., Feinberg S., Hollister S., Das S. Bone tissue engineering using polycaprolactone scaffolds fabricated via selective laser sintering. *Journal of Biomaterials* 2005; 26: 4817–4827. <https://doi.org/10.1016/j.biomaterials.2004.11.057>.
- [153] Duan B., Wang M., Zhou W., Cheung W., Li Z., Lu W. Three-dimensional nanocomposite scaffolds fabricated via selective laser sintering for bone tissue engineering. *Journal of Acta Biomaterialia* 2010; 6(12): 4495–4505.
- [154] Pereira T.F., Silva M., Oliveira M., Maia I., Silva J., Costa M., Thire R. Effect of process parameters on the properties of selective laser sintered Poly(3-hydroxybutyrate) scaffolds for bone tissue engineering. *Journal of Virtual and Physical Prototyping* 2012; 7: 275–285.
- [155] Dass A. and Moridi A. State of the Art in Directed Energy Deposition: From Additive Manufacturing to Materials Design. *Journal of Coatings* 2019; 9: 418. <https://doi.org/10.3390/coatings9070418>.
- [156] W. Yan, S. Lin, O.L. Kafka, C. Yu, Z. Liu, Y. Lian, S. Wolff, J. Cao, G.J. Wagner, W.K. Liu, Modeling process-structure-property relationships for additive manufacturing, *Front. Mech. Eng.* 13 (4) (2018) 482–492.
- [157] I.A. Roberts, C.J. Wang, R. Esterlein, M. Stanford, D.J. Mynors, A threedimensional finite element analysis of the temperature field during laser melting of metal powders in additive layer manufacturing, *Int. J. Mach. Tools Manuf.* 49 (12-13) (2009) 916–923.

- [158] J. Ding, P. Colegrove, J. Mehnert, S. Williams, F. Wang, P.S. Almeida, A computationally efficient finite element model of wire and arc additive manufacture, *Int. J. Adv. Manuf. Technol.* 70 (1-4) (2014) 227–236.
- [159] J. Zhao, L. Wu, C. Zhan, Q. Shao, Z. Guo, L. Zhang, Overview of polymer nanocomposites: computer simulation understanding of physical properties, *Polymer* 133 (2017) 272–287.
- [160] L.-T. Yan, X.-M. Xie, Computational modeling and simulation of nanoparticle self-assembly in polymeric systems: Structures, properties and external field effects, *Prog. Polym. Sci.* 38 (2) (2013) 369–405
- [161] Yan W, Ge W, Smith J, et al. Multi-scale modeling of electron beam melting of functionally graded materials. *Acta Materialia*, 2016, 115: 403–412
- [162] Yan W, Smith J, Ge W, et al. Multiscale modeling of electron beam and substrate interaction: A new heat source model. *Computational Mechanics*, 2015, 56(2): 265–276
- [163] Yan W, Ge W, Qian Y, et al. Multi-physics modeling of single/ multiple track defect mechanisms in electron beam selective melting. *Acta Materialia*, 2017, 134: 324–333
- [164] Yan W, Qian Y, Lin S, et al. Meso-scale modeling of multiple-layer fabrication process in selective electron beam melting: Inter-layer/ track voids formation. *Materials & Design*, 2018, 141: 210–219
- [165] Smith J, Xiong W, Cao J, et al. Thermodynamically consistent microstructure prediction of additively manufactured materials. *Computational Mechanics*, 2016, 57(3): 359–370
- [166] Liu Z, Bessa M, Liu W K. Self-consistent clustering analysis: An efficient multi-scale scheme for inelastic heterogeneous materials. *Computer Methods in Applied Mechanics and Engineering*, 2016, 306: 319–341

- [167] Liu Z, Moore J A, Liu W K. An extended micromechanics method for probing interphase properties in polymer nanocomposites. *Journal of the Mechanics and Physics of Solids*, 2016, 95: 663–680
- [168] Valino, A.D., Dizon, J.R.C., Espera Jr, A.H., Chen, Q., Messman, J. and Advincula, R.C., 2019. Advances in 3D printing of thermoplastic polymer composites and nanocomposites. *Progress in Polymer Science*, p.101162.
- [169] Lim, C.W.J., Le, K.Q., Lu, Q. and Wong, C.H., 2016. An overview of 3-D printing in manufacturing, aerospace, and automotive industries. *IEEE Potentials*, 35(4), pp.18-22.
- [170] Serdeczny, M.P., Comminal, R., Pedersen, D.B. and Spangenberg, J., 2020. Experimental and analytical study of the polymer melt flow through the hot-end in material extrusion additive manufacturing. *Additive Manufacturing*, 32, p.100997.
- [171] Ngo, Tuan D., et al. "Additive manufacturing (3D printing): A review of materials, methods, applications and challenges." *Composites Part B: Engineering* 143 (2018): 172-196.
- [172] Caminero, M.A., Chacón, J.M., García-Moreno, I. and Rodríguez, G.P., 2018. Impact damage resistance of 3D printed continuous fibre reinforced thermoplastic composites using fused deposition modelling. *Composites Part B: Engineering*, 148, pp.93-103..
- [173] Torrado, A.R., Shemelya, C.M., English, J.D., Lin, Y., Wicker, R.B. and Roberson, D.A., 2015. Characterizing the effect of additives to ABS on the mechanical property anisotropy of specimens fabricated by material extrusion 3D printing. *Additive Manufacturing*, 6, pp.16-29.
- [174] Nikzad, M., Masood, S.H. and Sbarski, I., 2011. Thermo-mechanical properties of a highly filled polymeric composites for fused deposition modeling. *Materials & Design*, 32(6), pp.3448-3456.

- [175] Gray IV, Robert W., Donald G. Baird, and Jan Helge Bøhn. "Effects of processing conditions on short TLCP fiber reinforced FDM parts." *Rapid Prototyping Journal* 4.1 (1998): 14-25.
- [176] Zhong, Weihong, et al. "Short fiber reinforced composites for fused deposition modeling." *Materials Science and Engineering: A* 301.2 (2001): 125-130.
- [177] Postiglione, G., Natale, G., Griffini, G., Levi, M. and Turri, S., 2015. Conductive 3D microstructures by direct 3D printing of polymer/carbon nanotube nanocomposites via liquid deposition modeling. *Composites Part A: Applied Science and Manufacturing*, 76, pp.110-114.
- [178] Zhang, H., Yang, D. and Sheng, Y., 2018. Performance-driven 3D printing of continuous curved carbon fibre reinforced polymer composites: A preliminary numerical study. *Composites Part B: Engineering*, 151, pp.256-264.
- [179] Frketic, J., Dickens, T. and Ramakrishnan, S., 2017. Automated manufacturing and processing of fiber-reinforced polymer (FRP) composites: An additive review of contemporary and modern techniques for advanced materials manufacturing. *Additive Manufacturing*, 14, pp.69-86.
- [180] Ning, F., Cong, W., Qiu, J., Wei, J. and Wang, S., 2015. Additive manufacturing of carbon fiber reinforced thermoplastic composites using fused deposition modeling. *Composites Part B: Engineering*, 80, pp.369-378.
- [181] Kestilä, A., Nordling, K., Miikkulainen, V., Kaipio, M., Tikka, T., Salmi, M., Auer, A., Leskelä, M. and Ritala, M., 2018. Towards space-grade 3D-printed, ALD-coated small satellite propulsion components for fluidics. *Additive Manufacturing*, 22, pp.31-37.
- [182] Zhu, L., Li, N. and Childs, P.R.N., 2018. Light-weighting in aerospace component and system design. *Propulsion and Power Research*, 7(2), pp.103-119.

- [183] Wu, C.S., 2018. Characterization, functionality and application of siliceous sponge spicules additive-based manufacturing biopolymer composites. *Additive Manufacturing*, 22, pp.13-20.
- [184] Hoff, B.W., Maestas, S.S., Hayden, S.C., Harrigan, D.J., Grudt, R.O., Ostraat, M.L., Horwath, J.C. and Leontsev, S., 2018. Dielectric strength heterogeneity associated with printing orientation in additively manufactured polymer materials. *Additive Manufacturing*, 22, pp.21-30.
- [185] Blok, L.G., Longana, M.L., Yu, H. and Woods, B.K., 2018. An investigation into 3D printing of fibre reinforced thermoplastic composites. *Additive Manufacturing*, 22, pp.176-186.
- [186] Dizon, J.R.C., Espera Jr, A.H., Chen, Q. and Advincula, R.C., 2018. Mechanical characterization of 3D-printed polymers. *Additive Manufacturing*, 20, pp.44-67.
- [187] Nieto, D.M., López, V.C. and Molina, S.I., 2018. Large-format polymeric pellet-based additive manufacturing for the naval industry. *Additive Manufacturing*, 23, pp.79-85.
- [188] Kalms, M., Narita, R., Thomy, C., Vollertsen, F. and Bergmann, R.B., 2019. New approach to evaluate 3D laser printed parts in powder bed fusion-based additive manufacturing in-line within closed space. *Additive Manufacturing*, 26, pp.161-165.
- [189] Kim, G., Barocio, E., Pipes, R.B. and Sterkenburg, R., 2019. 3D printed thermoplastic polyurethane bladder for manufacturing of fiber reinforced composites. *Additive Manufacturing*, 29, p.100809.
- [190] Golbang, A., Harkin-Jones, E., Wegrzyn, M., Campbell, G., Archer, E. and McIlhagger, A., 2020. Production and characterization of PEEK/IF-WS2 nanocomposites for additive manufacturing: Simultaneous improvement in processing characteristics and material properties. *Additive Manufacturing*, 31, p.100920.
- [191] Santos, V.M.R., Thompson, A., Sims-Waterhouse, D., Maskery, I., Woolliams, P. and Leach, R., 2020. Design and characterisation of an additive manufacturing

benchmarking artefact following a design-for-metrology approach. *Additive Manufacturing*, 32, p.100964.

- [192] Van de Werken, N., Tekinalp, H., Khanbolouki, P., Ozcan, S., Williams, A. and Tehrani, M., 2019. Additively Manufactured Carbon Fiber-Reinforced Composites: State of the Art and Perspective. *Additive Manufacturing*, p.100962.
- [193] Bhatt, P.M., Malhan, R.K., Rajendran, P. and Gupta, S.K., 2020. Building free-form thin shell parts using supportless extrusion-based additive manufacturing. *Additive Manufacturing*, 32, p.101003.
- [194] Tian, X., Liu, T., Yang, C., Wang, Q. and Li, D., 2016. Interface and performance of 3D printed continuous carbon fiber reinforced PLA composites. *Composites Part A: Applied Science and Manufacturing*, 88, pp.198-205.
- [195] Palaganas, N.B., Mangadlao, J.D., de Leon, A.C.C., Palaganas, J.O., Pangilinan, K.D., Lee, Y.J. and Advincula, R.C., 2017. 3D printing of photocurable cellulose nanocrystal composite for fabrication of complex architectures via stereolithography. *ACS applied materials & interfaces*, 9(39), pp.34314-34324.
- [196] Kumar, N., Jain, P.K., Tandon, P. and Pandey, P.M., 2018. Additive manufacturing of flexible electrically conductive polymer composites via CNC-assisted fused layer modeling process. *Journal of the Brazilian Society of Mechanical Sciences and Engineering*, 40(4), p.175.
- [197] Dickson, A.N., Barry, J.N., McDonnell, K.A. and Dowling, D.P., 2017. Fabrication of continuous carbon, glass and Kevlar fibre reinforced polymer composites using additive manufacturing. *Additive Manufacturing*, 16, pp.146-152.
- [198] Bryll, K., Piesowicz, E., Szymański, P., Ślaczka, W. and Pijanowski, M., 2018. Polymer Composite Manufacturing by FDM 3D Printing Technology. In *MATEC Web of Conferences* (Vol. 237, p. 02006). EDP Sciences.

- [199] Kim, H., Park, E., Kim, S., Park, B., Kim, N. and Lee, S., 2017. Experimental study on mechanical properties of single-and dual-material 3D printed products. *Procedia Manufacturing*, 10, pp.887-897.
- [200] Balla, V.K., Kate, K.H., Satyavolu, J., Singh, P. and Tadimeti, J.G.D., 2019. Additive manufacturing of natural fiber reinforced polymer composites: Processing and prospects. *Composites Part B: Engineering*, p.106956.
- [201] Slotwinski, J.A., 2014, February. Additive manufacturing: Overview and NDE challenges. In *AIP Conference Proceedings* (Vol. 1581, No. 1, pp. 1173-1177). American Institute of Physics.
- [202] Gnanasekaran, K., Heijmans, T., Van Bennekom, S., Woldhuis, H., Wijnia, S., de With, G. and Friedrich, H., 2017. 3D printing of CNT-and graphene-based conductive polymer nanocomposites by fused deposition modeling. *Applied materials today*, 9, pp.21-28.
- [203] Haider, S., Khan, Y., Almasry, W.A. and Haider, A., 2012. Thermoplastic nanocomposites and their processing techniques. *Thermoplastic: Composite Materials*, p.113.
- [204] Jia, Y., He, H., Geng, Y., Huang, B. and Peng, X., 2017. High through-plane thermal conductivity of polymer based product with vertical alignment of graphite flakes achieved via 3D printing. *Composites Science and Technology*, 145, pp.55-61.
- [205] Tekinalp, H.L., Kunc, V., Velez-Garcia, G.M., Duty, C.E., Love, L.J., Naskar, A.K., Blue, C.A. and Ozcan, S., 2014. Highly oriented carbon fiber–polymer composites via additive manufacturing. *Composites Science and Technology*, 105, pp.144-150.
- [206] Guo, Y., Chang, C.C., Halada, G., Cuiffo, M.A., Xue, Y., Zuo, X., Pack, S., Zhang, L., He, S., Weil, E. and Rafailovich, M.H., 2017. Engineering flame retardant biodegradable polymer nanocomposites and their application in 3D printing. *Polymer Degradation and Stability*, 137, pp.205-215.

- [207] Coiai, S., Passaglia, E., Pucci, A. and Ruggeri, G., 2015. Nanocomposites based on thermoplastic polymers and functional nanofiller for sensor applications. *Materials*, 8(6), pp.3377-3427.
- [208] Dul, S., Fambri, L. and Pegoretti, A., 2016. Fused deposition modelling with ABS–graphene nanocomposites. *Composites Part A: Applied Science and Manufacturing*, 85, pp.181-191.
- [209] Golbang, A., Harkin-Jones, E., Wegrzyn, M., Campbell, G., Archer, E. and McIlhagger, A., 2020. Production and characterization of PEEK/IF-WS2 nanocomposites for additive manufacturing: Simultaneous improvement in processing characteristics and material properties. *Additive Manufacturing*, 31, p.100920..
- [210] Lee, G., Carrillo, M., McKittrick, J., Martin, D.G. and Olevsky, E.A., 2020. Fabrication of ceramic bone scaffolds by Solvent jetting 3D printing and sintering: Towards load-bearing applications. *Additive Manufacturing*, p.101107.
- [211] Loh, G.H., Pei, E., Harrison, D. and Monzon, M.D., 2018. An overview of functionally graded additive manufacturing. *Additive Manufacturing*, 23, pp.34-44.
- [212] Gnanasekaran, K., Heijmans, T., Van Bennekom, S., Woldhuis, H., Wijnia, S., de With, G. and Friedrich, H., 2017. 3D printing of CNT-and graphene-based conductive polymer nanocomposites by fused deposition modeling. *Applied materials today*, 9, pp.21-28.
- [213] Kim, H., Park, E., Kim, S., Park, B., Kim, N. and Lee, S., 2017. Experimental study on mechanical properties of single-and dual-material 3D printed products. *Procedia Manufacturing*, 10, pp.887-897.
- [214] Prakash, K.S., Nancharaih, T. and Rao, V.S., 2018. Additive manufacturing techniques in manufacturing-an overview. *Materials Today: Proceedings*, 5(2), pp.3873-3882.

- [215] Reddy, K.V.P., Mirzana, I.M. and Reddy, A.K., 2018. Application of Additive Manufacturing technology to an Aerospace component for better trade-off's. *Materials Today: Proceedings*, 5(2), pp.3895-3902.
- [216] Bryll, K., Piesowicz, E., Szymański, P., Ślaczka, W. and Pijanowski, M., 2018. Polymer Composite Manufacturing by FDM 3D Printing Technology. In *MATEC Web of Conferences* (Vol. 237, p. 02006). EDP Sciences.
- [217] Thompson, M.K., Moroni, G., Vaneker, T., Fadel, G., Campbell, R.I., Gibson, I., Bernard, A., Schulz, J., Graf, P., Ahuja, B. and Martina, F., 2016. Design for Additive Manufacturing: Trends, opportunities, considerations, and constraints. *CIRP annals*, 65(2), pp.737-760.
- [218] Van de Werken, N., Tekinalp, H., Khanbolouki, P., Ozcan, S., Williams, A. and Tehrani, M., 2019. Additively Manufactured Carbon Fiber-Reinforced Composites: State of the Art and Perspective. *Additive Manufacturing*, p.100962.
- [219] Wang, S., Ma, Y., Deng, Z., Zhang, K. and Dai, S., 2020. Implementation of an elastoplastic constitutive model for 3D-printed materials fabricated by stereolithography. *Additive Manufacturing*, p.101104.
- [220] Singh, S., Ramakrishna, S. and Singh, R., 2017. Material issues in additive manufacturing: A review. *Journal of Manufacturing Processes*, 25, pp.185-200.
- [221] Salmi, M., Tuomi, J., Paloheimo, K.S., Björkstrand, R., Paloheimo, M., Salo, J., Kontio, R., Mesimäki, K. and Mäkitie, A.A., 2012. Patient-specific reconstruction with 3D modeling and DMLS additive manufacturing. *Rapid Prototyping Journal*.
- [222] Kumar, N., Jain, P.K., Tandon, P. and Pandey, P.M., 2018. Experimental investigations on suitability of polypropylene (PP) and ethylene vinyl acetate (EVA) in additive manufacturing. *Materials Today: Proceedings*, 5(2), pp.4118-4127.

- [223] Kumar, N., Jain, P.K., Tandon, P. and Pandey, P.M., 2018. Extrusion-based additive manufacturing process for producing flexible parts. *Journal of the Brazilian Society of Mechanical Sciences and Engineering*, 40(3), p.143.
- [224] Taufik, M. and Jain, P.K., 2017. Characterization, modeling and simulation of fused deposition modeling fabricated part surfaces. *Surface Topography: Metrology and Properties*, 5(4), p.045003.
- [225] Babal AS, Gupta R, Singh BP, e al. Mechanical and electrical properties of high performance MWCNT/polycarbonate composites prepared by an industrial viable twin screw extruder with back flow channel. *RSC advances*. 2014;4(110):64649-58.
- [226] www.thermos.com/mc
- [227] <http://solidspace.co.in/>
- [228] Daminabo, S. C., Goel, S., Grammatikos, S. A., Nezhad, H. Y., & Thakur, V. K. (2020). Fused deposition modeling-based additive manufacturing (3D printing): techniques for polymer material systems. *Materials today chemistry*, 16, 100248.
- [229] . <https://www.flashforge.com/product-detail/flashforge-dreamer-3dprinter>
- [230] Huang G, Huo S, Xu X, et al. Realizing simultaneous improvements in mechanical strength, flame retardancy and smoke suppression of ABS nanocomposites from multifunctional graphene. *Composites Part B: Engineering* 2019; 177: 107377.
- [231] Gackowski BM, Sharma M, Idapalapati S. Processing and characterization of tailorable 3D-printed acrylonitrile butadiene styrene composites with hybrid buckypapers. *Compos Commun*. 2022; 32:101162.
- [232] Abeykoon C, Sri-Amphorn P, Fernando A. Optimization of fused deposition modeling parameters for improved PLA and ABS 3D printed structures. *Int J Lightweight Mater Manufact*. 2020;3(3): 284-297.

- [233] Dul S, Fambri L, Pegoretti A. Filaments production and fused deposition modelling of ABS/carbon nanotubes composites. *Nanomaterials*. 2018;8(1):49.
- [234] Fang Z, Liu L and Gu A. Improved micro hardness and micro tribological properties of bismaleimide nanocomposites obtained by enhancing interfacial interaction through carbon nanotube functionalization. *Polym Adv Technol* 2009; 20: 849–856.
- [235] Yuan J, Li Q, Ding L, et al. Carbon black/multi-walled carbon nanotube-based, highly sensitive, flexible pressure sensor. *ACS Omega* 2022; 7: 44428–44437
- [236] Van Trinh P, Van Luan N, Phuong DD, et al. Microstructure, microhardness and thermal expansion of CNT/Al composites prepared by flake powder metallurgy. *Composites Part A: Applied Science and Manufacturing* 2018; 105: 126–137.
- [237] Ebadi M, Mirdamadian Z, Ghanbari D, et al. The effect of aminated carbon nanotube and phosphorus pentoxide on the thermal stability and flame retardant properties of the acrylonitrile–butadiene–styrene. *J Cluster Sci* 2014; 25: 541–548.
- [238] Zou Y, Liu P, Yan Y, et al. Effect of heteroatom in conductive polymercoating of cathode materials on electrochemical performance of lithium sulfur batteries. *Ionics*. 2023;29(3):1019-1028.
- [239] Kostas V, Baikousi M, Barkoula NM, et al. Synthesis, characterization and mechanical properties of nanocomposites based on novel carbon nanowires and polystyrene. *Applied Sciences* 2020; 10: 5737
- [240] Țucureanu V, Matei A and Avram AM. FTIR Spectroscopy for carbon family study. *Crit Rev Anal Chem* 2016; 46: 502–520.
- [241] Martins JN, Klohn TG, Bianchi O, et al. Dynamic mechanical, thermal, and morphological study of ABS/textile fiber composites. *Polym Bull* 2010; 64: 497–510.

- [242] Zia MA, Khosa MK, Noor A, et al. PMMA/ABS/CoCl₂ composites for pharmaceutical applications: thermal, antimicrobial, antibiofilm, and antioxidant studies. *Molecules* 2022; 27: 7669
- [243] Kapoor S, Goyal M and Jindal P. Effect of functionalized multi-walled carbon nanotubes on thermal and mechanical properties of acrylonitrile butadiene styrene nanocomposite. *J Polym Res* 2020; 27: 1–3
- [244] Jagadeesh Chandra RB, Shivamurthy B, Sathish Kumar M, Thimmappa BHS. Mechanical, thermal and electromagnetic shielding effectiveness of MWCN-ABS films. *Trans Electr Electron Mater.* 2021; 23:1-9. .
- [245] Mohammed MI, Wilson D, Gomez-Kervin E, Tang B, Wang J. Investigation of closed-loop manufacturing with acrylonitrile butadiene styrene over multiple generations using additive manufacturing. *ACS Sustain Chem Eng.* 2019;7(16):13955-13969.
- [246] Li M-Y, Gupta S, Chang C, Tai N-H. Layered hybrid composites using multi-walled carbon nanotube film as reflection layer and multi-walled carbon nanotubes/neodymium magnet/epoxy as absorption layer perform selective electromagnetic interference shielding. *Compos Part B Eng.* 2019; 161:617-626

List of Publications

- 1. Singh, P., Singari, R. M., & Mishra, R. S. (2024).** Enhanced mechanical properties of MWCNT reinforced ABS nanocomposites fabricated through additive manufacturing process. *Polymers for Advanced Technologies*, 35(2), e6308.
- 2. Singh, P., Singari, R. M., & Mishra, R. S. (2024).** Improved mechanical properties of multiwalled carbon nanotube reinforced acrylonitrile butadiene styrene nanocomposites prepared by twin screw extruder. *Proceedings of the Institution of Mechanical Engineers, Part E: Journal of Process Mechanical Engineering*, 238(2), 954-964.
- 3. Phool Singh, Ranganath M. Singari, R. S. Mishra** “A comprehensive review of additive manufacturing – a distinct parametric approach”. Published in *International Journal of Research in Engineering and Innovation*. Volume-7 Issue-5 (2023)

Conference Proceedings

- 1. Phool Singh, Ranganath M. Singari, R. S. Mishra G.S. Bajwa** “A review on recent development on polymeric Hybrid composites and analysis of their enhanced mechanical performance” Published in *Materials Today Proceedings* 56 (2022) 3692-3701.
- 2. Phool Singh, Ranganath M. Singari, R.S. Mishra** “A review of study on modeling and simulation of Additive Manufacturing” Published in *Materials Today Proceedings* 56 (2022) 3594-3603.

CURRICULUM VITAE

MR. PHOOL SINGH has obtained his Bachelor of Engineering Degree from the Faculty of Engineering and Technology, Jamia Millia Islamia University, Delhi 110025, India. He also obtained a Master of Engineering Degree in Production Engineering from Delhi College of Engineering, University of Delhi, India. Since 2005, He has been working in a prestigious college as a Sr. Technical Staff member in the Department of Mechanical Engineering of Delhi Technological University (Formerly Delhi College of Engineering), Delhi, India. He has also worked in various industries from 1987 to 2005 as a Senior. Position for research and development, new developments etc.. He is actively engaged in laboratory work, teaching and research work in various fields. He has 18 years of lab work experience. He has published 8 research papers in International Journal and Conferences Proceedings, etcetera.